ELECTRICAL PROPERTIES OF SILICATE GLASSES CONTAINING As_2O_3

A Thesis Submitted
In Partial Fulfilment of the Requirements
for the Degree of
MASTER OF TECHNOLOGY

By
HALLIYAL ARVIND

to the

INTERDISCIPLINARY PROGRAM IN MATERIALS SCIENCE
INDIAN INSTITUTE OF TECHNOLOGY KANPUR
JULY, 1976

CERTIFICATE

This is to certify that this work on "Electrical Properties of Silicate Glasses Containing As_2O_3" by Halliyal Arvind has been carried out under my supervision and that this has not been submitted elsewhere for a degree.

D Chakravorty

(D. Chakravorty)
Professor
Department of Metallurgical Engineering
Indian Institute of Technology, Kanpur

ACKNOWLEDGEMENTS

I express my deep sense of gratitude to Dr. D. Chakravorty for his excellent and enthusiastic guidance at every stage of the investigation.

I am thankful to Dr. E.C. Subbarao for his advice and encouragement.

My sincere thanks are due to Mr. Devendra Kumar, Mr. B.V. Hiremath and Mr. H.R. Aravinda for their invaluable help in experimental work.

I gratefully acknowledge the help rendered by Mr. B. Sharma, Mr. R.K. Prasad and Mr. O.P. Malaviya.

My thanks are due to Mr. R.N. Srivastava for his excellent typing and Mr. Vishwanath Singh for his help.

Part of the financial assistance received for the project from Council of Scientific and Industrial Research is gratefully acknowledged.

HALLIYAL ARVIND

CONTENTS

LIST OF FIGURES

FIGURE

SYNOPSIS

The electrical, switching and optical properties of glasses belonging to the system SiO_2 - B_2O_3 - Na_2O - As_2O_3 were studied.

Bulk conductivity of these glasses, and surface conductivity of virgin glasses, $Na^+ \rightleftharpoons Ag^+$ ion-exchanged and reduced specimens and simply reduced specimens were studied as a function of temperature.

The d.c. conductivity in bulk glasses is believed to arise due to the migration of Na ions. Surface conductivities depend very much on the nature of the surface and the ambient atmosphere. Ionic conduction, electronic conduction and proton conduction are suspected to be effective in determining the surface conductivity of these glasses at different temperature ranges. The surface resistivities of glasses for which reduction treatment or ion-exchange and reduction treatment was given follow different kind of variation with temperature than for virgin glasses. This difference is attributed to the surface treatment given to the glasses resulting in different conduction mechanisms.

The ion-exchanged and reduced glass with 5 mole % of Na_2O has shown threshold type of switching.

CHAPTER 1

INTRODUCTION

Many possible applications have led to great interest and activity in studying amorphous semiconductors, in which conduction processes are mainly electronic in nature. Amorphous materials in general exhibit a lack of long range periodicity. Among the many potential applications of amorphous semiconductors, their property of electrical switching holds a big promise. The electrical and optical properties of amorphous semiconductors can also be looked to for many applications. The applications[1-3] of amorphous semiconductors include switching and memory devices, photoconductors, light modulators, optical and infrared detectors, continuous dynode electron multipliers, phase contrast holograms, high energy particle detectors etc., not all realised. The advantages of producing amorphous semiconductors by means of thin film processes makes the fabrication of these devices comparatively easier.

1.1 Classification

Structural differences in amorphous semiconductors arise due to the difference in preparational techniques[4]

and chemical compositions. Considering this, amorphous semiconductors can be classified into 3 groups[5]

(1) Elemental:- Of these only S and Se can be obtained in amorphous form by slow cooling of their melts. Because of their chain or ring structure, the short range order extends over rather long distances, depending on temperature and thermal history of the material.

(2) Covalently bonded alloy glasses:- These alloys, e.g., those which contain group IV, V and VI elements possess compositional disorder in addition to translational disorder. Because of this all atoms locally satisfy their valence bond requirements. These are the simplest amorphous semiconductors.

(3) Ionic or tightly bound materials:- This category includes materials like SiO, Al_2O_3 and Ta_2O_5. These materials have band gaps larger than 2 eV. They have positional disorder and may contain impurities as an additional disorder. Alternatively, as a result of deviations from stoichiometry they may contain atoms in different valence states. These usually act as donors or acceptors and form a narrow band of states within the gap of the host material.

The common crystalline semiconductors Ge, Si etc. can be obtained in amorphous form by deposition of thin films from the vapour. One group of glasses has been studied intensly because of their potential applications. These are chalcogenide glasses[6], those containing the group VI (chalcogenide) elements S, Se, Te alone or in combination with group V elements P, As, Sb and Bi (e.g., As_2S_3, As_2Te_3, Si-Ge-As-Te etc.). Many oxide glasses with transition metal ions such as vanadium andiron show semiconducting behaviour. Alkali borosilicate glasses containing Bi_2O_3[7] show semiconducting and switching properties.

Two important aspects of crystalline semiconductors are missing in amorphous semiconductors[4]. The first is the probability of changing by doping the conductivity of crystalline semiconductors. The second is the possibility of forming p-n junctions by choosing different doping elements. This is because, in a crystalline semiconductor a donor or acceptor doping element acts as such because it is forced to take the place of a crystalline host atom and hence has either an excess or a deficiency of a valence electron. On the other hand in an amorphous semiconductor the local order is not the same everywhere, as a result of which, each atom can satisfy its valence requirements and hence does not act as a conventional donor or acceptor as

in crystalline semiconductors. Amorphous semiconductors behave similar to intrinsic semiconductors.

1.2 Ionic Conduction in Glasses

In most oxide glasses the electrical conductivity results from ionic motion. In oxide glasses the basic ingredients are a network former (e.g., SiO_2), network modifier (e.g., Na_2O) and an intermediate (e.g., Al_2O_3). A chemical reaction takes place during fusion, so that strong Si-O-Si bonds are broken and the bridging oxygens are converted to nonbridging oxygens. The alkali ions are electrostatically attached to the nonbridging oxygen ions and they are the principal carriers in ionic conduction. To calculate ionic conductivity in oxide glasses[8], the appropriate structural knowledge viz., the number of bridging and nonbridging oxygens surrounding the alkali ion, the distribution of alkali ions, the structure of silicon-oxygen network etc. must be known.

The mobility of divalent ions and other higher valence ions is low relative to alkali ions. In $BaO-SiO_2$ and $CaO-SiO_2$ glasses the ionic conductivity is due to the divalent ions[9] Ba^{2+} and Ca^{2+} respectively. In Cabal ($CaO-B_2O_3-Al_2O_3$) glasses the conductivity may be due to the transport of oxygen ions[10]. It seems that the

the conductivity of lead silicate[11], calcium silicate[12] and barium aluminum borate[13] glasses is due to the mobility of hydrogen ions.

Two methods have been used to measure electrical conductivity of solid ionic conductors; one technique uses direct current and the other uses alternating current. In a d.c. measurement a space charge is often set-up in the glass because of partial blocking of the ionic current by the electrodes; then the current decreases rapidly with time, and its value must be extrapolated to zero time if an accurate value of conductivity is desired. To avoid these electrode problems an alternating current is usually used, of a frequency from 10^3 to 10^6 cycles/sec. Silicate glasses show dielectric losses at these frequencies, however, so care must be taken to make the measurements over a wide frequency range.

1.2.1 Relation between ionic conductivity and ionic diffusion

If the electrical current in a glass is carried by a single ionic species, the electrical conductivity of the glass is related to the diffusion coefficient of the ion by Nernst-Einstein relation

$$\sigma = \frac{Z^2F^2Dc}{RT} \qquad (1.1)$$

where Z is the ionic charge, F is the Faraday, D is the diffusion coefficient in cm^2/sec, R is the gas constant, c is the concentration of ions and T is the absolute temperature. The above equation will be useful in understanding the conductivity mechanisms in glasses.

1.2.2 The dependence of ionic conductivity on temperature

For most of the oxide glasses, over fairly wide temperature ranges, the electrical resistivity is generally described by the Rasch-Hinrichsen[14] relation

$$\log \rho = A + \frac{B}{T} \qquad (1.2)$$

where A and B are constants.

By considering the alkali ions to be in a potential well undergoing thermal vibrations, Stevels[15] derived the equation

$$\rho = \frac{6kT}{\nu ba^2 e^2 n} (\exp^{E/kT}) \qquad (1.3)$$

where ν is the vibrational frequency, b is the number of adjacent wells an ion can jump into, a is the average jump distance, n is the number of mobile ions per c.c. and E is the energy barrier. If the variation of E with temperature is small, equation (1.3) leads to equation (1.2) and a

plot of log ρ vs 1/T gives a straight line, the slope of which gives the activation energy for conduction. Improvements over Stevels analysis have been made by Mazurin[16] and Owen[17].

The activation energies for electrical conduction decrease with increasing concentration of alkali ions. Stevels[15] reasoned that as more alkali ions are added to the glass, fewer and fewer bridging oxygen ions remain. The network coherence decreases, making it easy for the ions to move.

The addition of an oxide of a higher valent metal ion to an alkali silicate glass leads to a decrease in the ionic mobility of the alkali ion[17]. The decrease is related to the ionic size of the added ion for divalent ions. The largest change was found for Ba ions with a decreasing effect for Pb, Sr and Ca ions.

1.2.3 Mixed-alkali effect

When a second alkali oxide is added to an alkali silicate glass (e.g., replacement of Na ions by Li or K ions) the conductivities decrease sharply[18]. Activation energy also shows similar anamolous behaviour. Since the alkali ions are considered to be the sole current carriers, some very drastic effects must take place when one alkali

ion is replaced by another alkali ion. The simple concept of a random silicon-oxygen network in which the alkali ions are free to move about is not acceptable in the light of such results. Measurements of diffusion coefficients in such glasses show that the mobility of each ion is decreased by the addition of the other[19]. The decrease in conductivity results from these reductions in mobility, but the reasons for the mobility reductions are not clear.

1.3 Electronic Conduction

The electrical conductivity of many amorphous semiconductors including chalcogenide glasses are observed to vary with temperature as[20]

$$\sigma = \sigma_o \exp(-E/kT) \qquad (1.4)$$

where E is the activation energy for conduction process and σ_o is a constant. The electrical conductivity of many chalcogenide glasses[20] resembles that of intrinsic semiconductors even down to quite low temperature, as shown in figure 1. The intrinsic conductivities of Ge and InSb films are also shown in the figure. The electrical resistivity of non-crystalline solids ranges from 10^{-3} ohm-cm to greater than 10^{15} ohm-cm at room temperature and the mechanism of conduction throughout this range can be primarily electronic.

The electronic conduction in oxide glasses is essentially due to the presence of transition metal ions of different valencies in the glass. For example, in a glass containing Fe^{2+} and Fe^{3+}, an electron can move from Fe^{2+} to Fe^{3+}, a mechanism analogous to that in crystalline transition metal oxides. In iron phosphate glasses the conductivity is maximum when the ratio $Fe^{3+}/Fe(total)$ is about 0.4 to 0.6[21]. Whereas in crystalline semiconductors even very small concentration of impurities cause large changes in conductivity and in the type of charge carriers (electrons or holes), impurity concentrations upto a few percent usually cause relatively minor changes in the conductivity of amorphous semiconductors.

Other important parameters for characterisation of amorphous semiconductors are the a.c. conductivity, thermoelectric power, optical absorption and Hall coefficient.

Since Denton et al.[22] showed that V_2O_5 - P_2O_5 glasses exhibit bulk electronic conduction in 1954, the interest in electronic conduction of glassy materials has increased. Various other oxide glasses have been studied by various workers after that. A range of vanadate-phosphate, vanadate-germanate have been studied by Mackenzie[23,24] and Ioffe and Regel[25]. Other glasses studied include iron-oxide based glasses[21], As-Te-Ge

and As-Te-Se systems[26], Si-As-Te glasses[27], $4As_2Te_3 . As_2Se_3$[28], $As_2Se_2 . Tl_2Se$[29] etc. A survey of the earlier work done is given by Bandyopadhyay[30] and Nagesh[31]. Amorphous Ge, InSb, Te, Se and As_2Se_3 have been studied in detail by Stuke[32] in comparison with their crystalline counterparts.

1.3.1 Theories of amorphous semiconduction

In crystals, there are certain features of the electronic structure and of the energy bands, in particular, which are universal for all crystals, being consequences only of periodicity of the crystals. Although no definite theory yet exists for disordered systems, we can anticipate that the electronic structures of disordered systems will also show universal features.

For perfect crystals, if we assume the electron wave functions to be given by Bloch-Floquet theorem, we get corresponding one electron energies which fall into continuous bands of allowed levels separated by forbidden gaps. The energy $E_n(k)$ will be a continuous function of k within each band, except at band edges which correspond to the absolute minimum or maximum of E as a function of k for each band. The density of states n(E) has square root singularities at these edges as shown in fig. 2(a). Other critical

points, saddle points also occur within the band, also giving rise to square root singularities in n(E).

1.3.2 Density of states

Density of states n(E) as a function of energy E for (a) a perfect crystal, (b) a crystal containing only one localized imperfection and (c) a crystal containing a low concentration of localized imperfection are shown in fig. 2.[33] In all the 3 cases there are continuous bands of energy levels separated by gaps with square root singularities at these band edges. The square root singularities associated with the saddle points within the band in (a) and (b) are eliminated by scattering in (c). If the potential change ΔV introduced by the imperfection is strong enough in (b), localized levels split off from the bands (off the bottom for attractive ΔV or the top for repulsive) which broaden into bands in (c).

We come to similar results if we consider disorder introduced by phonons. Their consequence for electron transport in intrinsic semiconductors are readily apparent from the Kubo-Greenwood[34] formula for the electrical conductivity

$$\sigma = \sum_b \int dE n_b(E) e \mu_b(E) f_b(E) \qquad (1.5)$$

Here, b is a band index with v for valence and c for conduction, $n_b(E)$ is the density of states. $\mu_b(E)$ is the average mobility of charge carriers of energy E. $f_c(E)$ is the electron occupation probability in the conduction band and $f_v(E)$ is the hole occupation probability in the valence band. With a density of states as in the fig. 2(a), the integration over E gives

$$\sigma = \sigma_o \exp(-\frac{E}{kT}) \qquad (1.6)$$

as is observed for intrinsic semiconductors, the activation energy E being half the band gap $(E_c - E_v)$. This well defined activation energy is a consequence of the fact that the sharp band edges of the perfect crystal are not wiped out by the imperfections.

When the potential change associated with a localized imperfection is large enough, there can be localized states in the energy gap, one associated with each imperfection. Their degeneracy is lifted by overlap, however and we face the problem of impurity band, which is not yet completely solved.

1.3.3 Energy Bands in Amorphous Semiconductors

An essential feature of all the models proposed for the electronic structure of disordered materials is

the presence of tails of localized states. The concept of localized states is used extensively for the crystalline semiconductors in which impurity atoms and point defects give rise to localized levels or traps in the forbidden energy gap. But a continuous range of energies in which all electronic states are localized is not that familiar. The causes for the occurrence of localized states have been discussed by Mott[34].

A band model proposed by Mott[35] is shown in fig. 3(a). There is a valence band with a tail of localized states above E_v and a conduction band with a tail of localized states below E_c. Thus only a pseudogap exists between the valence and conduction bands.

This simplest model is probably not adequate for elemental and compound amorphous semiconductors. Though these materials are translationally disordered, the short range order is in general so well defined that structural defects can occur. These defects can be expected to have well defined energy levels associated with them. These would not be sharp as in a crystal, but varying somewhat, with local environment would give rise to peaks or monotonicity in the density of states as in the fig. 3(c).

For amorphous covalent alloys such as these based on the chalcogenides Se and Te, the above models are not

adequate. Such alloys contain atoms of varying valences in large concentrations. There is compositional disorder in addition to translational disorder enhanced by the requirement that valences are locally satisfied. The tails of the valence and conduction bands therefore overlap leading to a finite density of states at the Fermi energy $n(E_F)$ and a finite concentration of localized states near E_F. This model was proposed by Cohen, Fritzsche and Ovshinsky[36], (known as CFO model). Mott and Davis[37] have suggested a smaller degree of tailing and have proposed the existence of a 'defect band' perhaps arising from unsatisfied or dangling bonds near the gap centre (fig. 3(c)). A review of different models proposed has been done by Cohen[38].

All the models developed so far have continuous densities of states. It is therefore difficult to understand how σ can obey equation (1.6) over a wide range of temperatures, particularly so for alloys where the band tailing is pronounced. From the Kubo-Greenwood formula it is clear that some kind of an edge must occur in the integrand of equation (1.5) to obtain equation (1.6). For crystalline materials it is a band edge. For amorphous semiconductors, however it can only have to do with the critical energies E_v and E_c. There the states change their character from extended to localized. The transport mechanism must also

change from one characteristic of extended states such as propagation with occasional scattering to that characteristic of localized states, phonon assisted hopping at finite temperatures. Therefore to explain the validity of equation (1.6) for amorphous semiconductors, one needs only to suppose that the mobility changes by several orders of magnitude within an energy range of order kT near E_c and E_v. Such an energy dependence for μ is shown in fig. 3(b). This explains the dependence of σ on temperature according to equation (1.6). E_v and E_c are mobility edges. The drop there in μ is termed, the mobility shoulders. The energy range $E_g = (E_c - E_v)$ is called the mobility gap[38].

Thus in amorphous semiconductors, transport in delocalized electronic states for which the mean free path is of the same order as the interatomic spacing and transport by thermally activated hopping between localized states are the modes of conduction that occur. This is similar to the hopping or band-like conduction with short mean free path in heavily doped crystalline semiconductors.

Amorphous covalent alloys of group IV, V and VI elements have been described as low-mobility electronic intrinsic semiconductors with a temperature activated electrical conductivity. These alloys transmit infrared light upto an exponential absorption edge[39] from which

an energy gap E_g can be estimated. This E_g is usually smaller than 2 E, often by as much as 10-20%. Photoconductivity and recombination radiation measurements have been interpreted as giving evidence for the presence of localized states in the gap. If the nearest neighbour distance and co-ordination number remain unchanged from those found in the crystalline phase, then the density of electronic states remains essentially the same. The main experimental evidence for this is the optical absorption edge, which occurs at roughly the same photon energy in crystalline and amorphous phases of the material, indicating an energy gap of about the same magnitude. But when the energy gap in the crystal is determined to some extent by interactions of long range, than nearest neighbour separations, this is not true. Electrical measurements show a large density of states of about 10^{19}/eV cm^3 at the Fermi energy in the middle of the gap, whereas optical absorption measurements indicate a much smaller value such as 10^{16}/eV cm^3, except near the critical energies. Fritzsche has proposed a heterogeneous model[40] to account for these differences. A random phase model[41] of conduction in glassy semiconductors has been proposed by Hindly. A review of current theories is given by Hulls[42].

1.4 Switching in Amorphous Solids

The switching effect comprises a sudden change of electrical resistivity by several orders of magnitude when a sufficiently high electric field is applied to the material. Two types of switching characteristics are observed in amorphous solids.

(1) Threshold Switching: where above a certain voltage, threshold voltage, the material goes from high-resistance state to low-resistance state and when the current through it is reduced below a certain current called holding current, it comes back to its high-resistance state.

(2) Memory Switching: where the material retains its low resistance state even after the removal of the applied voltage.

Switching effects have been observed in thin films and a large number of amorphous semiconductors like, chalcogenide glasses[43] such as AlTlSe and $TiAs(Se, Te)_2$, in vanadate glasses[44], in sodium borosilicate glasses[44], in amorphous Si and Ge[45], in organic semiconductors[46], calcium borate glasses with iron[47] and a number of other semiconducting glasses. Interesting memory effects have been observed in crystalline stibnite Sb_2S_3[48], in transition metal glasses[49] and in As-Te-I glasses[50].

Many theories have been put forward to explain the switching mechanisms – thermal breakdown theory[51], electronic theory with charge accumulation[52], phase change mechanism[53,54], and many others. Switching has been described by Ovshinsky[50] and Owen[55].

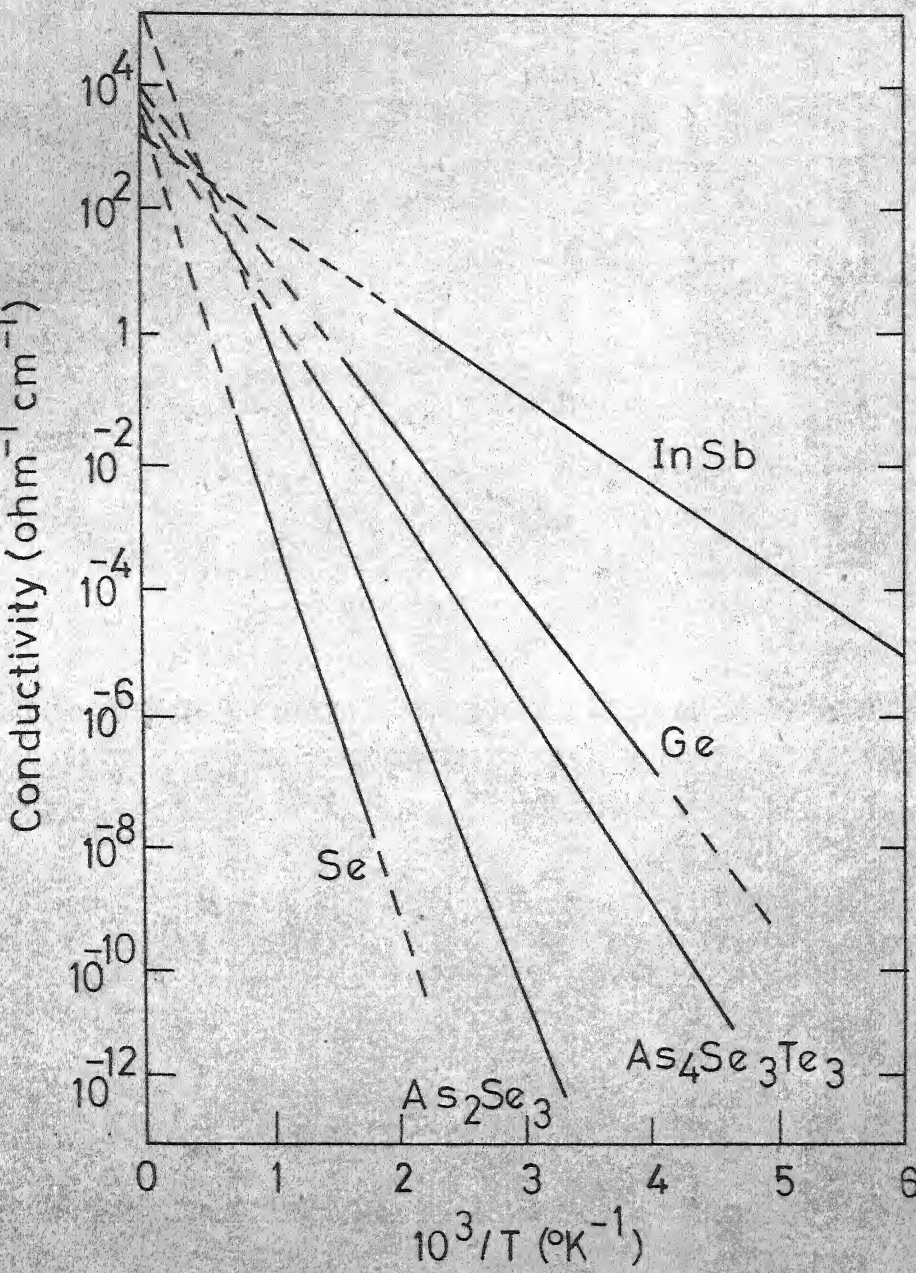

FIG. 1 TEMPERATURE VARIATION OF ELECTRICAL CONDUCTIVITY OF VARIOUS AMORPHOUS SEMICONDUCTORS (Ref. 20)

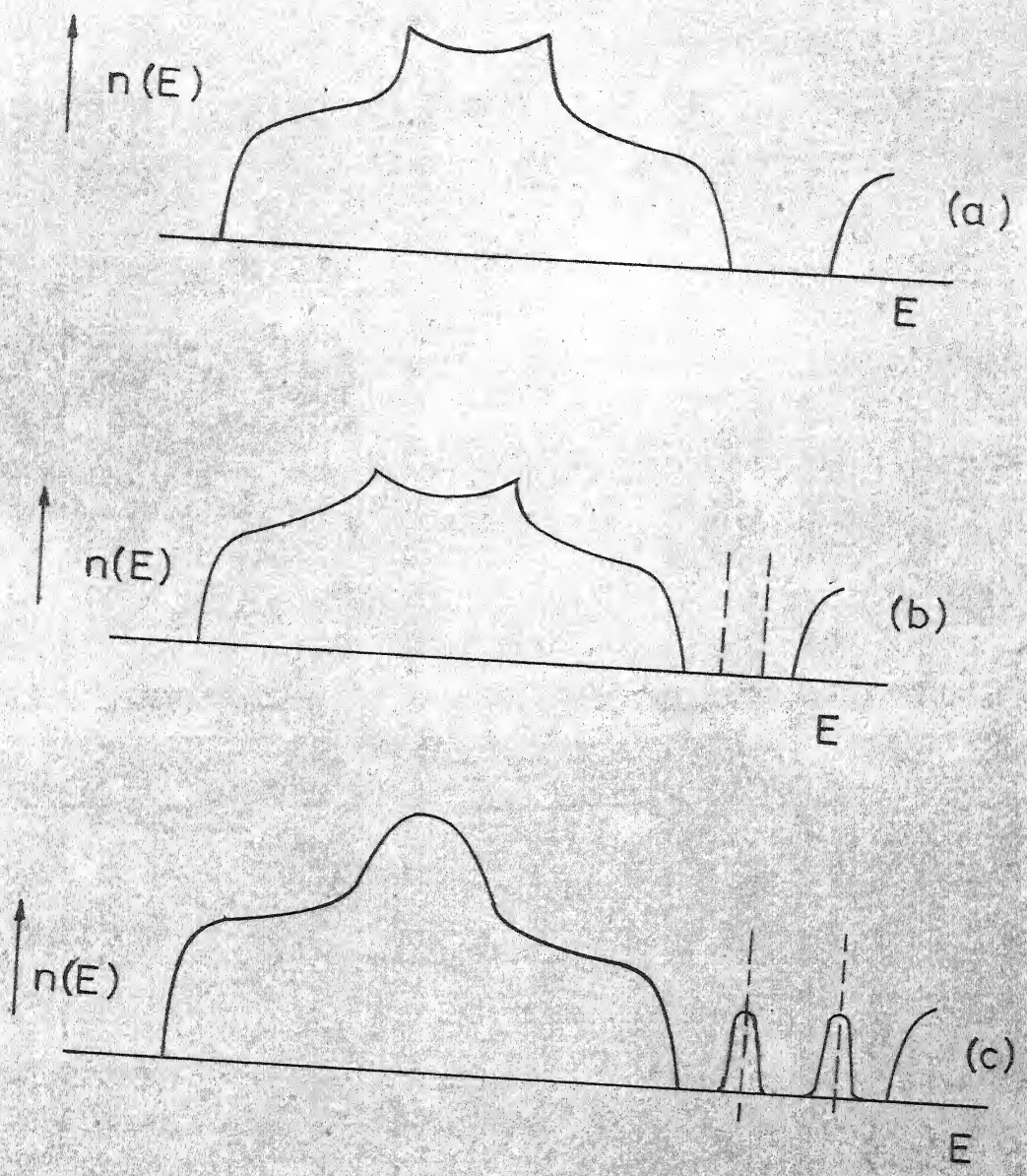

FIG 2 DENSITY OF STATES n(E) AS A FUNCTION OF E FOR (a) A PERFECT CRYSTAL (b) A CRYSTAL WITH ONE LOCALIZED IMPERFECTION (c) A CRYSTAL WITH LOW CONCENTRATION OF LOCALIZED IMPERFECTIONS.

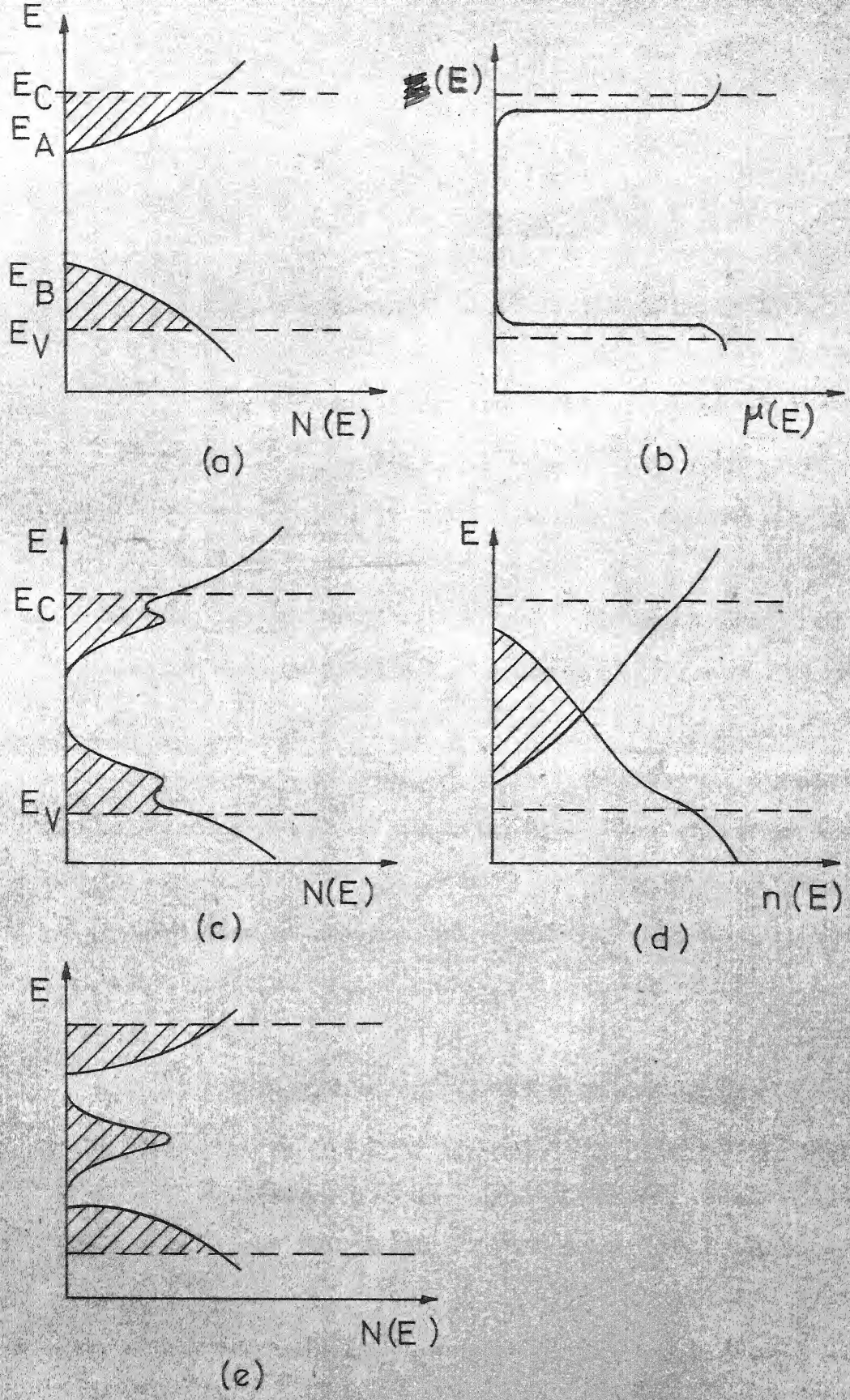

FIG. 3 DENSITY OF STATES AND MOBILITY AS FUNCTIONS OF ENERGY IN AMORPHOUS SEMICONDUCTORS FOR VARIOUS ENERGY BAND MODELS.

CHAPTER 2

SURFACE ELECTRICAL PROPERTIES OF GLASSES

Apart from their theoretical interest the electrical properties of glass surfaces are of great practical importance. Glass is widely used for making electrical insulators and the vacuum envelopes of thermionic and photo-electric devices. The surface electrical properties of glass will determine whether there is an accumulation or leakage of charges. If there is adsorption of moisture by glass, the surface electrical resistivity of glass will be markedly lower than the volume resistivity. The chemical durability is an essential requirement in good electrical glass since moisture film thickness and surface conductivity both are increased if there are soluble products of unstable composition.

The composition of the surface layers may differ from that of the bulk material, depending on the thermal and chemical treatment to which the glass has been subjected. This difference in composition arises due to several reasons[56].

(1) The contribution of the surface-free energy is different for the various constituents of glasses.

Hence to maintain minimum surface free energy, those constituents of the glass which lower the free energy will be concentrated in the surface layer.

(2) Certain constituents of glasses will be more volatile than others, and they will be lost from the surface during forming process.

(4) There may be selective solution or absorption at the surface in contact with liquids such as water.

In alkali silicate glasses, sodium ions lower the surface tension of the glasses and hence they tend to concentrate in the surface layer of the molten glass. On the other hand, alkali ions are very volatile. The actual composition of a glass surface, then will be a complex function of the time temperature history of the surface.

2.1 Absorption of Water by Glass Surfaces

Frazer[57] studied the absorption of water by fresh glass surfaces, by admitting water vapour on the specimen kept in a vacuum chamber. He observed that the thickness of the adsorbed layer (6 Å at 13 mm of Hg) increased rapidly above 13 mm pressure. Yager and Morgan[56] studied the adsorption of water with increasing humidity. They observed that the first additional monolayer is formed at a relative humidity of 50%, a rapid increase in thickness

of adsorbed layer taking place at greater humidities (at 97% relative humidity the water condensed is equivalent to 90 layers).

2.2 Surface Structure

The surface structure of oxide glasses depends on the reactions of dangling oxide bonds. In a silicate glass a surface leads to Si-O- and Si-bonds that are unsatisfied. These bonds react with atmospheric water to form SiOH groups. Therefore the surface of an oxide glass is normally composed of metal hydroxyl groups. The thickness and structural arrangement of the hydrated surface layer depend on the composition of the glass, its thermal history, humidity and surface treatment after melting and cooling. Hydroxyl group on glass surfaces can be examined by infrared spectroscopy[58]. In addition to physically adsorbed molecular water and isolated SiOH groups, hydrogen bonded SiOH groups and internal SiOH groups exist near a silica surface. The internal SiOH groups result from diffusion of water molecules into silica and their subsequent reaction with silica lattice to form two SiOH groups. This process becomes important above about 100°C[59]. At room temperature these internal silica groups do not form because of the low diffusion coefficient of water in bulk silica at this temperature. Schematic

diagrams of these hydroxyl groups are given in fig. 4(b).

The surfaces of silicate glasses with additional components will probably have the same types of groups as pure silica, modified by the following considerations. If other glass formers are in the glass network, they will also provide sites for hydroxyl groups. Thus AlOH, BOH and POH groups are likely. Monovalent cations R^+ in a silicate glass can exchange with water by the following reaction.

$$H_2O + SiOR^+ = SiOH + ROH \qquad (2.1)$$

This reaction gives rise to SiOH groups at the cation sites. Internal hydroxyl groups are less likely in multicomponent silicate glasses because the diffusion of water molecules in the more dense structure of these glasses is retarded. However a hydrated layer can form more easily because of the above exchange reaction. When other glass formers are also present, apart from silica, it is possible that one of them will appear preferentially at the surface giving a distribution of surface hydroxyl groups different from what would be expected from the bulk composition.

A large number of experimental techniques[60] have been used to examine the glass surfaces apart from IR spectroscopy[58], like electron microscopy[61], electron microprobe[61] and electron diffraction[62]. A discussion

of other properties of glass surfaces such as surface tension, adhesion and wetting, cleaning, hardness, corrosion properties, chemical durability, adsorption of gases can be found in Ref. (60) and in a recent article by Ernsberger[63].

2.3 Physical Adsorption and Reaction

The nature of physical or chemical adsorption on a glass surface is strongly dependant on the surface structure. The surface hydroxyl groups are the most important sites for adsorption and reaction. Water will be adsorbed on silica surface even at room temperature. Various other gases including oxygen react with the SiOH groups. Hydrogen and oxygen in glass determine its oxidation state and can reduce or oxidize ions in the glass.

Water reacts with the Si-O bond as follows.

$$-\overset{|}{\underset{|}{Si}}-O-\overset{|}{\underset{|}{Si}}- + H_2O = -\overset{|}{\underset{|}{Si}}-OH \qquad HO-\overset{|}{\underset{|}{Si}}- \qquad (2.2)$$

forming pairs of adjacent silanol groups. These groups and the hydroxyl ions so formed are very immobile, even at 1000°C. Thus water molecules must diffuse in and out of the silicate lattice to form or remove these hydroxyl groups. In alkali silicate glasses, the water solubility increases with the alkali content.

Hydrogen also reacts with silica to form hydroxyl groups. In pure silica it occurs at higher temperatures or pressures. The reaction is

$$-\overset{|}{\underset{|}{Si}}-O-\overset{|}{\underset{|}{Si}}-+H_2 \;=\; -\overset{|}{\underset{|}{SiOH}}+H-\overset{|}{\underset{|}{Si}}- \qquad (2.3)$$

In this case the rate of introduction or removal of OH groups is controlled by the diffusion of hydrogen molecules, which is much faster than the diffusion of the larger water molecules.

Hydrogen can reduce[64] ions in various oxide glasses to the atomic state, e.g., Au, Ag, Pb, Bi and Sb oxides. At lower temperatures these reactions are often limited to layers of the glass near its surface because of the slow diffusion of hydrogen in the glass at these temperatures. In addition, hydrogen can reduce the valence of an ion in glass without reducing it completely to the atomic state.

2.4 Formation of Gel Layer

Acid solutions tend to leach out metal oxides from glass surfaces leaving the more inert silica component behind and with chemically resistant glasses, (e.g.,

soda-lime-silicate) the silica outer layer forms a barrier to further attack. Some glasses may show a high rate of attack. With such glasses the silica may remain on the glass in a porous state in which case the silica layer is likely to be in the form of a gel which can be easily removed from the surface. Russian workers advanced the theory[66] that silica gel was formed on a glass surface during polishing and that this layer was continuously removed by the cutting action of the particles of the polishing medium which were embedded in the polisher. The water absorbed in the pores of a pure silica gel may play a major role in the electrical conduction process. Gel layer on the glass surface can also form due to ion-exchange and hydrolysis of Si-O-Si bonds.

2.5 Surface Conductivity

The surface resistivity of clean glass in dry air will be very high; 10^{14} ohm/square or higher. The systematic investigation of surface conductivity was first done by Fulda (1927) who tried to find a correlation between the surface conductivity and the bulk composition of the glass. He attributed the conductivity values obtained to an electrolyte film formed on the glass surface in wet atmosphere. Curtis (1915) investigated the humidity dependence and established that surface conductivity

increased with the humidity when the humidity is higher. The temperature dependence combined with humidity variation was investigated by Gutkin et al. (1952). The variation of surface conductivity with humidity is shown in fig. 4(a) for some of the glasses[65]. The dotted line at the top indicates the order of additional insulation (w.r.t. surface σ) which can be achieved by means of special surface treatments.

2.5.1 Surface Layers and Surface Characterization

Boksay[67] et al. did a series of experiments to find the relation between surface conductivity, the ion distribution profile and the leaching time. They concluded that the mobility of ions is considerably higher in the gel layer than in the interior of the glass. An estimation shows that the volume conductivity of the surface layer with an unchanged network exceeds that for the bulk glass by about 8 orders of magnitude. Tomozawa et al.[68] have found that low frequency dielectric measurements can be used to characterize glass surface structure.

A method has been developed by Wikby[69] to locate the high resistance layer by step wise dissolution and analysis of the surface layer combined with measurements of the resistance. Boksay et al.[67] studied the dependence of surface conductivity of $22Na_2O5.5Al_2O_372.5SiO_2$ (mole%)

glass on humidity. They observed that σ remains constant upto 60% relative humidity and begins to increase appreciably at about 80% relative humidity. Since the humidity has no influence on the electrical conduction when the vapour concentration is not too high, it appears plausible to assume that an interior layer insulated from the atmosphere is responsible for the constant surface conductivity. They also observed that no appreciable amount of gel layer formation takes place on this glass surface but only a slight loosening of the structure of the glass. The activation energy of σ vs. 1/T plot was 0.30 eV which is less than half of the activation energy for sodium ion movement in the bulk glass. Hence in the stratum with an almost unchanged structure, the current is carried by species other than sodium ions.

The interior stratum evidently contributes to the surface conductivity in the whole humidity range. Thus the values in the humidity dependent region comprise of two terms. The additional term which depends on humidity is due to a layer exposed directly to the influence of the atmosphere. This coating if any, may be a very thin gel layer or a dilute electrolyte or both. Its contribution to the conductance decreases with loss in water and at a certain humidity value, the interior stratum becomes the

only conduction limiting factor. Between these conducting strata a barrier layer is located, which seems to be responsible for keeping water molecules away from the interior stratum. Since the conducting strata represent almost negligible fractions in the cross section of the sample, but are predominant in the total conductance it is obvious that their volume conductivities exceed that for the bulk by several orders of magnitude.

2.5.2 Conduction by Protons

The surface layer displays high conductance in a number of experiments and high resistance in others. When we measure the conductance using a current parallel to the surface, parts of the layer act as parallel conductors in a circuit. In the resulting value, the contribution of the stratum with the highest conductance predominates while that for the resultant stratum is negligible. On the other hand when the field strength is perpendicular to the glass surface, the resistance of the layers are additive and so the two highly conductive layers have no influence, resulting in a high surface resistance. Thus the nature of the surface layer is complex within which both a high maximum and a deep minimum in σ can be observed.

The occurrence of the maximum located in the interior can be explained as follows. The increased σ with low activation energy is due to the presence of penetrating protons as charge carriers. The protons are thought to be present in hydroxyl groups bound to Si atoms and when migrating to jump from a hydroxyl group to a nearby terminal oxygen atom. Thus the conductivity increases with the concentration of both the hydroxyl groups and the terminal oxygen atoms. Since the sum of these concentrations is constant, there is an optimum ratio of concentration at which the conductivity is greatest.

Any deviation from the optimum ratio lowers the conductivity. As the hydroxyl concentration decreases with increasing depth, and beyond the conductivity maximum finally tends to zero, the role of protons is taken over gradually by the less mobile sodium ions. This change leads to a reduced conductivity characteristic of the bulk. On the other side of the conductivity maximum interface, both the hydroxyl group concentration and the sodium ion concentration are at lower levels. Since the former is needed for the proton conduction and the latter is necessary for the sodium ion conduction, the overall σ decreases rapidly with decreasing depth. This may be however a reasonable factor in the formation of the high resistance stratum.

From the above discussion it follows that the underlying layers of glass influence the electrical conduction to a great extent. Unfortunately little attention has been paid so far to the development and state of the surface layer, the condition of which may be rather uncertain, especially at the commencement of the interaction between glass and water. To avoid uncertainty and to obtain more relevant data, a controlled leaching procedure for glass samples prior to the electrical measurements is advisable.

2.6 Conduction in Reduced Surface Layers

A number of methods have been developed for obtaining highly conductive layers on glasses. These include metallizing procedures wherein Pt, Au or Cu salts are heated to reduction on the glass, vaporization of metals such as Al onto the surface, firing silver oxide or metal powder on with the aid of auxiliary fluxes, etc. With these methods, control of the conductivity of the applied layer is not feasible, as the insulating nature of the oxide surface will predominate upto the point where sufficient metal has been applied to give the surface the conductivity of the metal itself. This means that the surface will be insulating as long as the metallic particles are not in contact, and when they are, conduction will be in the metal layer and

will depend solely upon its properties. Green and Blodgett[64,70] developed techniques for inducing conductivity in a thin layer within the glass surface by treating the glasses with hydrogen. The oxides of Pb, Bi and Sb if present in glass are readily reduced[71] by hydrogen. The samples became black after treating with hydrogen at high temperature. In all cases it was found that ground surfaces develop lower resistance after hydrogen treatment than polished surfaces do.

Blodgett[70] who studied in detail a $PbO-SiO_2-BaO$ glass found that mere blackening of the surface after hydrogen treatment does not always impart conductivity to the surface layer. The amount of conductivity which is developed in a glass at any temperature T in hydrogen depends on the value of T and the entire hydrogen treatment given prior to the time at T (i.e., the time spent at each lower temperature through which the sample passed while being brought upto T). In order to separate these factors Blodgett did 2 sets of experiments; treatment in hydrogen at constant temperature and treatment in hydrogen at two or more temperatures.

Curve A in fig. 5 shows how the end values of resistances vary with the temperature of the hydrogen treatment, after 7 hours of treatment at constant temperatures.

The curve passes through a minimum at about 395°C. After passing through the minimum the curve returns to the high value for untreated glass at temperatures above 520°C.

Curve B is a plot of the resistances obtained in which the sample was heated from 320°C to T in hydrogen by slow heating. The resistance values on curve B lie lower than the minimum of curve A although the length of time required for the B treatment were only a small fraction of the 7 hours chosen for the A curve. Thus to develop conductivity in glass the initial stages of the hydrogen treatment must be carried out at low temperature (favourable temperature range is 300-380°C). High temperature treatment alone produces no conductivity. The reason for this is explained in a later section.

2.6.1 Effect of Composition on Conductivity

With PbO glasses the conductivity developed was found to increase with the PbO content. The surface resistivity of reduced glasses containing only PbO and SiO_2 could be represented by the formula

$$\log \rho_s = 0.097C + 12.84 \qquad (2.4)$$

where C was the mole % of PbO. Substitution of 8.3 mole % of B_2O_3 for SiO_2 did not affect the above relation, but

34.8 mole % B_2O_3 greatly increased ρ_s. Replacement of SiO_2 by Bi_2O_3 reduced the resistance. $PbO-SiO_2-Sb_2O_3$ glasses showed low values of ρ_s when Sb_2O_3 content in the glass was increased.

2.6.2 Theory of Conduction in Reduced Glasses

Green and Blodgett[64] advance the following theory for electrical conduction in the reduced glasses. The oxides of Pb, Bi and Sb originally held in the random oriented glass network are reduced to the free metal atoms, and the hydrogen is removed as water. As the PbO content decreases, higher temperature is needed to produce the maximum number of Pb atoms which will contribute to conduction. In glasses with lower percentage of PbO the Pb ions are held more tightly and consequently higher temperatures are needed to produce sufficient reduction enabling conduction in these as compared to the higher percentage of PbO glasses, wherein these ions are held more weakly. Hence in lead silicate glasses of high PbO content, the role of Pb ions is such as to weaken the continuous SiO_4 networks, i.e., PbO acts as a network modifier.

The two factors which determine the resistivities of the reduced glasses are (1) the distance between the particles and (2) influence of the surrounding oxide lattice.

(1) Distance between the particles:- This parameter is determined by the temperature of reduction and also by the composition of the glass. The first factor can be clarified by considering the variations in resistivity of a given composition due to different temperatures at which reduction is carried out (fig. 6). For temperatures below T_1, the forces binding the reducible ions in the networks are strong and not all are reduced. The average distance between conducting particles is hence greater than in the range $(T_1 - T_2)$ where a greater percent of the atoms have been formed. Consequently the resistivities will be lower if reduction is carried out below T_1. However, above T_2, even though more ions may be reduced, the resulting atoms tend to aggregate into configurations more stable than the atomic dispersions. This process depletes certain zones of conducting particles and as the gaps between groups increase, resistivity increases. It can be assumed that the structures will show their maximum conductivities when a maximum number of ions have been reduced and when the coalescence of these atoms into groups is at a minimum.

(2) Influence of surrounding oxide lattices:- On the other hand, the conduction mechanism also depends on the nature of the continuous network as well as on the presence of other nonreducible ions which may be present. Due to

their positive ionic charges and their location in the interstices of the networks, the alkali ions in these electronic conductors interfere with the movement of the electrons in their jump from atom to atom resulting in an increased electronic resistivity of the glasses. The alkali ions may act as local electron traps which increase with the increasing alkali content. The result is that the free paths of the electrons are shortened and this appears at higher resistivities.

Partial substitution of B_2O_3 for SiO_2 will have no pronounced effect on the conduction process. This is because the B-O configurations directly replace SiO_4 structures and consequently, bond types are not changed. The substitution of a Bi or Sb atom for a Pb atom reduces the resistivity obtainable. This may be due to the fact that the Bi or Sb ions being part of the continuous networks, when reduced to atoms, produce new gaps or voids in the structures through which electrons may jump. The chemical reduction of Pb ions on the other hand, would only eliminate the ionic forces with which these were originally held.

2.6.3 Effect of Heat Treatment

The higher resistivities can be explained by the tendency for the reduced atoms to aggregate if the glass is reduced over long periods at temperatures higher than a given range. On the other hand, the PbO glasses show decrease in resistivity, if after the initial reduction treatment, they are reheated to higher.temperatures in hydrogen for short periods. This effect is due to the further reduction of ions which withstand the initial treatment. Since the reheating times are of short duration, further aggregation of the atoms is restricted.

It is observed that glasses with mixture of two or more oxides are reduced readily and when reduced are more stable as regards aggregation of the resulting atoms, than those with a single oxide only.

2.7 Ion-Exchanged and Reduced Glasses

When a glass is immersed in a molten salt bath, ions move in and out of the glass due to an ion-exchange mechanism occurring at the glass-salt interface. If the exchange is carried out at a temperature above the glass transition temperature T_g, the network of glass expands or contracts to accommodate the size difference of the ions.

When the exchange temperature is lower than T_g, such an adjustment of the network is not fully possible[72]. The result is the appearance of stresses in the glass. If the salt bath ions are larger than the host ions in the glass, the strength of the glass increases due to a resultant compression layer in the surface of the glass.

Chakravorty and Murthy[7,73-75] carried out switching and microstructural studies of glasses belonging to the system $Na_2O - B_2O_3 - SiO_2 - Bi_2O_3$ and $Na_2O - B_2O_3 - SiO_2 - Sb_2O_3$, after ion-exchanging them with Ag^+ ($Na^+ \rightleftharpoons Ag^+$) and reducing by hydrogen. The ion-exchange was carried out by immersing specimens in a molten bath of $AgNO_3$ and keeping at 330°C for 6 hours. Reduction treatments were carried out in the temperature range 250-400°C over periods extending to 16 hours.

The surface resistances of all virgin specimens as well as ion-exchanged ones were higher than 10^{14} ohm/square. The ion-exchanged and reduced specimens developed high surface conductance, of the order of a few ohms. The conductance induced in the glass surfaces after the ion-exchange and reduction treatments increased with the amount of Na_2O present in the virgin specimen.

The microstructural studies[73] indicated that the virgin surface of Bi_2O_3 glass consists of a dispersion

of spherical particles with diameters of 50-250 Å, embedded in a glassy matrix. These particles were identified to be metallic Bi. After ion-exchange and reduction larger particles with a maximum diameter of about 2000 Å were found to appear in the glass matrix which were identified to be metallic Ag.

The microstructural characteristics of Sb_2O_3 containing glasses showed that the droplet phase in the virgin specimen was rich in Sb phase which however was not in metallic state. The ion-exchanged and reduced specimens had a structure consisting of fine droplets of diameter 50-100 Å.

2.7.1 Conduction in Ion-Exchanged and Reduced Glasses

The conduction in Bi_2O_3 containing silicate glasses can be explained by the presence of droplets of Bi in the ion-exchanged and reduced glasses. The electronic conduction may be due to the hopping of the electrons between the conducting islands of Bi. The activation energy for electron hopping in such a situation has been shown by Neugebauer and Webb[76] to be given by $\phi = (e^2/kr)$ where ϕ is the activation energy for electronic conduction, e is the electronic charge, k is the dielectric constant

of the glassy matrix and r is the diameter of the conducting island. Assuming k = 6 and a distribution of activation energies in the range .02 to 0.3 eV (determined by variation of σ with T), we get a range of r values extending from 10 Å to 150 Å. This is consistent with the microstructural features of these glasses.

Memory switching was observed in the surface layers of glasses subjected to ion-exchange and reduction treatments as well as in the bulk specimens of the glasses belonging to the system $SiO_2 - B_2O_3 - Bi_2O_3 - Na_2O$[75] and $SiO_2 - B_2O_3 - Sb_2O_3 - Na_2O$[77]. Also, glasses containing Sb_2O_3 show interesting electrical properties after ion-exchange and reduction of the surface or just reduction of the surface by hydrogen.

Since arsenic also belongs to the V group of the periodic table, it was thought it would be interesting to study the incorporation of As_2O_3 in the system $SiO_2 - B_2O_3 - Na_2O$ and to see whether these glasses also exhibit similar behaviour. The present investigation concerns with the bulk and surface electrical properties of alkali borosilicate glasses containing As_2O_3.

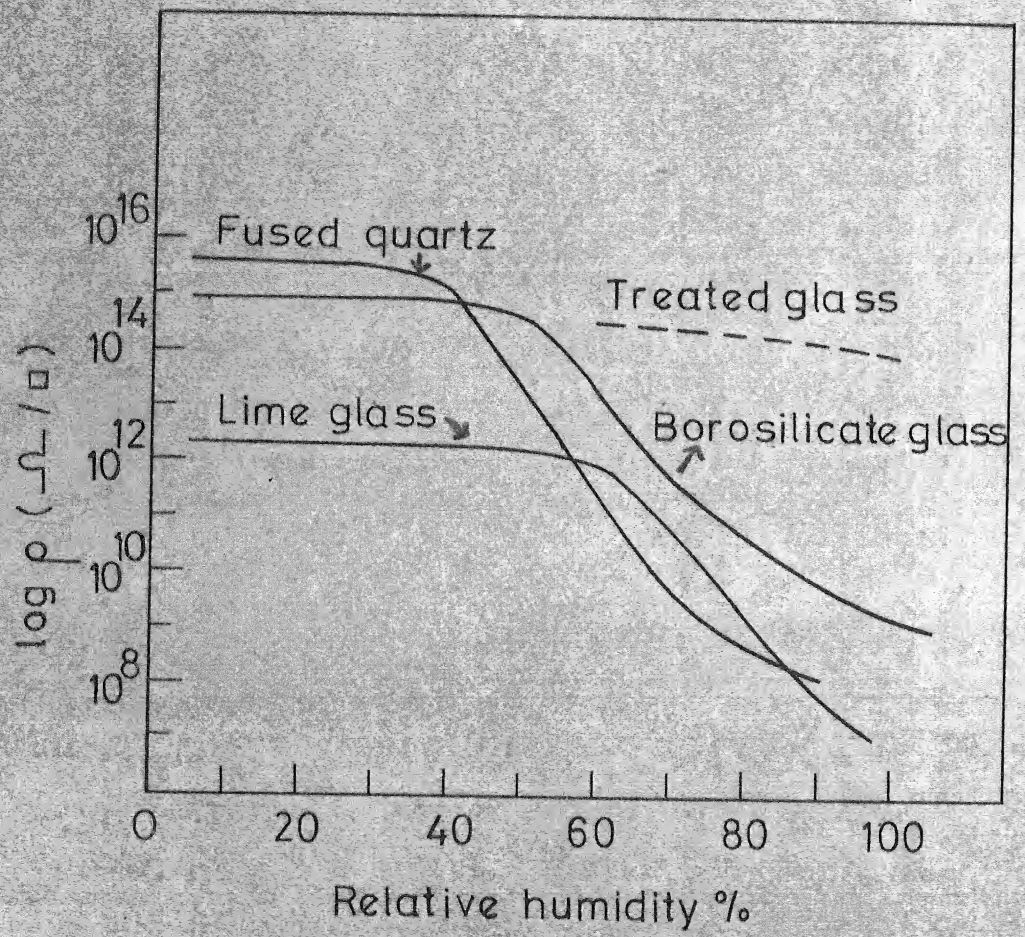

FIG. 4(a) SURFACE RESISTIVITY AS A FUNCTION OF RELATIVE HUMIDITY AT 20°C.

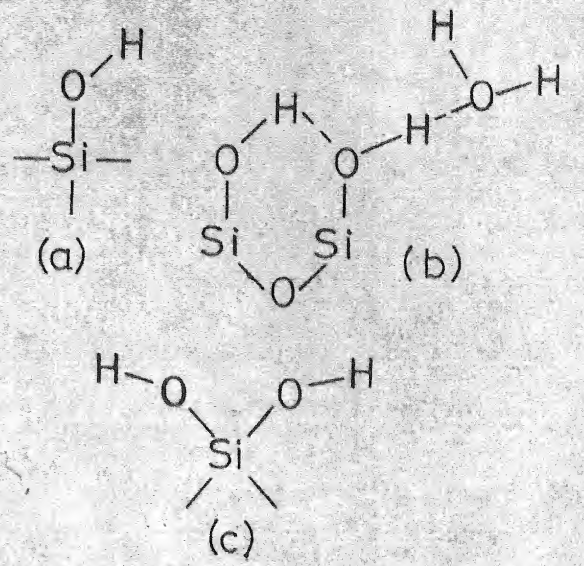

FIG. 4(b) SCHEMATIC DIAGRAMS OF HYDROXYL GROUPS ON A SILICA SURFACE.

(a) ISOLATED GROUP

(b) HYDROGEN BONDED GROUPS WITH AN ADSORBED WATER MOLECULE

(c) TWO HYDROXYLS ON ONE SILICON ATOM.

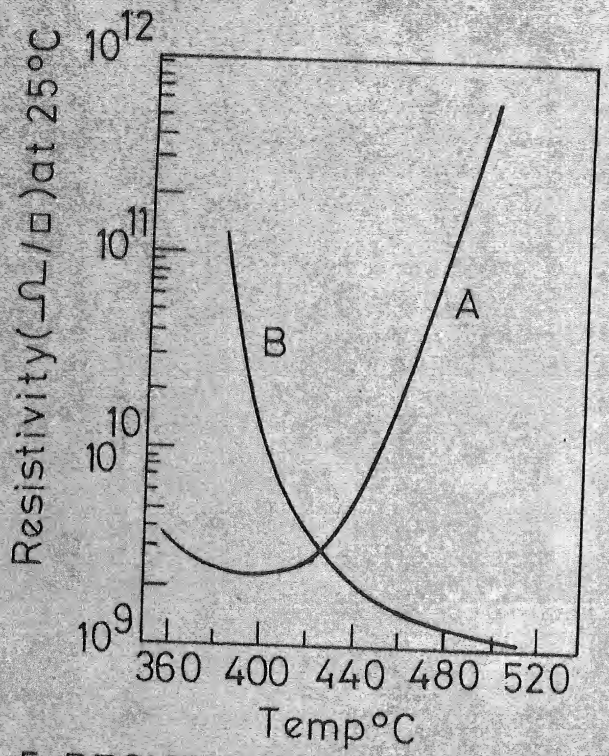

FIG.5 RESISTIVITY (A) AFTER 7 Hrs. REDUCTION AT CONSTANT TEMPERATURE T AND (B) AFTER SLOW HEATING FROM 320 °C TO T.

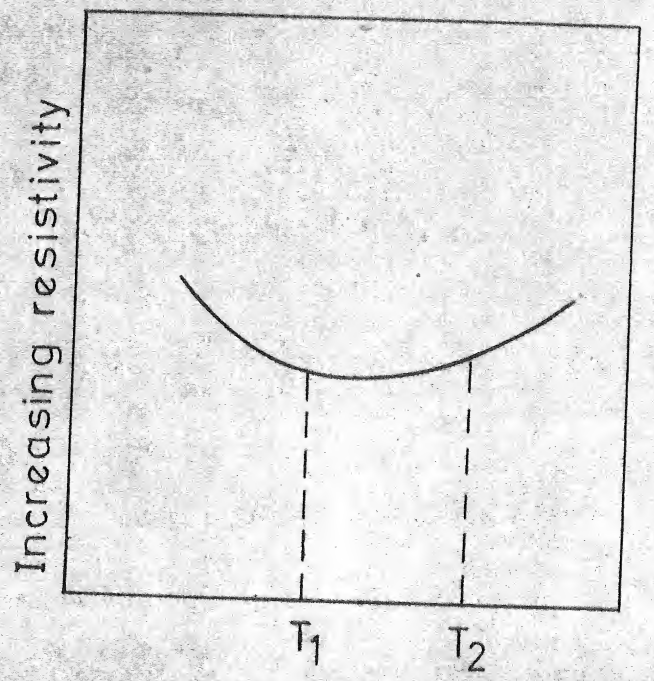

FIG.6 VARIATION OF RESISTIVITY OF REDUCED GLASS WITH TEMPERATURE OF REDUCTION TREATMENT (Schematic)

CHAPTER 3

OBJECTIVES OF INVESTIGATION

It has been observed earlier that sodium borosilicate glasses containing Bi_2O_3 [74] or Sb_2O_3 [77] show memory type of switching after ($Na^+ \rightleftarrows Ag^+$) ion exchange and reduction treatment. However no work has been reported on the effect of introducing As_2O_3 into $Na_2O - B_2O_3 - SiO_2$ glass matrix. The present investigation was undertaken to study the basic mechanism of conduction in the glass system $Na_2O - B_2O_3 - SiO_2 - As_2O_3$ and to make an assessment of the influence of ionic and electronic transport on the overall conductivity characteristics of these glasses.

Also, it was observed that the variation of surface conductivity with temperature of Sb_2O_3 containing glasses upon surface modification by ion-exchange and reduction or simply upon reduction is very peculiar. Surface resistivity measurements of As_2O_3 containing glasses were undertaken to find out whether similar behaviour is observed for these glasses.

The objectives of the present investigation were to study the following:

(1) Variation of bulk resistivity of glasses with temperature

(2) Variation of surface resistivity of virgin glasses with temperature

(3) Variation of surface resistivity of reduced glasses with temperature

(4) Variation of surface resistivity of ion-exchanged and reduced glasses with temperature

(5) Switching effects in these glasses

(6) Optical absorption properties of these glasses.

CHAPTER 4

EXPERIMENTAL DETAILS

4.1 Preparation of Glass

Glasses belonging to the system SiO_2 - B_2O_3 - Na_2O - As_2O_3 were prepared. The compositions are shown in table 1. Starting materials for B_2O_3 and Na_2O were H_3BO_3 and Na_2CO_3 respectively. Reagent grade chemicals were used. Calculated amount of all the components were mixed thoroughly using acetone. The dry mixture was transferred to an alumina crucible and heated in an electric furnace fitted with globar rods, in which a maximum temperature of 1400°C could be reached. Except glass no. 1 all the glasses could be melted in the temperature range 1250-1400°C. The glasses were melted for one hour to ensure homogeneity. Molten glasses were very viscous even at the highest temperature. Glass plates were cast from the molten glass free from air bubbles by pouring glass melts into alumina molds. The cast glasses were transferred quickly to a furnace at 450°C for annealing (the glasses were furnace cooled). Glass no. 1 had a higher m.p. (about 1450°C). It was melted in a gas fired furnace.

Some attempts were made to incorporate As metal into SiO_2 - B_2O_3 - Na_2O base glass. The powdered base glass was mixed with calculated quantity of As metal (99% pure) and the mixture was taken in a double walled quartz tube which was sealed after evacuation. The sealed tube was heated in a furnace at a temperature of about 900-1000°C, for 24 hours with intermittent shaking. When the quartz tube was taken out to room temperature, many times the As metal could be seen as separate coagulated mass. More often the Na_2O in the glass would attack quartz tube. Many attempts were made to incorporate As metal into base glass but such attempts were not successful.

4.2 Sample Preparation

4.2.1 For Bulk Conductivity Measurements

After annealing the plates, specimens of dimensions 2 cm x 1.5 cm x 1 cm were cut and the surfaces ground and polished using silicon carbide grit of different mesh sizes (120, 240, 400, 600 and 800) to thicknesses approximately 0.5 to 0.8 mm. The specimens were uniform in thickness to within $\pm$0.02 mm. Silver electrodes were applied on both sides by painting silver paste (supplied by NPL, India) and thin copper wires were stuck on to the silver electrodes.

After the silver paint dried, the specimens were sandwiched between two glass slides using araldite. For the electrode system, a guard ring arrangement was used.

4.2.2 For Surface Conductivity Measurements

For the preparation of ion-exchanged and reduced specimens, glass specimens having dimensions approximately 1.5 cm x 1 cm x 0.5 cm were cut and polished using 120 mesh size silicon carbide powder. Specimens were immersed in a molten bath of $AgNO_3$ contained in a pyrex crucible and the bath was heated to about 320°C in an electrically heated furnace for a period of 6 hours, for ($Na^+ \rightleftarrows Ag^+$) ion-exchange to occur. The furnace used was a horizontal one, having canthal wire turnings for electrical heating. After the diffusion run, the specimens were kept under running water for 24 hours to remove completely any $AgNO_3$ sticking to the glass surface.

After ion-exchange treatment of the sample, reduction treatment was carried out at about 340°C for 12 hours by passing hydrogen over the samples. The flow rate of hydrogen was 100 c.c./min. (the same horizontal furnace was used).

Virgin glasses (without any ion-exchange treatment), after polishing with 120 mesh size silicon carbide powder

were also reduced at 340°C by following the same procedure as described above.

To these samples, (ion-exchanged and reduced and simply reduced) parallel electrodes were attached on one side using silver paste and copper wire, with a gap of approximately 0.6 to 1 mm at the centre.

For measuring the surface conductivity of virgin samples, parallel electrodes were attached to the samples after polishing with 120 mesh size silicon carbide powder.

4.3 Resistivity Measurements

Bulk conductivity and virgin surface conductivity measurements were made in the temperature range 0 to 400°C. For ion-exchanged and reduced and simply reduced samples the measurements were made in the temperature range 0 to 340°C only. It was not possible to do measurements below 0°C, as the resistances were very high below 0°C. Since reduction treatments were carried out at 340°C, for ion-exchanged and reduced and simply reduced specimens, measurements were carried out upto 340°C only, to avoid any effects which may result from the heat treatment given to the sample by heating it beyond the temperature at which heat treatment was given to the sample during reduction of the sample by hydrogen.

4.3.1 High Temperature Measurements

For high temperature resistivity measurements, the sample was kept in a horizontal furnace provided with a temperature controller. The sample was surrounded by a metallic tube and the tube was earthed for better shielding. The schematic diagram of the circuit used is shown in fig. 7. ECIL Digital Picoammeter, (EA813A, which can measure currents in the range 10^{-3} to 10^{-11} amperes) was used to measure the current flowing in the circuit. At every temperature (at an interval of 10 to 20°C) the current vs. voltage across the specimen were noted over a decade of voltage and the sample resistance was calculated from the slopes of the linear V-I plots. Temperature was measured using a potentiometer and chrome-alumel thermocouple.

4.3.2 Low Temperature Measurements

The same circuit, as used for high temperature measurements was used. To attain steady temperatures below room temperature, a set up as shown in the fig. 8 was used. Liquid nitrogen was taken in a 5 litre dewar. A metallic tube (Al. tube) was mounted on top of dewar and the gap was closed by quick fix. A heating coil wound on mica was kept at the bottom of dewar. Liquid nitrogen was heated by applying voltage with a variac. Different rates of

evaporation of liquid nitrogen could be obtained. The sample was inserted inside the tube mounted over dewar so that it was near the mouth of dewar. The evaporating nitrogen cooled the sample while passing out of the tube. Different steady temperatures could be obtained. Resistances were measured at different constant temperatures.

4.4 Switching Properties

Switching properties were measured for some of the glasses at room temperature and higher temperatures. The circuit employed was the same as shown in fig. 7. A high resistance (10^5 ohm) was connected in series with the sample to control the current in the ON state of the glass. The ON state characteristics were recorded using Hewlett-Packard recorder.

4.5 Optical Absorption Spectra

Optical absorption spectra were recorded using a Cary-14 spectrometer. The samples were polished to a thickness of 0.3 to 0.5 mm. Absorption spectra were recorded in the wavelength range 2000-6000 Å for different glasses. Absorption spectra for some of the thin reduced specimens were also recorded.

4.6 Transport Number Measurements

An attempt was made to measure the transport number for some of the glasses by Tubandt method[78]. Transport number is defined as the ratio of current carried by a particular species to the total current carried by all the species $t_i = (\sigma_i/\sigma_{total})$.

To carry out the measurements, 3 samples of the same glass of uniform dimensions (approximately 1 cm x 1 cm x 0.1 cm) were taken and polished till the surfaces became very flat. One surface of the glass was coated with silver paste for two samples for making electrical contacts. All the 3 samples were weighed individually. The three samples were stacked one above the other with the silver coated surfaces of the 2 samples forming outer surfaces. The assembly was kept in a sample holder. The sample holder was kept in a vertical furnace and current was passed at about 400°C for a period of 24-48 hours. The total charge passed through the circuit was measured with a silver coulometer. The current passing in the circuit was measured by noting down the voltage drop across a standard resistance. The samples were weighed again after passing the current.

For a single alkali glass the transport number t_R of the alkali ion R is given by

$$t_R = \left(\frac{m}{m_{Ag}}\right)\left(\frac{E_{Ag}}{E_R}\right) \qquad (3.1)$$

where m = mass lost by the silver coated anode glass disc

m_{Ag} = mass of silver deposited in the coulometer.

E_{Ag} and E_R are the electrochemical equivalent weights. The weight of an element deposited when a current of I amps. is passed for a period of t seconds is given by

$$w = ItE \qquad (3.2)$$

where E is the electrochemical equivalent weight. For t = 50 hours and for Na ions with $E = 0.24 \times 10^{-3}$ gm/coulomb, we get

$$w = 30\ I \qquad (3.3)$$

From the resistivity-vs. temperature plots of various glasses (fig. 9) we know that even at 400°C, the resistances of all the glasses are more than 10^6 ohm. For an applied voltage of 100 volts and a total resistance of 10^7 ohm in the circuit, current through the samples will be 10^{-5} amps.

Hence mass lost by the anode glass will be approximately 3×10^{-4} gms. Detection of such small changes in weight is very difficult, by usual methods. No weight change in the anode glass was detected even after passing the current for 50 hours and hence transport number could not be measured, for any of the glasses.

4.7 DTA Studies

DTA was carried out using 'MOM Derivetograph' from room temperature to 500°C. Rate of increase of temperature was 5°/min. Platinum-platinum/rhodium thermocouple and αAl_2O_3 reference material were used in the investigation. DTA curves were recorded for powdered glasses.

TABLE 1

The chemical compositions of the glasses chosen for the present investigation

Glass No.	Composition in mole %					
	SiO_2	B_2O_3	As_2O_3	Na_2O	PbO	ZnO
1	64	18	8	10	-	-
2	60	27	8	5	-	-
3	60	29	8	3	-	-
4	60	31	8	1	-	-
5	60	31	6	3	-	-
6	6	19	1	-	60	14

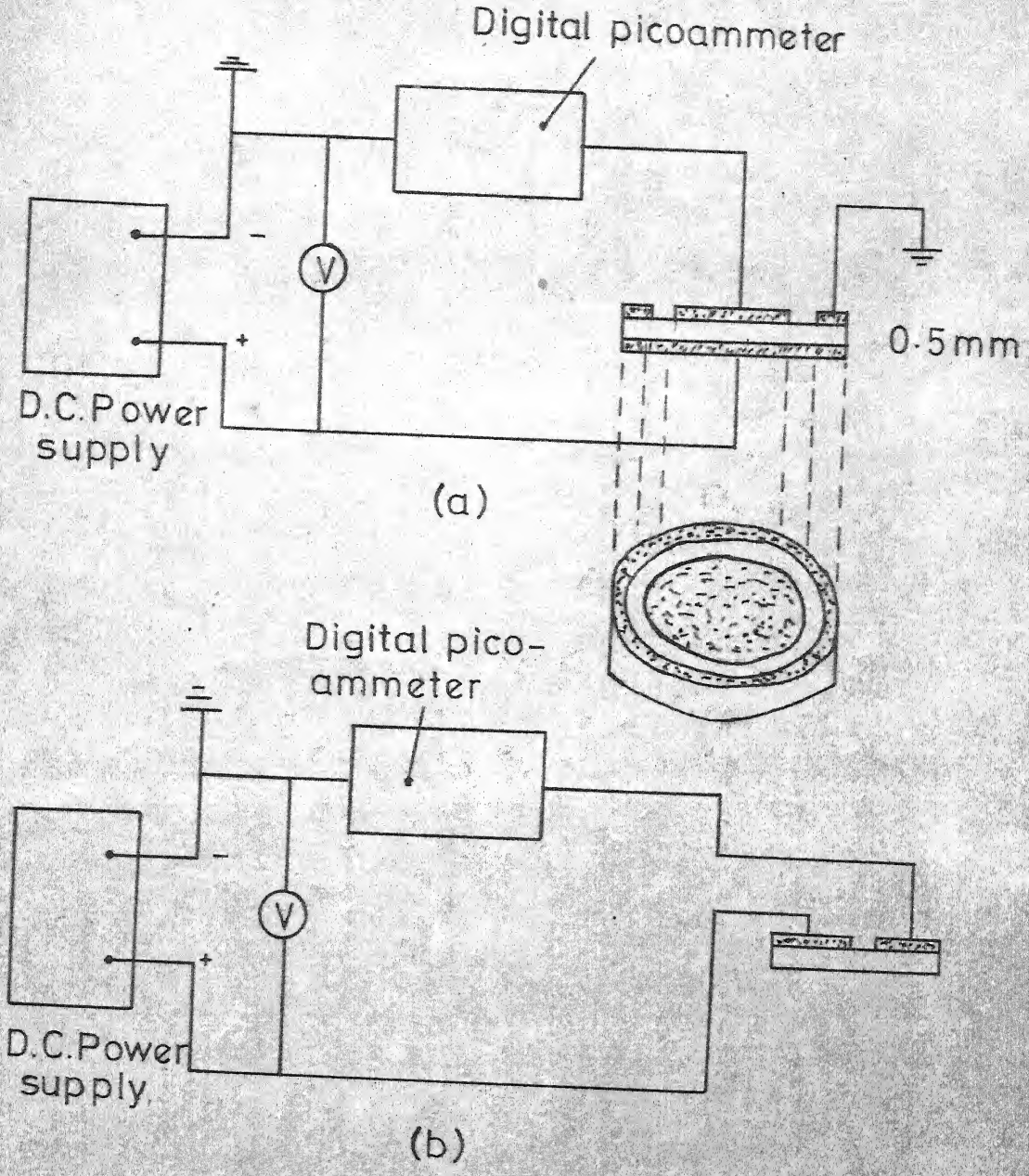

FIG. 7 SCHEMATIC CIRCUIT DIAGRAM FOR
(a) Bulk resistivity measurement
(b) Surface resistivity measurement

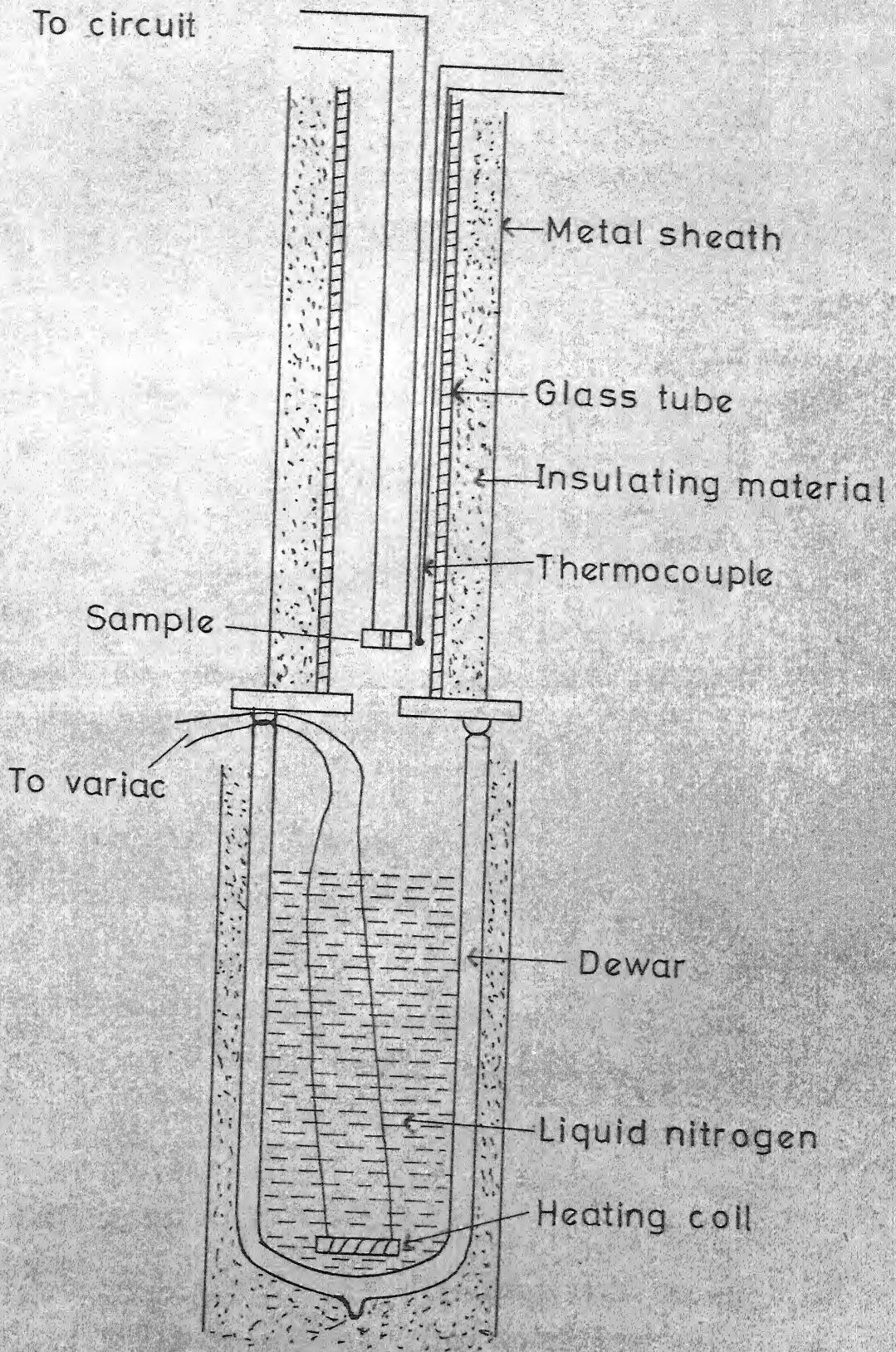

FIG. 8 SET UP FOR LOW TEMPERATURE RESISTIVITY MEASUREMENT

CHAPTER 5

RESULTS

The temperature variation of resistivity of glasses as described in Chapter 1 is given by the expression

$$\rho = \rho_0 \exp^{(E/kT)} \qquad (5.1)$$

where E is the activation energy for conduction and ρ_0 is a constant. From the plot of log ρ vs. 1/T, obtained by measuring resistivities at different temperatures, the activation energy E can be determined.

5.1 Bulk Resistivity Measurements

Bulk resistivities were determined in the temperature range 30-400°C for different glasses. Logarithm of the resistivity as a function of inverse of the absolute temperature is plotted in fig. 9 for glass nos. 1, 2, 3, and 5. All the plots are straight lines. The activation energy E was calculated using the standard least squares method of fitting the data, for each glass. These values are given in table 2. The variation of activation energy for all the glasses as a function of mole % of Na_2O is shown in fig. 10. The activation energy for these glasses decreases with Na_2O content of the glass.

5.2 Surface Resistivity Measurements

5.2.1 Virgin Glasses

Surface resistances of virgin glasses with no ion-exchange or reduction treatments were measured in the temperature range 0 to 400°C, both while heating and cooling the sample. Surface resistivities were calculated from these values by using the relation $R = \rho t/w$, where R is the specimen resistance in ohms, ρ is the surface resistivity in ohms/ square, t is the separation between the electrodes in cm. and b is the width of the electrodes in cm. In each case plots of log ρ (ohm/□) vs. 1/T were made, from which activation energies were calculated, which are given in table 2.

The variation of surface resistivities with temperature are shown for all the glasses in figures (11-15), where plots of log ρ(ohm/square) vs. 1/T are made. All the glasses show somewhat peculiar but similar variation of resistivity with temperature e.g., for glass no. 1 (fig. 11), the resistivity near room temperature (37°C) is 5.30×10^{12} ohm/□ . It increases sharply to a value of 4.01×10^{14} ohm/□ , as the temperature of the sample is lowered to 24°C. Again, the resistivity of the sample increases, as it is heated above room temperature, reaching a maximum

value of 3.34×10^{13} ohm/□ at 59°C. For further rise in temperature, the resistivity starts falling. Resistivities were measured while cooling the sample also. Resistivity values in cooling cycle agree with the resistivity values of heating cycle. The dip in resistivity observed near room temperature is common to almost all the glasses studied. For other glasses, the resistivities determined in the cooling cycle do not agree with the resistivities determined in the heating cycle, and in general they are slightly higher than the resistivities of heating cycle.

Glass nos. 3, 4 and 5 show a rise in resistivity against at about 280-300°C, showing a second maximum in resistivity plot. However this peak was not observed during cooling cycle for any of the glasses.

Resistivity measurements were made on a sample of glass no. 5 after giving 12 hours of heat treatment at 120°C (6 hours before putting the electrodes, and 6 hours after putting the electrodes). Though this glass showed a maximum in resistivity at about 115°C, it did not show a maximum at higher temperatures, as observed in the case of a sample of the same glass, for which no heat treatment was given.

The characteristic features of log ρ vs. 1/T plots for surface resistivity measurements of all the glasses are tabulated in table 3. The table gives the resistivity

near room temperature, the temperature and resistivity below room temperature at which the maximum resistivity was measured, the temperature and resistivity at which the maximum resistivity occurs as the sample is heated above room temperature and the temperature at which the second peak was observed.

5.2.2 Ion-Exchanged and Reduced (IER) Glasses

All the glasses were first given ion-exchange ($Na^+ \rightleftharpoons Ag^+$) treatment for 6 hours at 320°C and later reduced by hydrogen at 340°C for 12 hours. Surface resistivity measurements were made for all the samples in the temperature range 0-340°C. In each case plots of log ρ (ohm/$\square$) vs. 1/T were made. Activation energies of different linear regions in the graph were calculated. These values are given in table 2.

The variation of surface resistivities with temperature are shown for all the glasses in figures (16-20). Ion-exchanged and reduced glasses also show the same kind of variation of resistivity with temperature, as shown by virgin glasses e.g., for ion-exchanged and reduced glass no. 1 the resistivity near room temperature (33°C) is 4.97×10^{12} ohm/$\square$, which increases to 3.37×10^{14} ohm/$\square$

as the temperature is lowered to 2°C. This increase is not very sharp, unlike in the case of virgin surface resistivity variation of the same glass (fig. 11). As the sample is heated above room temperature, the resistivity starts decreasing. In cooling cycle the resistivities are somewhat higher than in the heating cycle.

But other IER glasses show a maximum in resistivity as the sample is heated above room temperature Glass nos. 2, 3 and 5 show a maximum at about 130-160°C whereas glass no. 4 shows a maximum at about 51°C. For glass no. 4 the resistivity decreases very fast after 51°C, as the sample is heated above this temperature.

None of the IER glasses show a maximum in resistivity at about 300°C (which was observed in the case of virgin glasses), except glass no. 2 which shows a small hump at about 270°C.

It is important to note that whereas for virgin glasses the maxima in resistivity occurred in the temperature range 110-130°C, the maxima for IER samples occur in the temperature range (130-160°C), except for glass no. 4 which shows a maximum at about 51°C.

5.2.3 Reduced Glasses

Reduction treatments were given to the specimens of all the glasses by passing hydrogen over the samples at 340°C for 12 hours. Surface resistivity measurements were made for all the samples, in the temperature range 0 to 340°C and plots of log ρ (ohm/□) vs. 1/T were made. Activation energies of different regions of the curves were calculated, which are given in table 2.

The variation of surface resistivities with temperature are shown for all the reduced glasses in figures (21-26). The behaviour of all the glasses is in general similar to the behaviour of virgin glasses and IER glasses, except for a few differences. Taking glass no. 1, as an example, we see that, (fig. 21) its room temperature (37°C) resistivity is 4.11×10^{11} ohm/□, which increases sharply as the temperature is lowered below room temperature, reaching a resistance of 4.26×10^{14} ohm/□ at 11°C. As the sample is heated above room temperature, the resistivity increases rapidly reaching a maximum at 79°C. The resistivity at 79°C is 1.03×10^{14} ohm/□. During the cooling cycle the resistivity values are slightly higher.

Glass nos. 4 and 5 show a rise in resistivity again at about 260°C, showing a second maximum in resistivity. Again this peak was not observed during cooling cycles for both the glasses.

The maxima in resistivity for reduced glasses occur in the temperature range 70-110°C, which are lesser than the temperature range in which maxima for virgin glasses (110-130°C) and IER glasses (130-160°C) occur.

The resistivity measurements were carried out on a PbO glass of composition 6 given in table 1, in the temperature range 50-200°C. (This glass melts at about 800°C. The reduction treatment was carried out at 200°C). The plot of log ρ vs. 1/T for this glass is shown in figure 26. The resistivity of this glass goes on decreasing as the temperature of the sample is increased. It did not show any maximum in resistivity in the above temperature range.

5.3 Switching Studies

I-V characteristics of IER glass nos. 2 and 3 and bulk glass no. 1 were studiedbelow room temperature and also at higher temperatures.

IER glass no. 2 showed threshold type of switching at about 28°C. I-V characteristics of this glass at 28°C are shown in figures (27-29). It switches from OFF state (resistance, 10^{11} ohm) to ON state (resistance, 10^{5} ohm) at about 7 volts during the first two cycles. The I-V chararacteristics were recorded using a recorder. Square wave pulse was applied to the specimen, and switching

was observed on an oscilloscope. After applying square wave pulse, the switching was found to be more stable. I-V characteristics were recorded again using the recorder for 20-30 cycles. It showed stable switching at about 15 volts, as shown in the figure 29. However, this specimen of glass no. 2 did not show any switching at higher temperatures upto 350°C even though high voltages upto 1000 volts were applied. A kilowatt power supply was used to apply high voltages.

I-V characteristics of IER glass no. 3 and bulk glass no. 1 were also studied at room temperature and also at higher temperatures upto 350°C, applying voltages upto 1000 volts. The samples did not break even though such high voltages were applied. I-V characteristics of these samples were found to be nonlinear. I-V characteristics of IER glass no. 3 at different temperatures are given in figure 30. and 31.

5.4 Optical Absorption

Optical absorption curves were recorded for thin specimens (0.5 mm thick) of all the glasses and for a few reduced samples in the wavelength range 2500-6500 Å. U.V. absorption was observed for all the specimens in the wavelength range 2800-3100 Å.

From the recorded absorption densities, the absorption coefficients were calculated at different wavelengths, using the relation

$$\alpha = \ln \frac{I_o}{I} \frac{1}{x} \text{ cm}^{-1} \qquad (5.2)$$

where x is the thickness of the sample and I is the transmitted intensity. Usually for chalcogenide glasses, the optical absorption edge E_{opt} is taken as the energy of the wavelength corresponding to $\alpha \simeq 10$ cm^{-1}. A more justifiable procedure is to estimate an optical gap by attempting to fit the absorption curve above the exponential edge to the standard formulae for optical transition in semiconductors. By the reasons given by Tauc et al.[79], a plot of $(\alpha h\nu)^{\frac{1}{2}}$ vs. $h\nu$ gives E_{opt}, by extrapolating the linear part of the curve.

Plots of $(\alpha h\nu)^{\frac{1}{2}}$ vs. $h\nu$ were made from the absorption curves recorded for all the samples (fig. 32). Optical gaps thus obtained lie in the range of 2.8 to 3.1 eV. Table 4 gives the optical gaps for all the samples.

5.5 DTA Studies

DTA curves for glass nos. 4 and 5 are shown in figure 32(a). For both the glasses a sharp minimum is observed at about 160°C. For glass no. 4 another well defined dip is observed at about 190°C.

TABLE 2

Activation energies E calculated from log ρ vs. 1/T plots for different regions of the curves for glasses studied, as computed using Least Squares Method

Glass No.	Fig. No.	Temperature region for which E is calculated. Range of 1/T From	To	Region marked on the graph	Activation energy eV	Standard deviation
			I BULK CONDUCTIVITY			
1	9	1.65	2.60	(a)	0.85	.006
2	9	1.55	2.35	(b)	1.27	.02
3	9	1.4	2.15	(c)	1.40	.06
5	9	1.4	2.15	(d)	1.43	.04
			II SURFACE CONDUCTIVITY			
			A. Virgin Glasses			
1	11	1.6	3.0	(a)	0.90	.003
		3.2	3.4	(b)	2.50	.68
2	12	1.5	2.5	(a)	1.01	.03
		2.5	3.0	(b)	-1.00	.22
		3.25	3.45	(c)	4.18	1.19
3	13	1.9	2.5	(a)	0.76	.06
		3.25	3.4	(b)	4.77	1.39
4	14	2.6	3.2	(a)	-0.99	.18
		1.9	2.5	(b)	0.53	.10
		3.25	3.4	(c)	7.47	.99
5	15	1.9	2.5	(a)	0.82	.04
		3.28	3.5	(b)	5.32	1.29
		1.5	2.5	(c)	0.75	.03

TABLE 2 (Continued)

Glass No.	Fig. No.	Temperature region for which E is calculated. Range of 1/T From	To	Region marked on the graph	Activation energy eV	Standard deviation
		B. Ion-Exchanged and Reduced Glasses				
1	16	1.6	2.6	(a)	0.81	.03
		2.9	3.6	(b)	0.84	.04
2	17	2.6	3.1	(a)	-1.68	.19
		1.9	2.5	(b)	0.81	.04
3	18	1.8	2.4	(a)	0.65	.04
		3.25	3.35	(b)	6.28	1.55
4	19	2.2	3.1	(a)	1.11	.04
		3.25	3.45	(b)	6.24	.86
		2.1	2.8	(c)	1.58	.07
5	20	1.6	2.3	(a)	0.95	0.03
		3.25	3.6	(b)	1.70	0.19
		C. Reduced Glasses				
1	21	1.6	2.8	(a)	0.91	.002
		3.23	3.5	(b)	1.88	.33
		1.6	2.6	(c)	0.98	.01
2	22	2.8	3.25	(a)	1.88	.20
		1.6	2.5	(b)	0.96	.03
		3.25	3.5	(c)	3.26	.77
3	23	1.9	3.2	(a)	0.75	.05
		3.2	3.35	(b)	3.69	.32
		1.6	2.5	(c)	0.86	.04
4	24	2.7	3.2	(a)	-1.02	.11
		1.9	2.6	(b)	0.60	.03
		3.3	3.4	(c)	8.23	.95
5	25	2.2	2.9	(a)	0.76	.03
		3.25	3.45	(b)	2.5	.44
6	26	2.0	2.6	(a)	0.92	.04
		2.0	2.6	(b)	1.07	.01

TABLE 3

Characteristic features of log ρ (ohm/□) vs. 1/T plots of virgin, reduced, and ion-exchanged and reduced glasses studied

Glass No.	Figure No.	Resistivity near room temperature		Maximum resistivity measured below R.T.		Maximum resistivity measured above R.T.		Temperature at which second peak occurs °C
		Temp.°C	ρ(ohm/□)	Temp.°C	ρ(ohm/□)	Temp.°C	ρ(ohm/□)	
				A. Virgin Glasses				
1	11	37	5.31×10^{12}	24	4.01×10^{14}	59	3.34×10^{13}	-
2	12	38	9.66×10^{11}	10	4.68×10^{14}	127	4.70×10^{13}	-
3	13	33	7.64×10^{10}	22	1.76×10^{14}	117	2.77×10^{13}	295
4	14	30	5.67×10^{10}	21	3.27×10^{14}	117	1.75×10^{13}	307
5	15	32	2.37×10^{9}	17	2.11×10^{14}	125	9.04×10^{13}	288
5	15	41	4.68×10^{10}	-	-	115	1.15×10^{13}	-
				B. IER Glasses				
1	16	33	4.97×10^{12}	2	3.37×10^{14}	-	-	-
2	17	54	5.61×10^{8}	-	-	130	7.69×10^{12}	276
3	18	33	2.64×10^{11}	25	2.97×10^{14}	140	1.65×10^{13}	-
4	19	36	1.22×10^{11}	20	3.19×10^{14}	51	1.86×10^{13}	-
5	20	32	8.31×10^{10}	-1	3.41×10^{14}	165	3.46×10^{14}	-

TABLE 3 (Continued)

Glass No.	Figure No.	Resistivity near room temperature Temp.°C	Resistivity near room temperature ρ (ohm/□)	Maximum resistivity measured below R.T. Temp.°C	Maximum resistivity measured below R.T. ρ (ohm/□)	Maximum resistivity measured above R.T. Temp.°C	Maximum resistivity measured above R.T. ρ (ohm/□)	Temperature at which second peak occurs °C
				C. Reduced Glasses				
1	21	37	4.11×10^{11}	11	4.26×10^{14}	79	1.03×10^{14}	-
2	32	34	2.33×10^{9}	10	4.68×10^{14}	81	4.37×10^{13}	-
3	23	34	8.31×10^{12}	27	4.38×10^{14}	-	-	-
4	24	30	2.35×10^{10}	21	3.29×10^{14}	114	9.69×10^{13}	294
5	25	32	1.98×10^{12}	16	4.28×10^{14}	73	2.20×10^{12}	255

TABLE 4

Absorption edges calculated from the plots of $(\alpha h\nu)^{\frac{1}{2}}$ vs. $h\nu$ for the glasses studied

Glass No.	Thickness of the sample, mm	Absorption edge (in eV)
1	0.37	3.05
2	0.33	2.75
2 (Reduced)	0.50	2.70
3	0.43	3.3
3 (Reduced)	0.64	3.3
5	0.53	3.4
5 (Reduced)	0.63	3.4

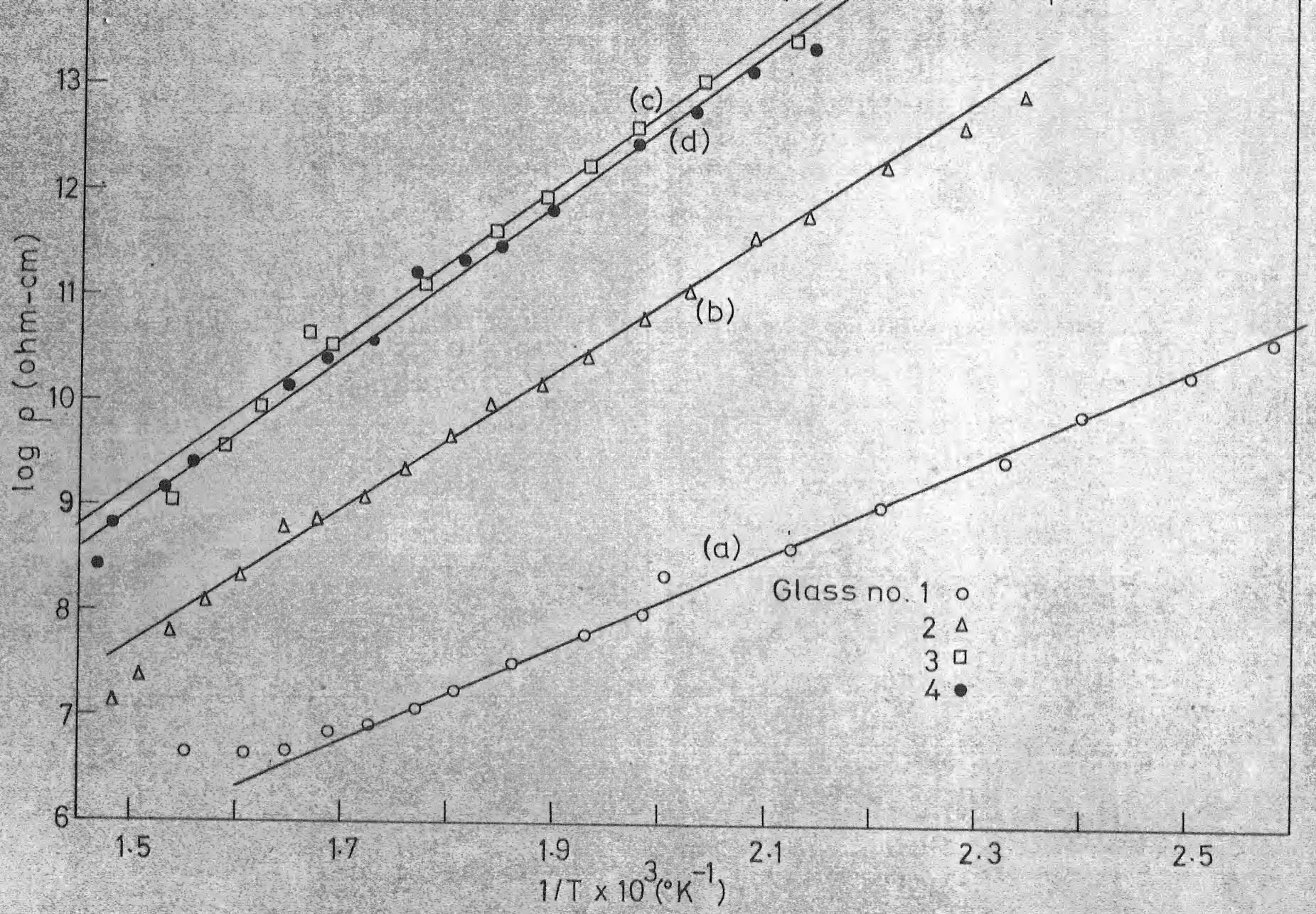

FIG.9 VARIATION OF RESISTIVITY WITH INVERSE OF ABSOLUTE TEMPERATURE

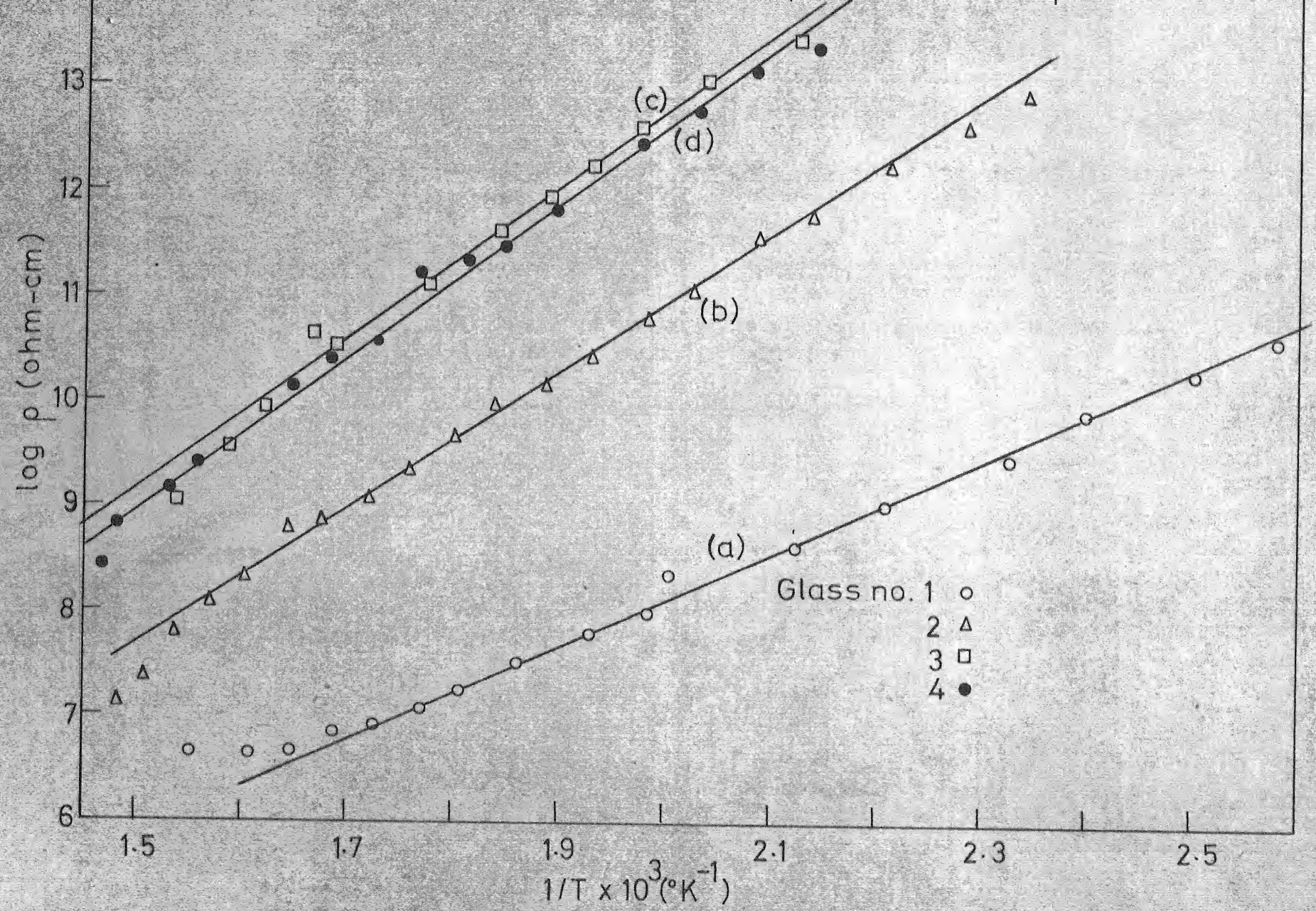

FIG.9 VARIATION OF RESISTIVITY WITH INVERSE OF ABSOLUTE TEMPERATURE

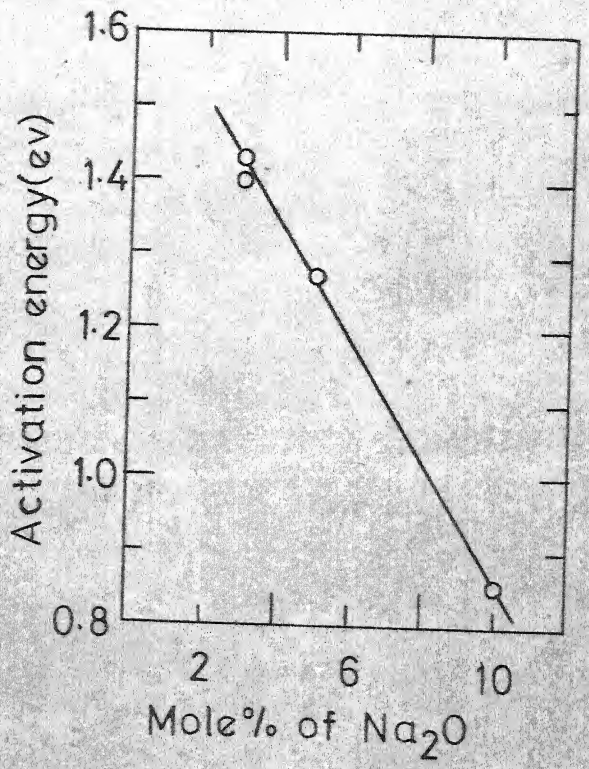

FIG.10 VARIATION OF ACTIVATION ENERGY WITH MOLE % OF Na_2O FOR BULK CONDUCTIVITY.

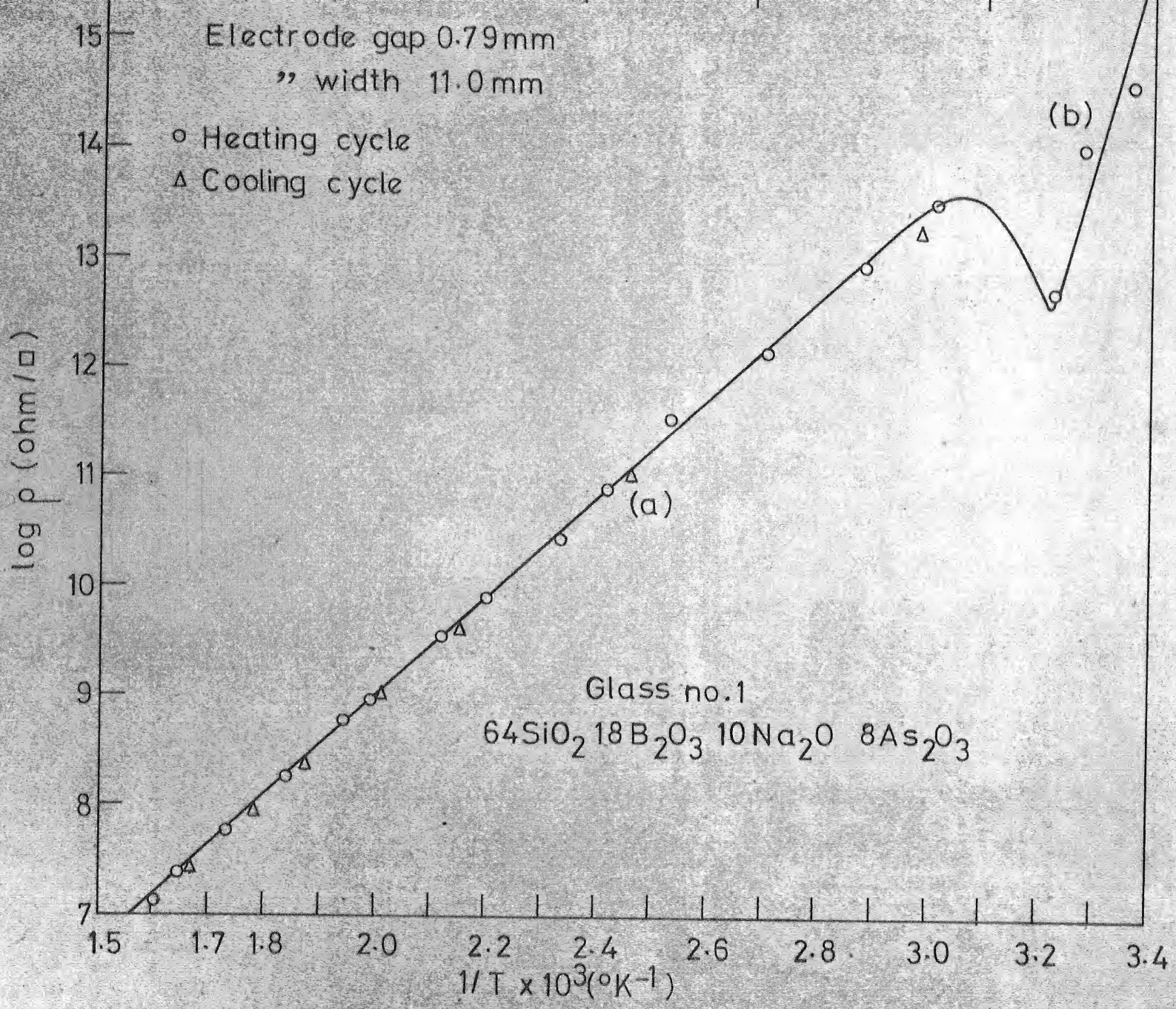
Electrode gap 0.79mm
" width 11.0mm
o Heating cycle
Δ Cooling cycle
(a)
(b)
Glass no.1
64SiO2 18B2O3 10Na2O 8As2O3
log ρ (ohm/□)
1/T x 10^3(°K^-1)
15
14
13
12
11
10
9
8
7
1.5
1.7
1.8
2.0
2.2
2.4
2.6
2.8
3.0
3.2
3.4

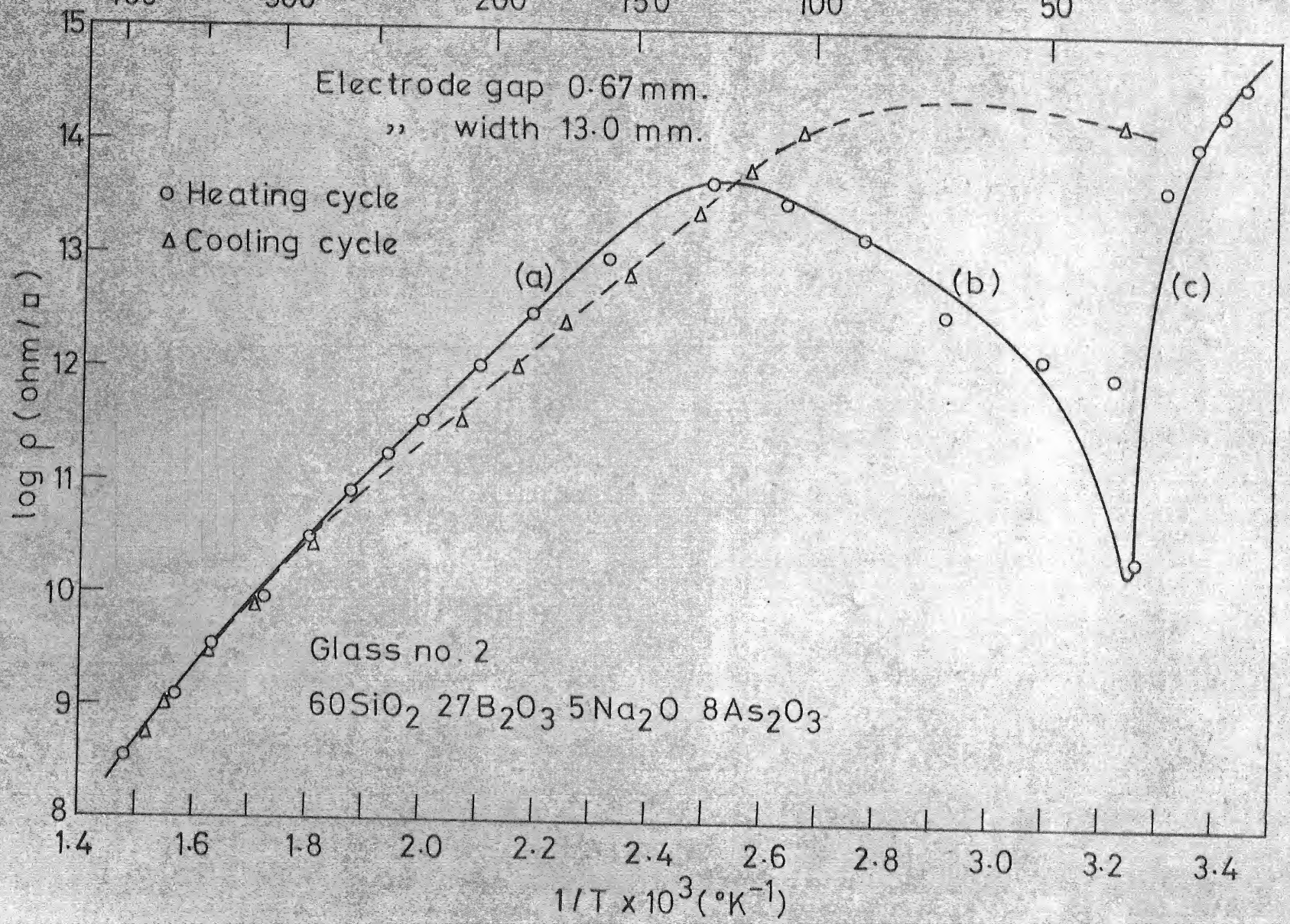

FIG.12 VARIATION OF SURFACE RESISTIVITY WITH INVERSE OF ABSOLUTE TEMPERATURE.

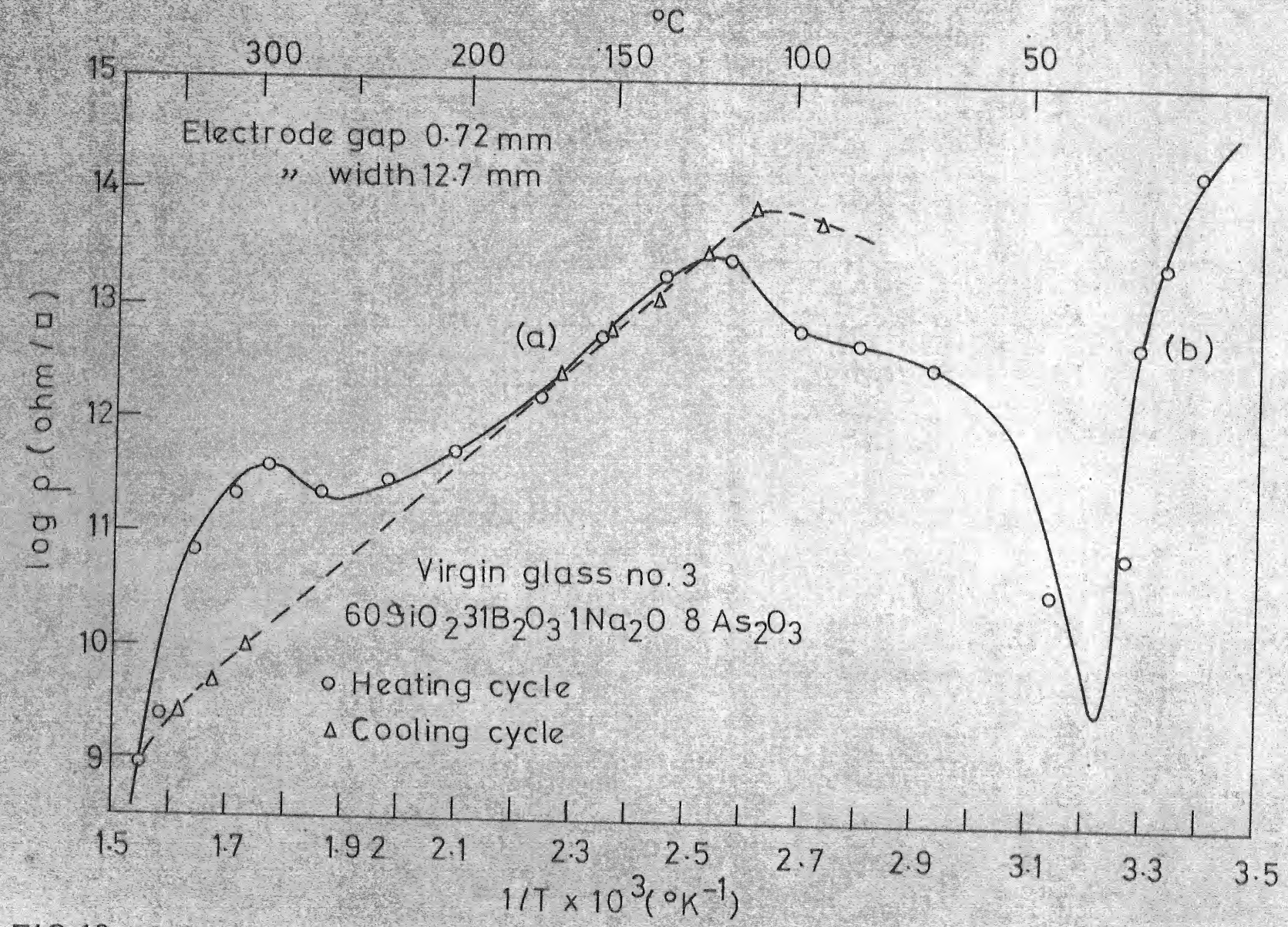

FIG. 13 VARIATION OF SURFACE RESISTIVITY WITH INVERSE OF ABSOLUTE TEMPERATURE

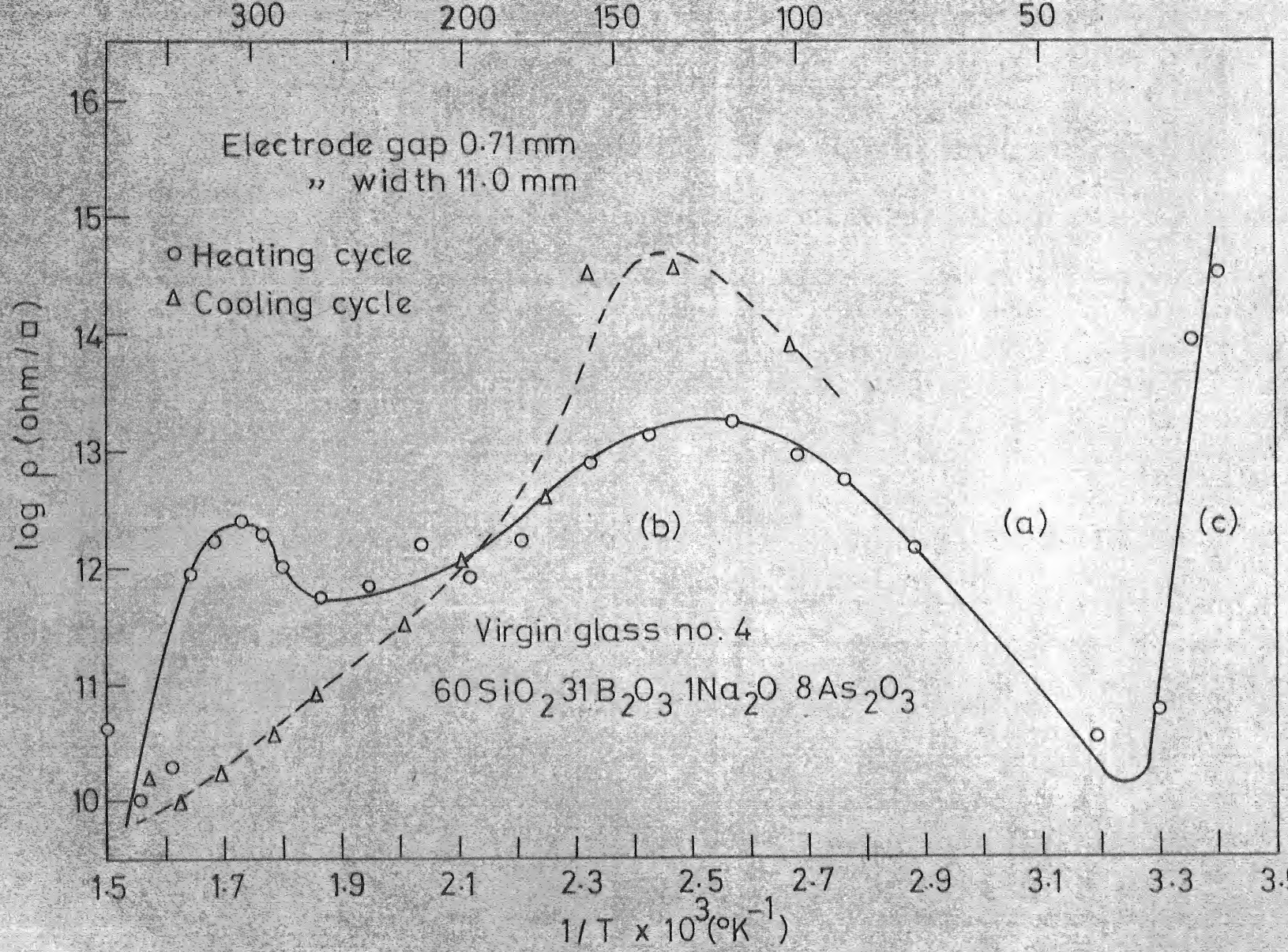

FIG. 14 VARIATION OF SURFACE RESISTIVITY WITH INVERSE OF ABSOLUTE TEMPERATURE.

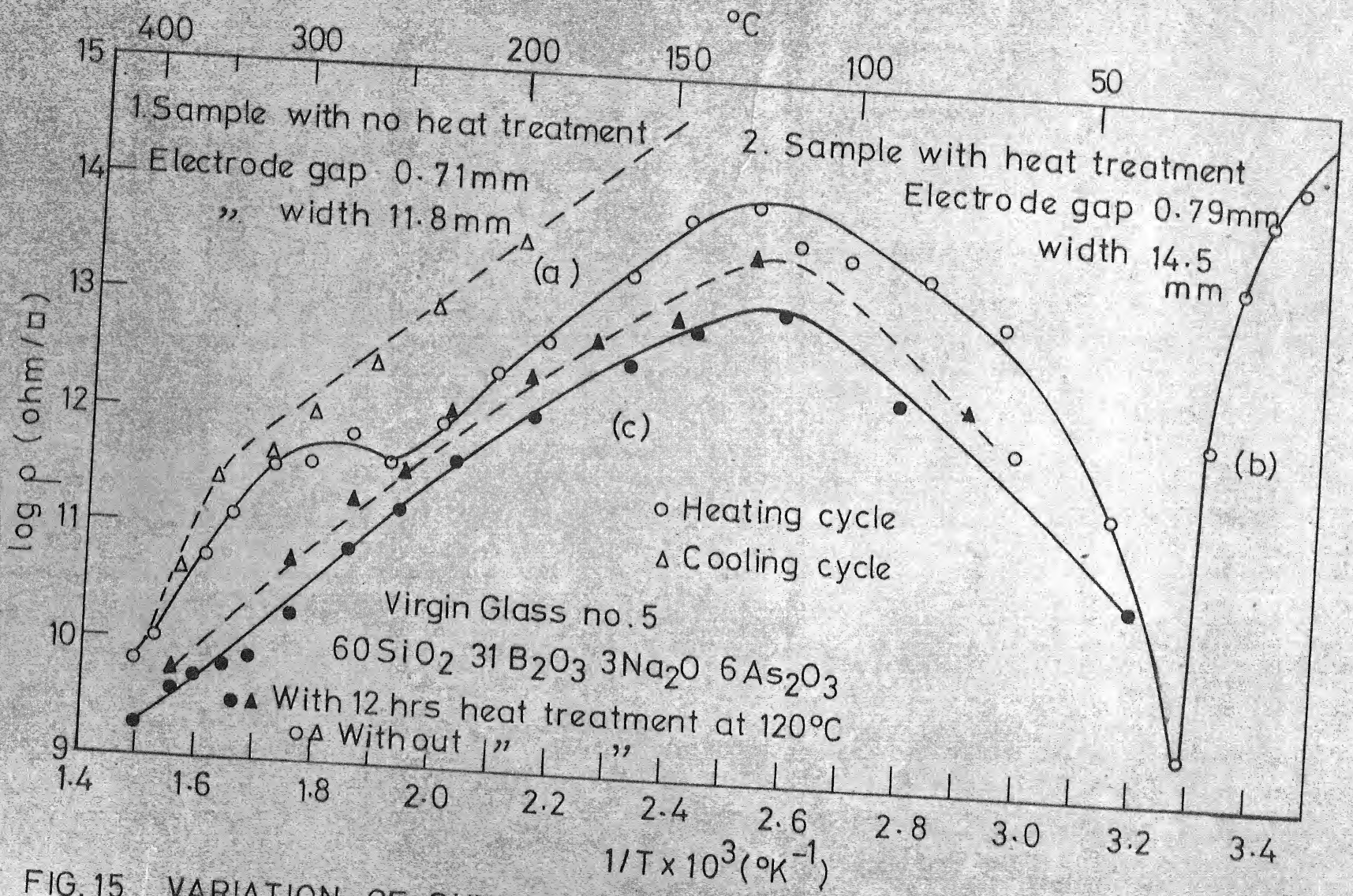

FIG. 15 VARIATION OF SURFACE RESISTIVITY WITH INVERSE OF ABSOLUTE TEMPERATURE

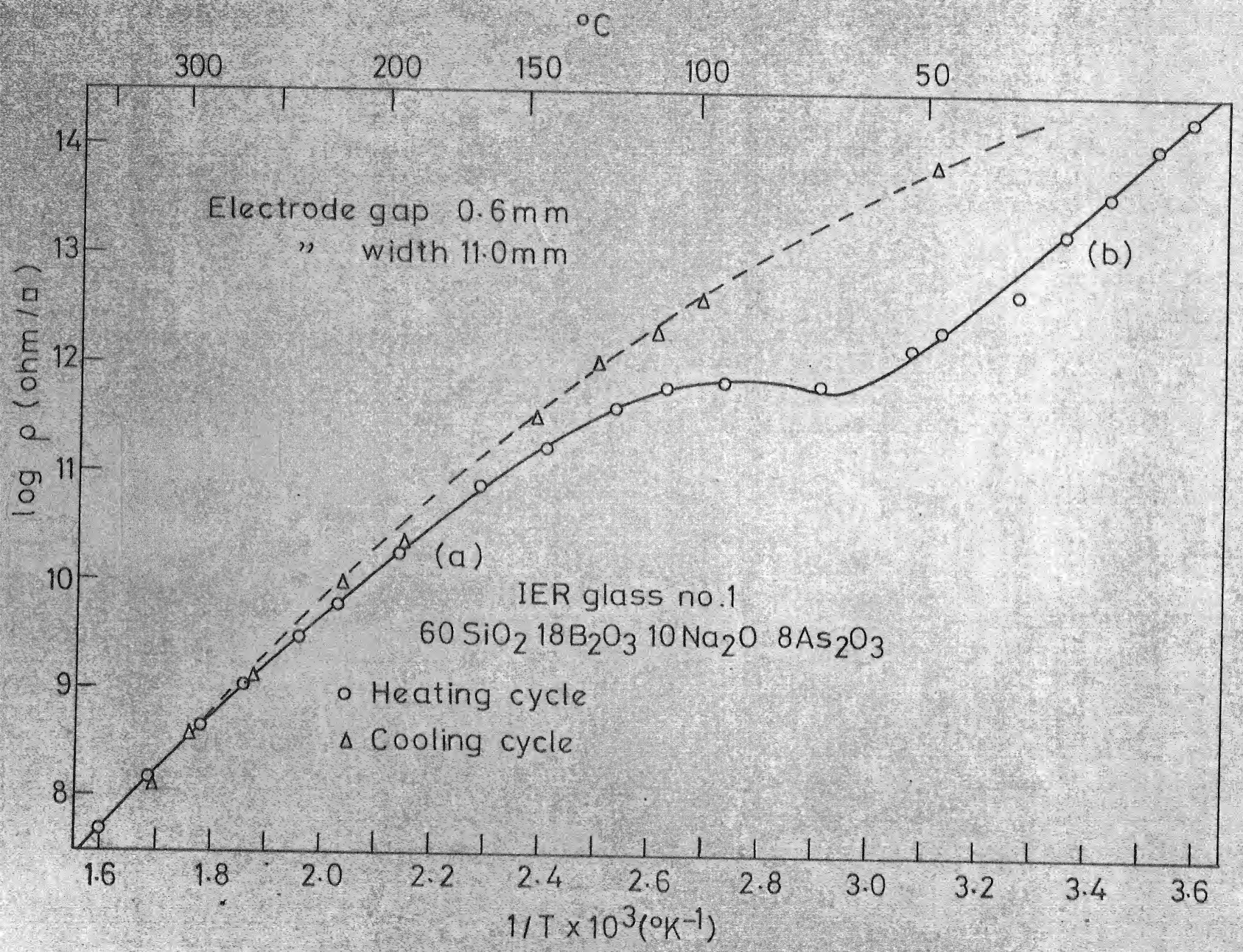

FIG.16 VARIATION OF RESISTIVITY WITH INVERSE OF ABSOLUTE TEMPERATURE

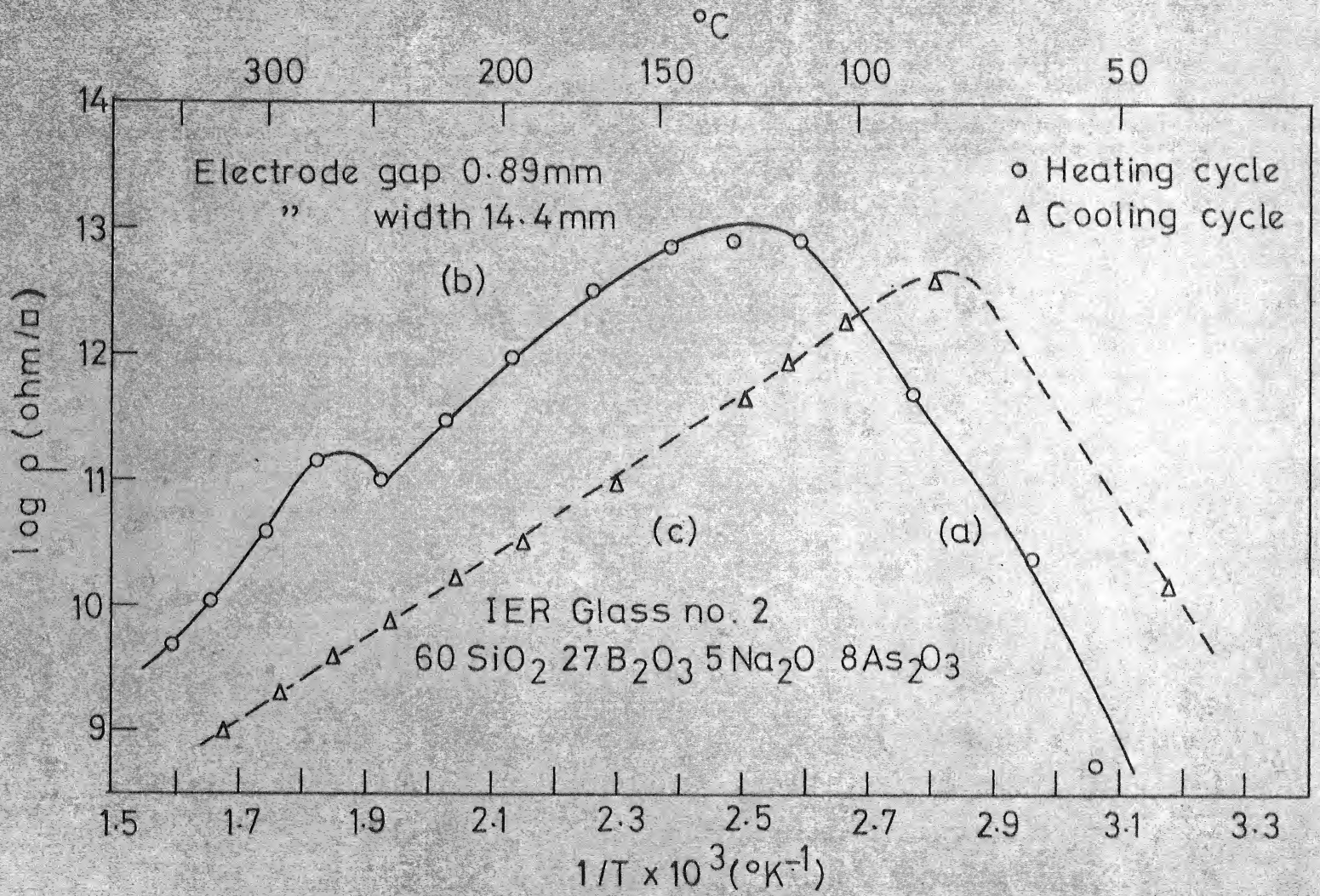

FIG.17 VARIATION OF RESISTIVITY WITH ABSOLUTE TEMPERATURE

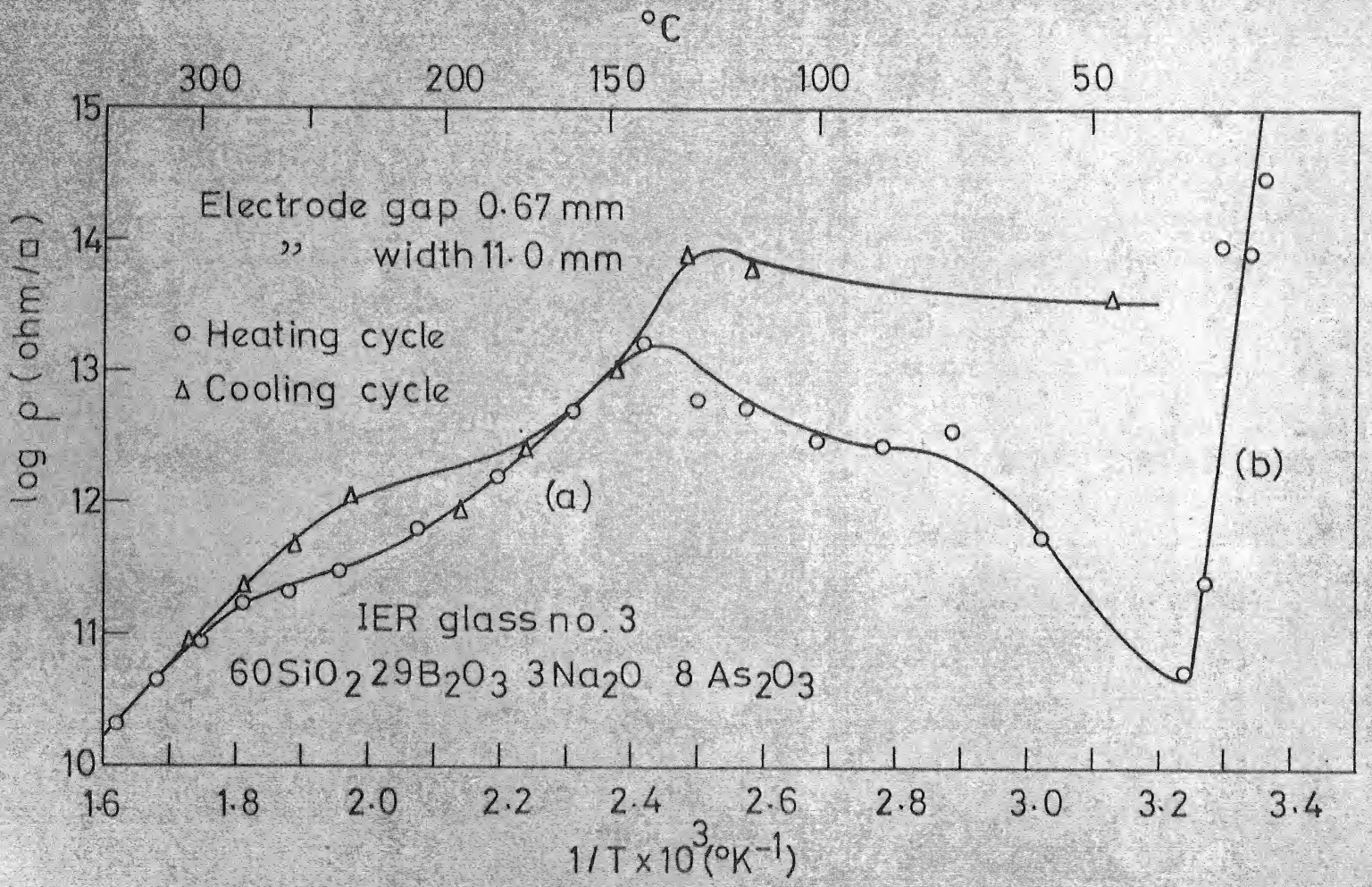

FIG. 18 VARIATION OF RESISTANCE WITH INVERCE OF ABSOLUTE TEMPERATURE

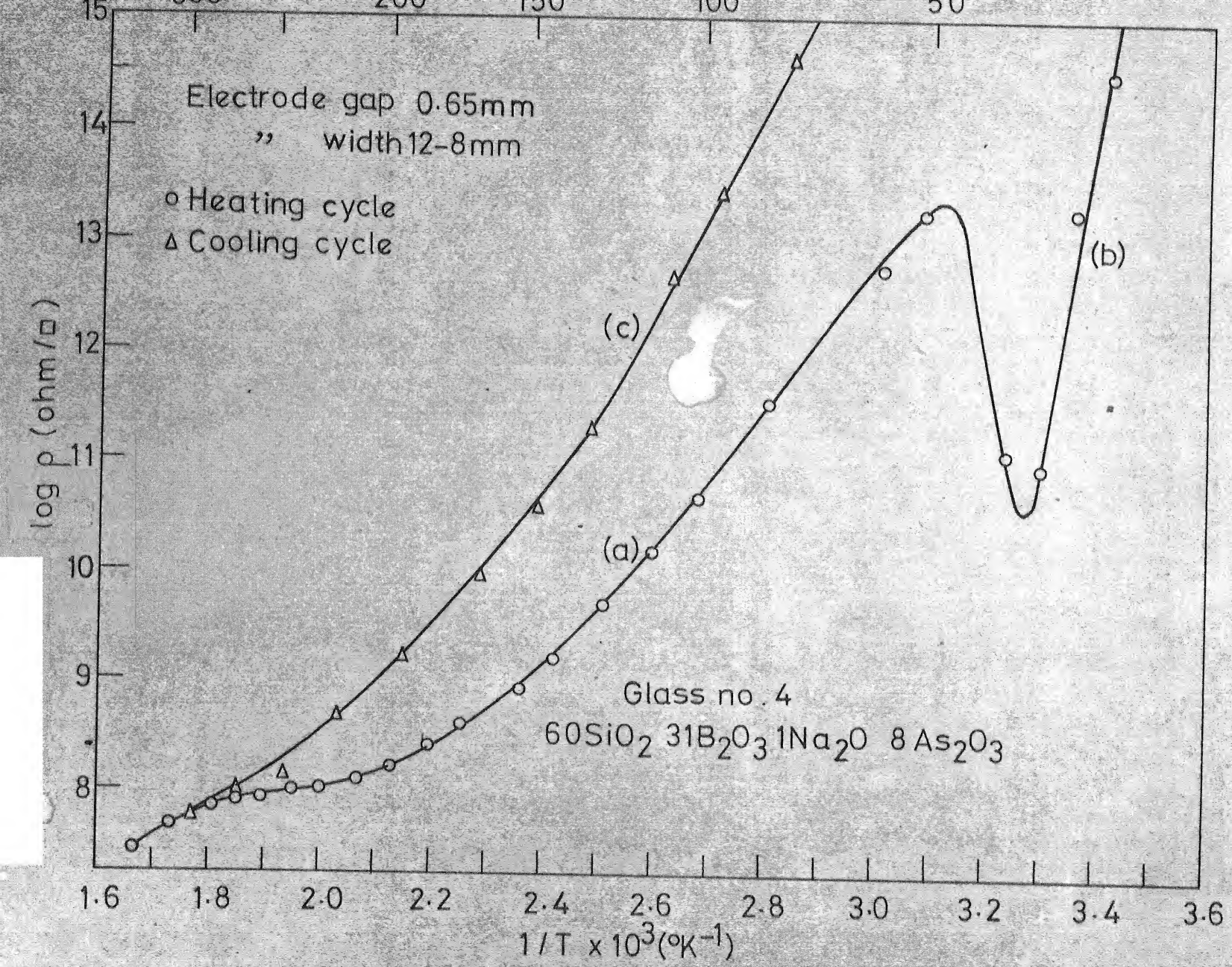

FIG. 19 VARIATION OF RESISTIVITY WITH INVERSE OF ABSOLUTE TEMPERATURE

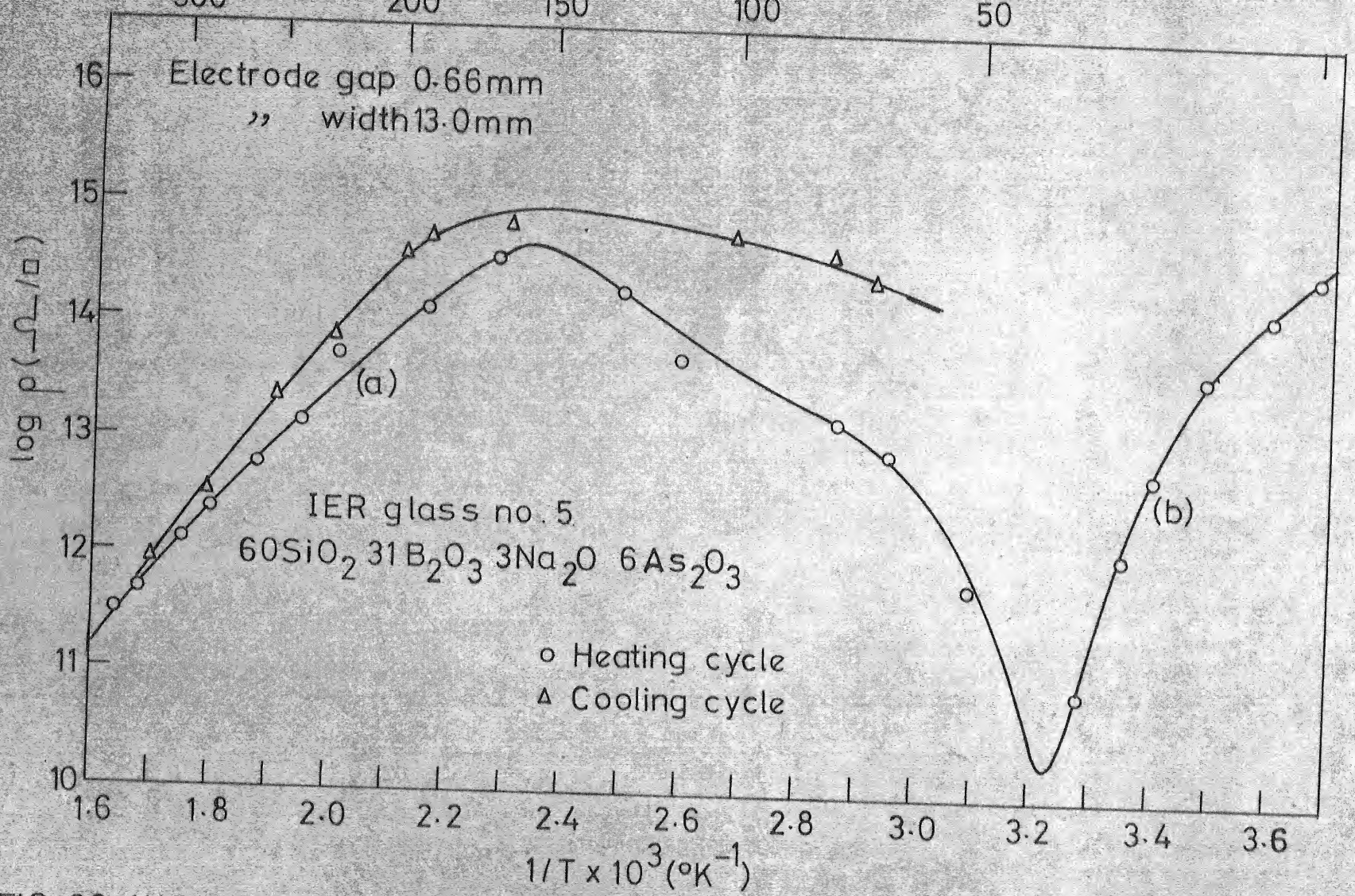

FIG. 20 VARIATION OF RESISTIVITY WITH INVERSE OF ABSOLUTE TEMPERATURE

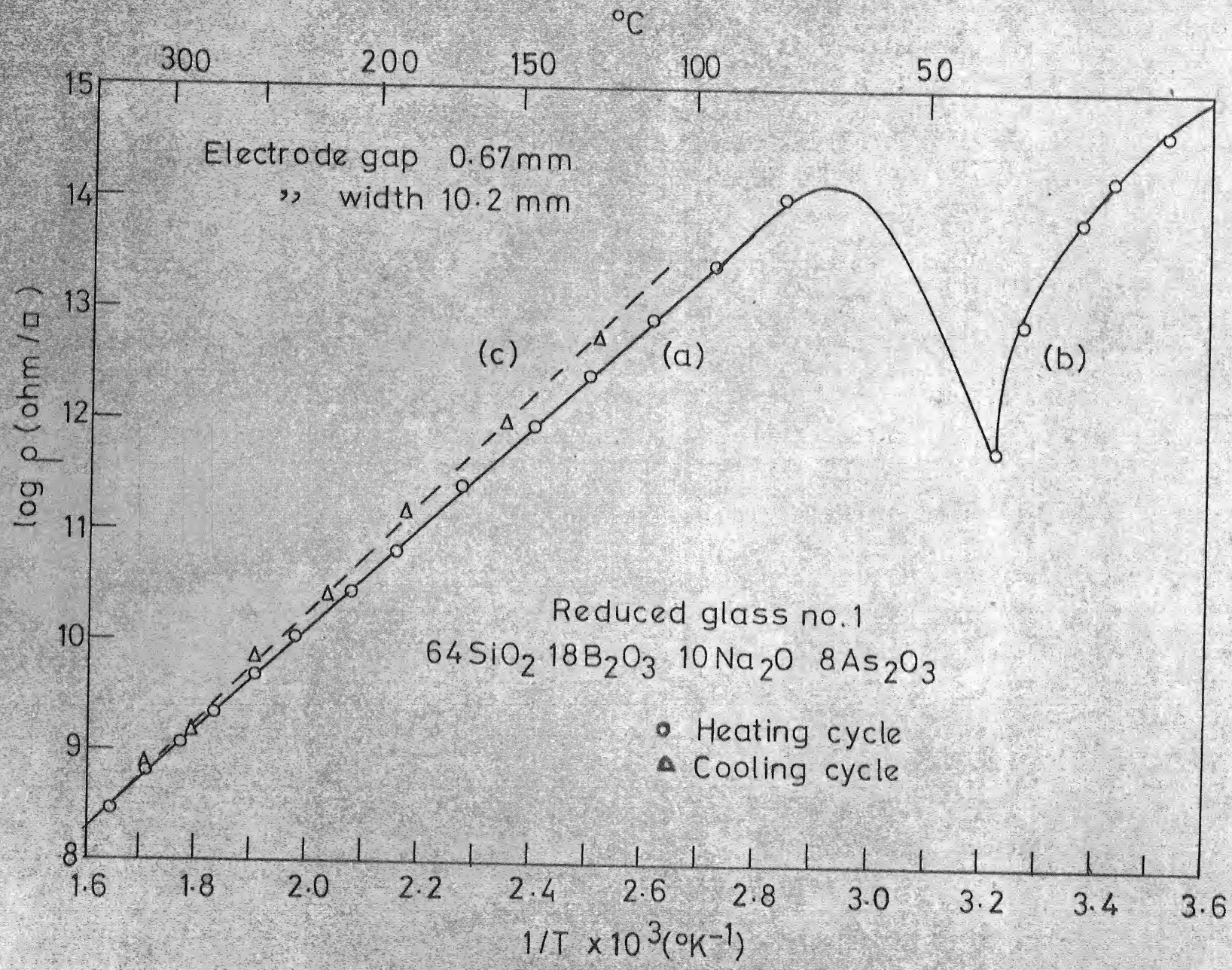

FIG. 21 VARIATION OF RESISTIVITY WITH INVERSE OF ABSOLUTE TEMPERATURE

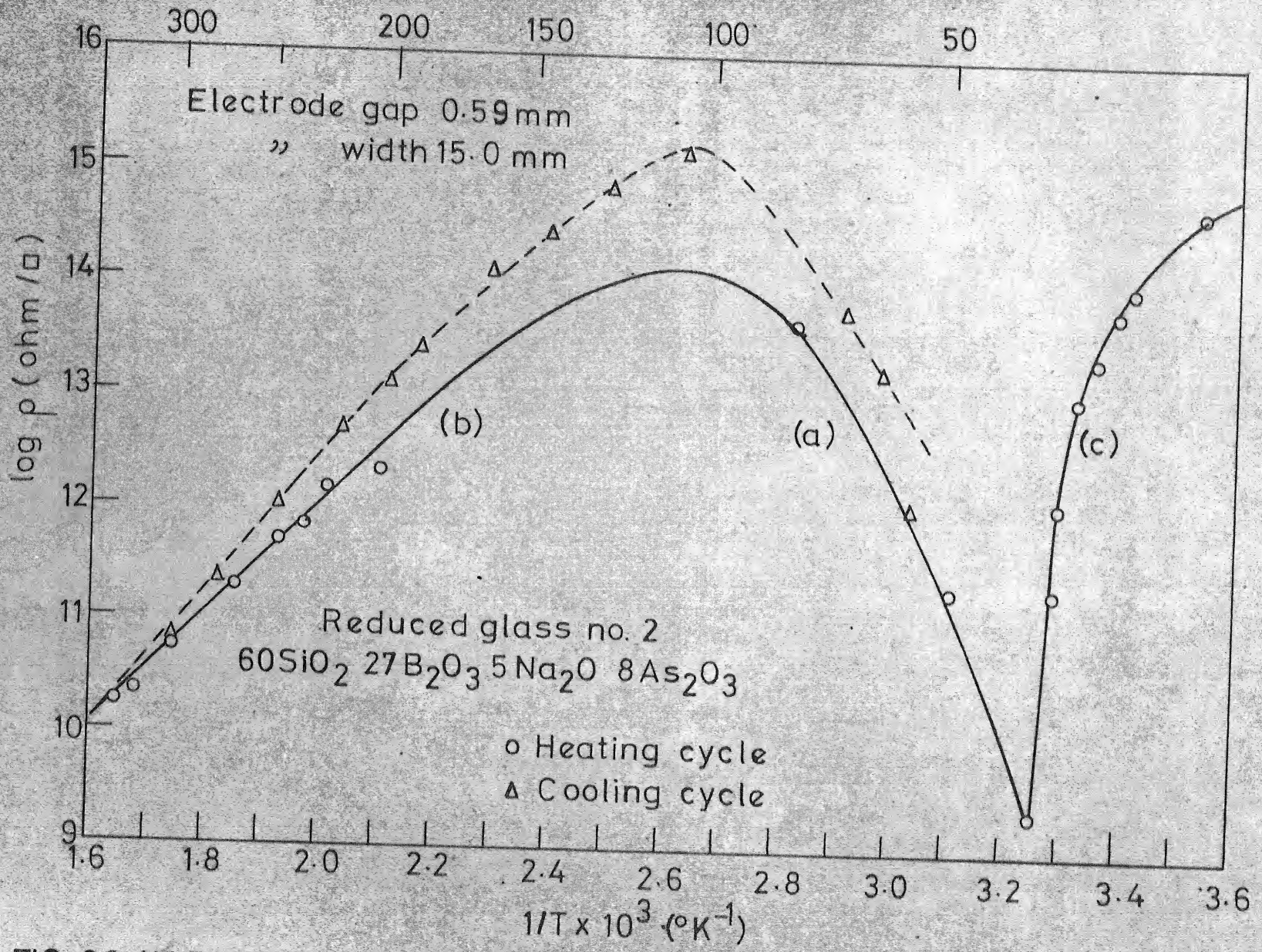

FIG. 22 VARIATION OF RESISTIVITY WITH INVERSE OF ABSOLUTE TEMPERATURE

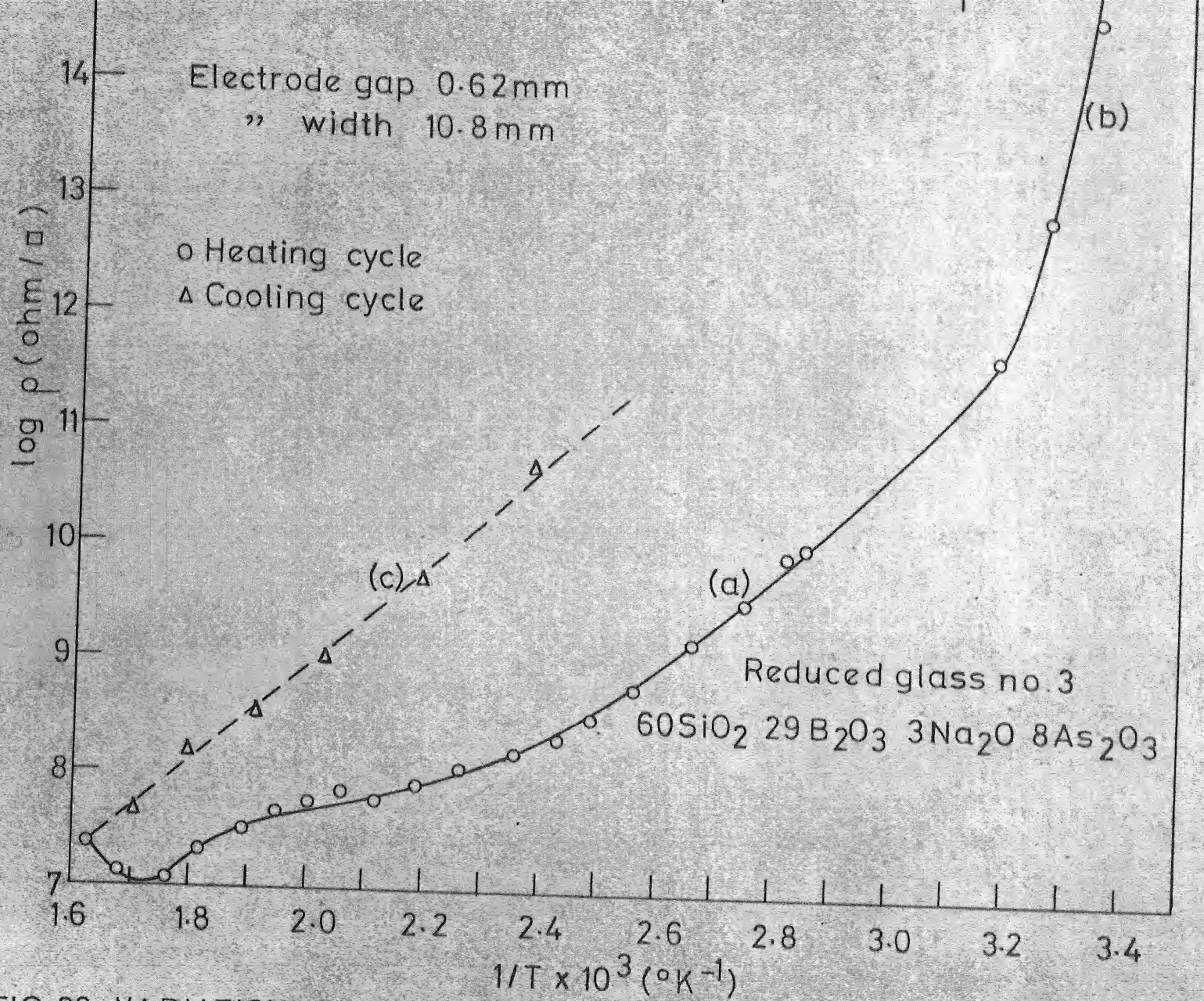

FIG. 23 VARIATION OF RESISTIVITY WITH INVERSE OF ABSOLUTE TEMPE -RATURE

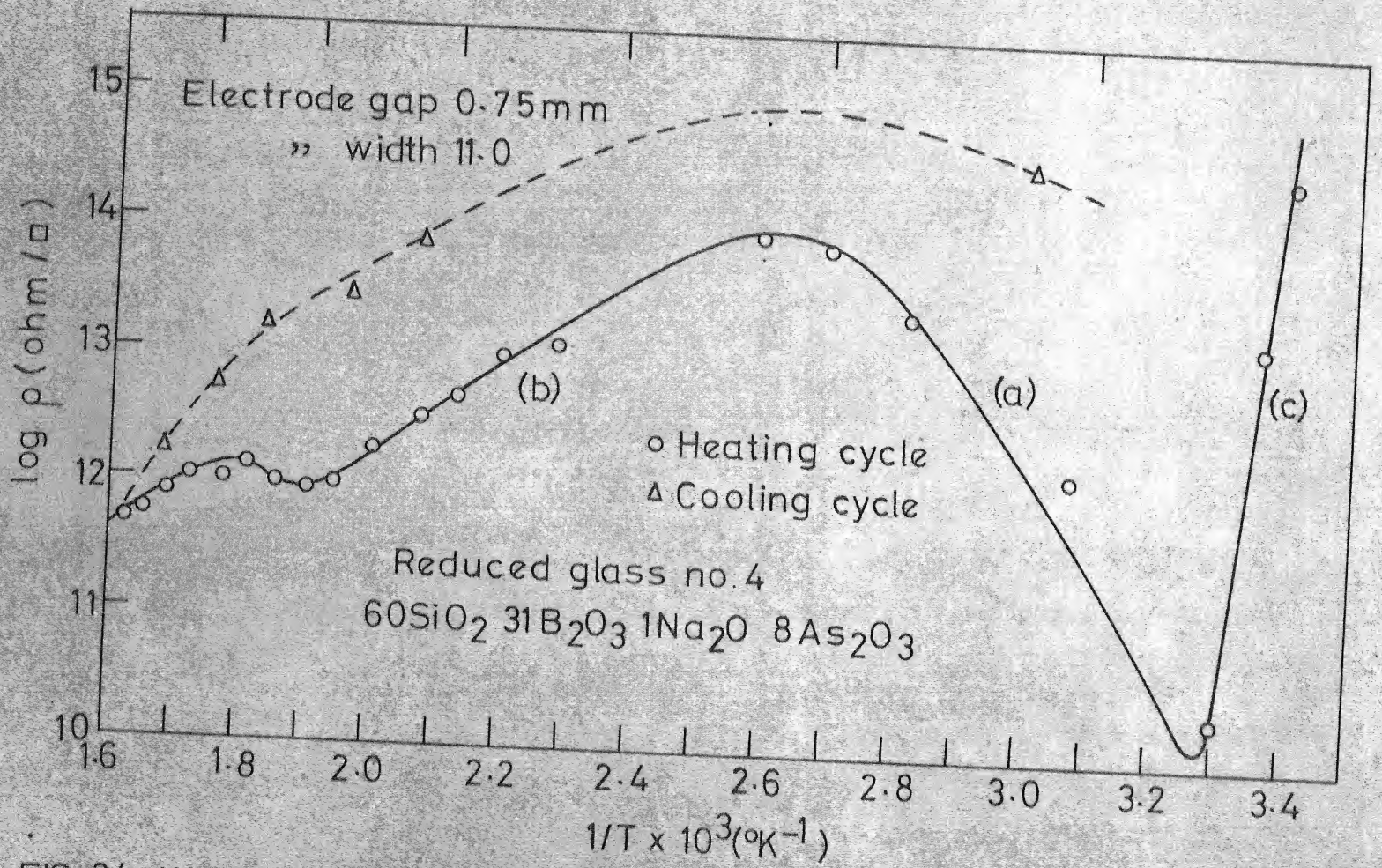

FIG. 24 VARIATION OF RESISTIVITY WITH INVERSE OF ABSOLUTE TEMPERATURE

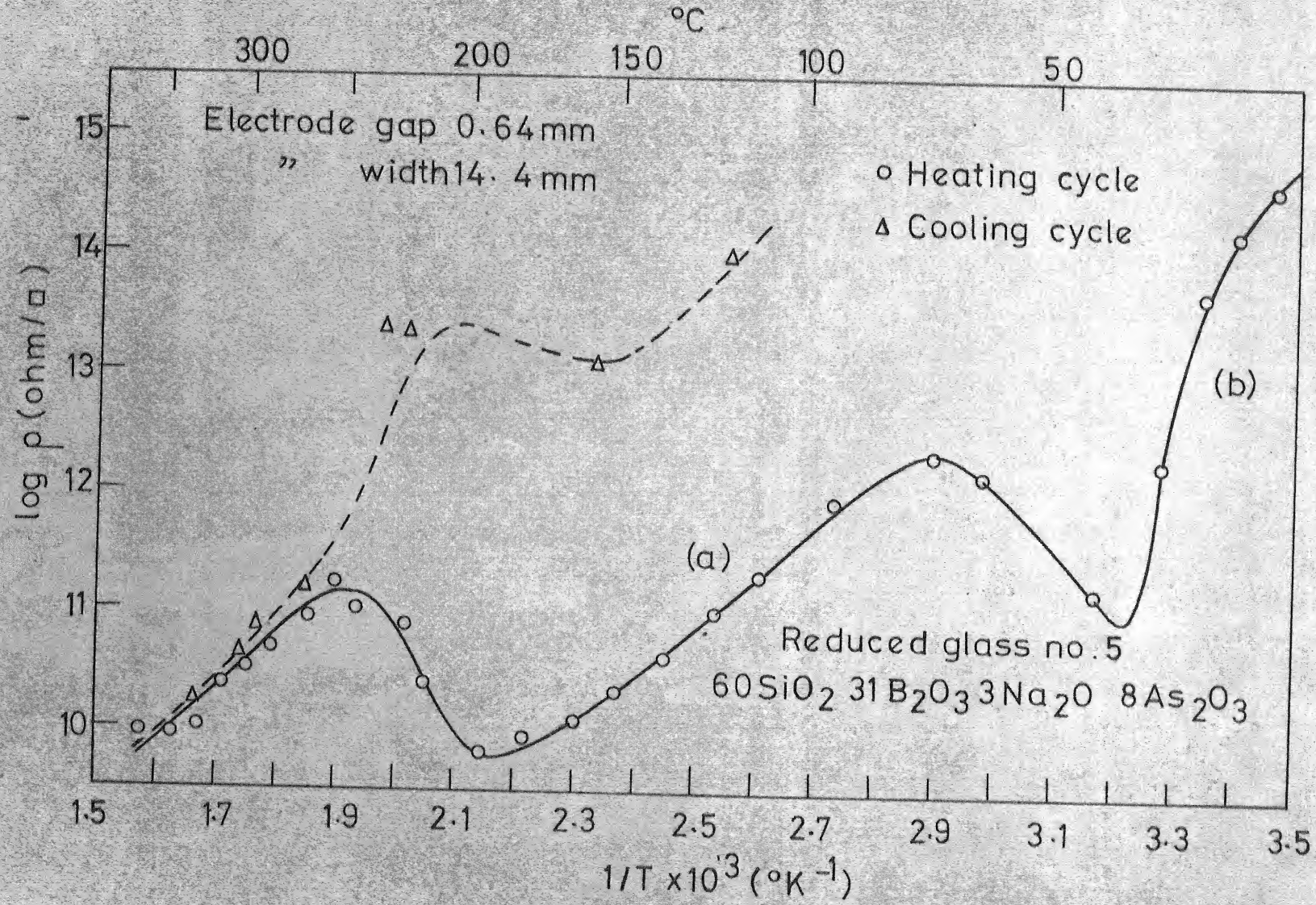

FIG. 25. VARIATION OF RESISTIVITY WITH INVERSE OF ABSOLUTE TEMPERATURE.

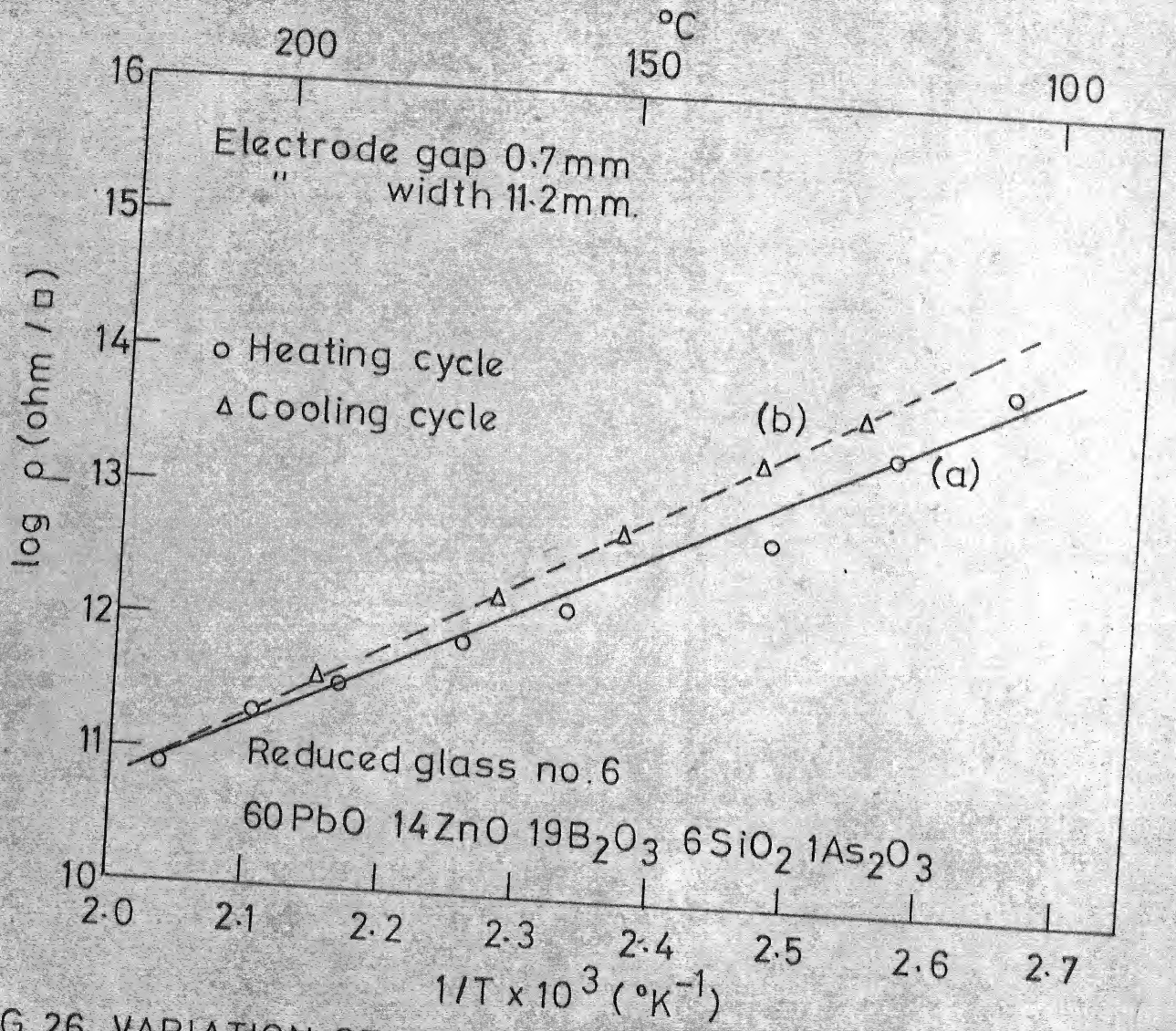

FIG. 26 VARIATION OF RESISTIVITY WITH INVERSE OF ABSOLUTE TEMPERATURE

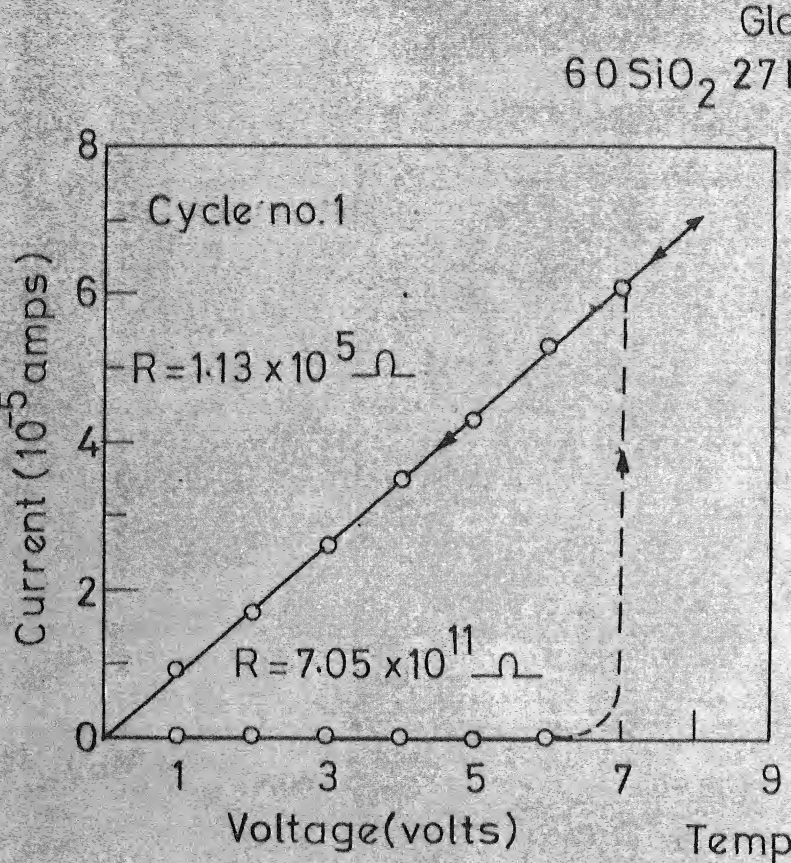

FIG. 27 I-V CHARACTERISTICS OF IER GLASS NO. 2.

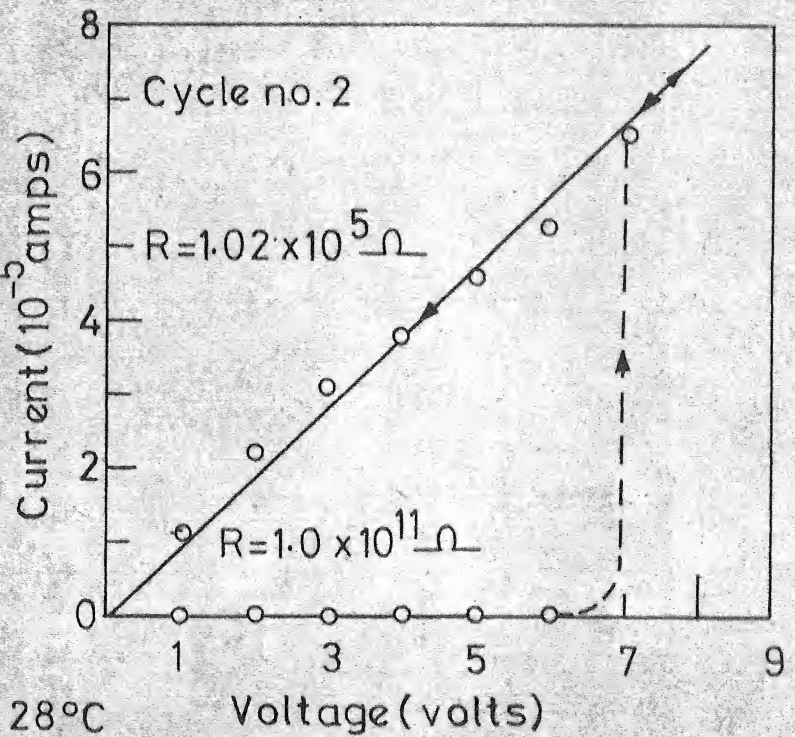

FIG. 28 I-V CHARACTERISTICS OF IER GLASS NO. 2.

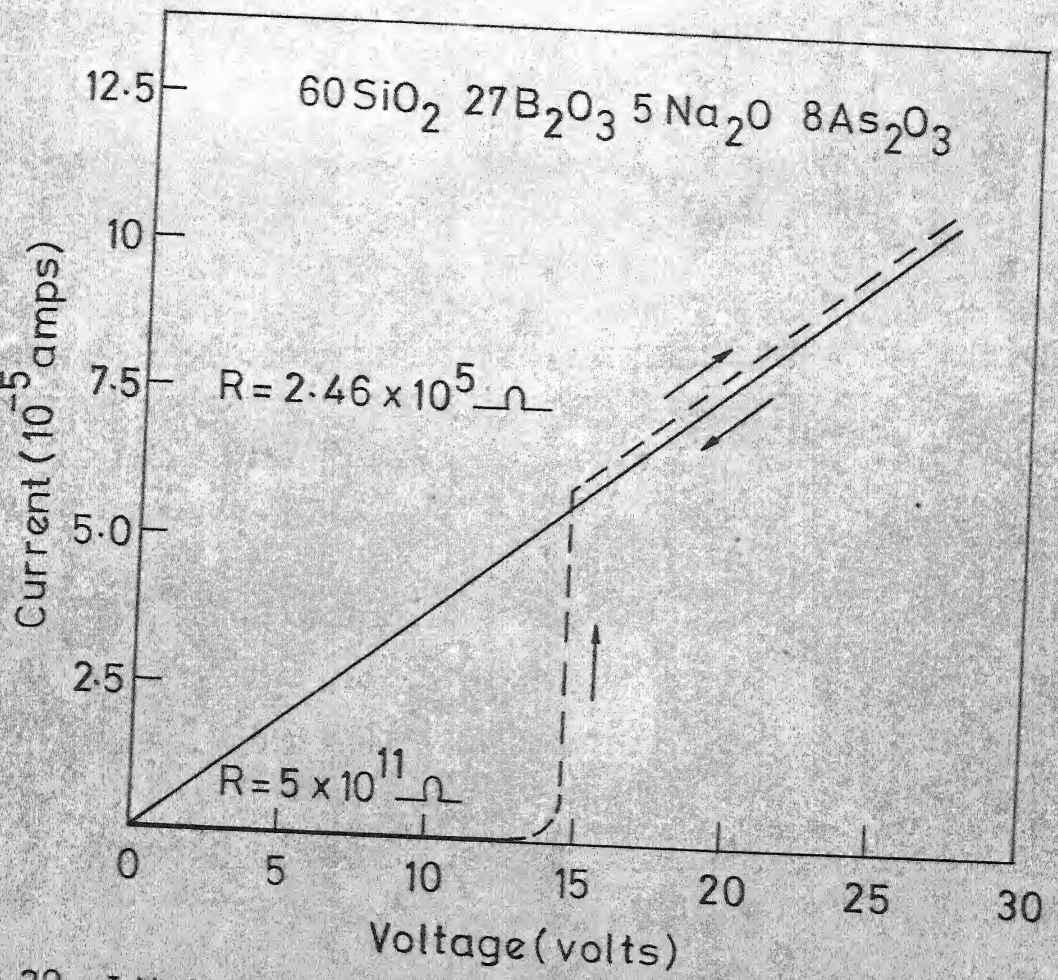

FIG.29 I-V CHARACTERISTIC OF IER GLASS No.2 AFTER APPLYING SQUARE WAVE PULSE.

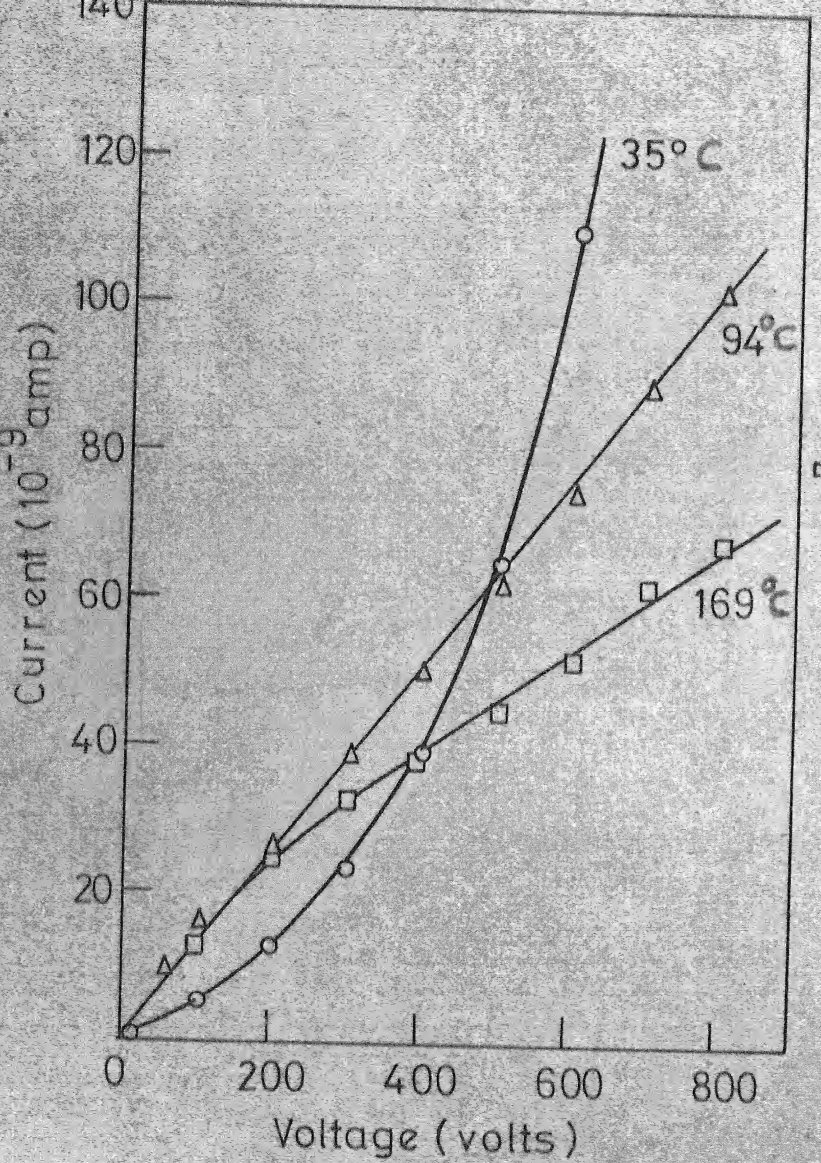

FIG.30 I-V CHARACTERISTICS AT DIFFERENT TEMPERATURES FOR GLASS NO. 3.

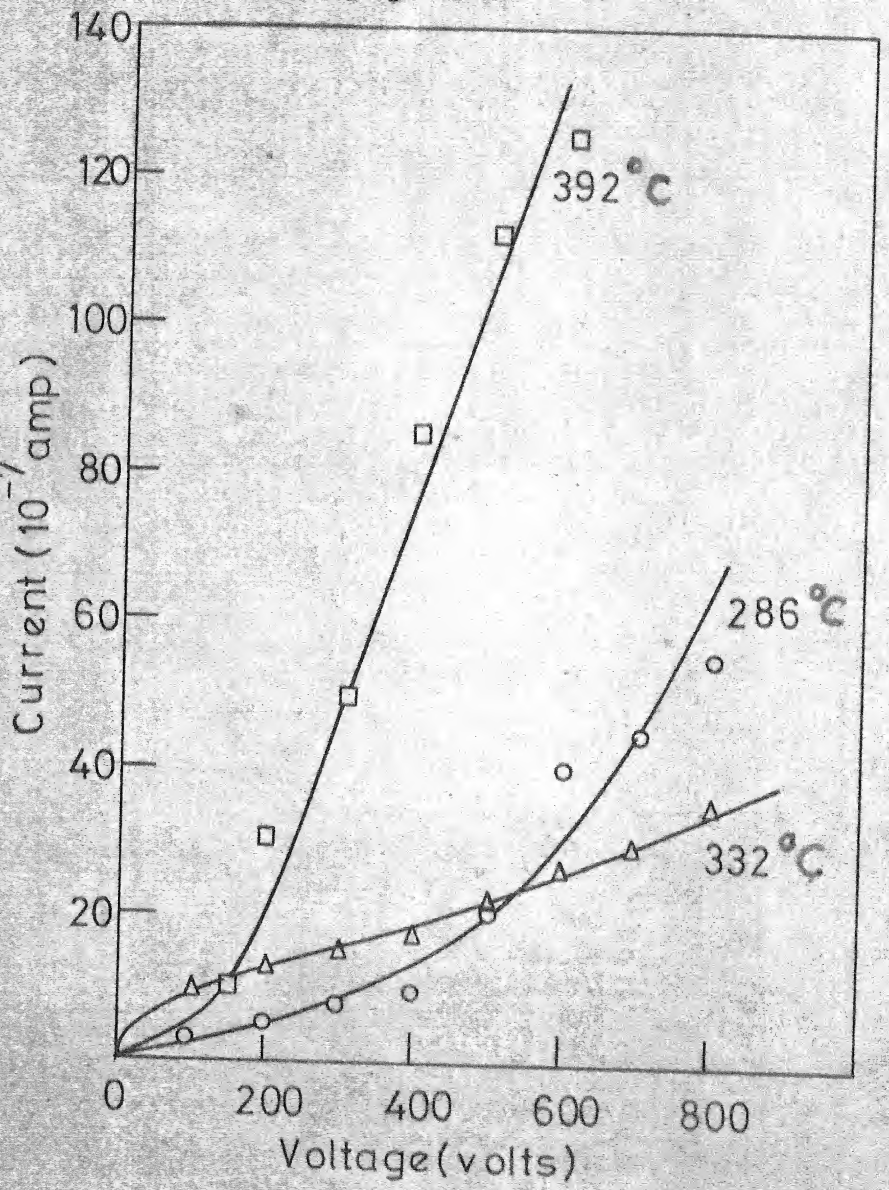

FIG.31. I-V CHARACTERISTICS AT DIFFERENT TEMPERATURES FOR GLASS NO 3

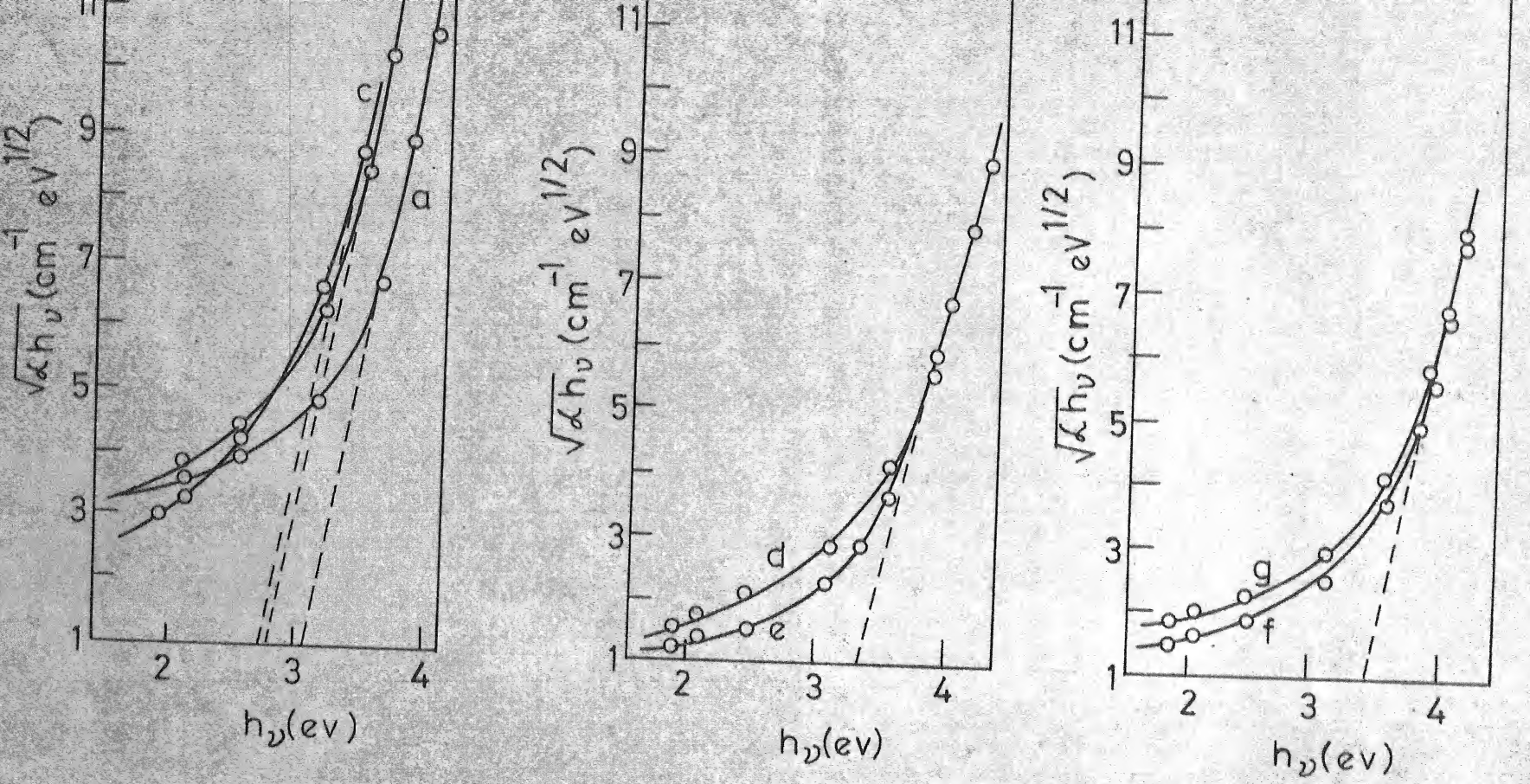

FIG. 32 PLOT OF $\sqrt{\alpha h\nu}$ vs. $h\nu$ FOR DIFFERENT GLASSES

(a) GLASS No. 1 (0.37) (b) GLASS No. 2 (0.33)
(c) GLASS No. 2 REDUCED (0.5) (d) GLASS No. 3 (0.43)
(e) GLASS No. 3 REDUCED (0.64) (f) GLASS No. 5 (0.53)
(g) GLASS No. 5 REDUCED (0.63)

Numbers in brackets indicate thickness of the specimen in mm.

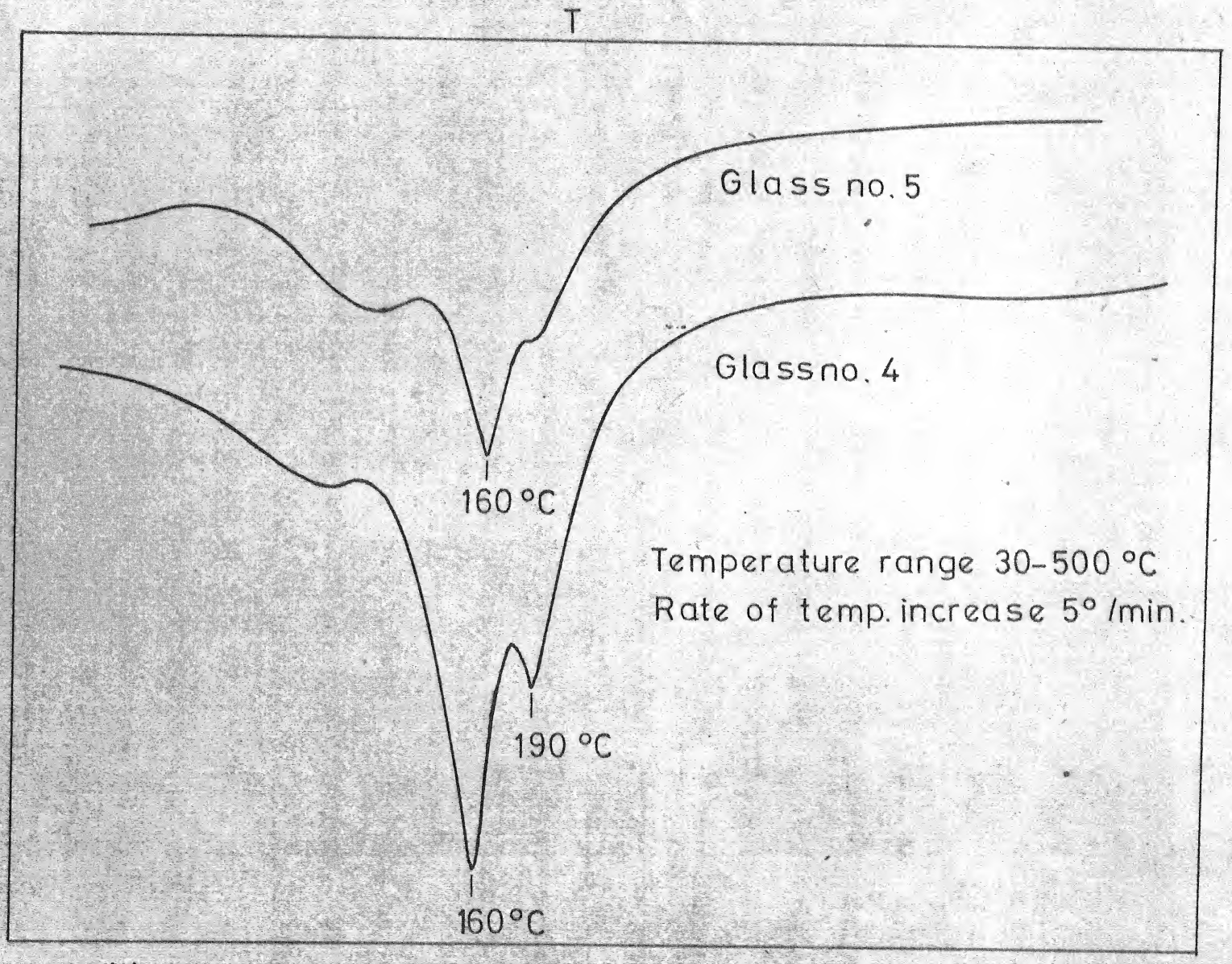

FIG. 32 (a) DTA CURVES FOR GLASS Nos. 4 & 5 FROM ROOM TEMPER-

CHAPTER 6

DISCUSSION

6.1 Bulk Resistivity

For bulk resistivity log ρ vs. 1/T plots are all straight lines for all the glasses in the temperature range for which resistivities were measured (fig. 9). Resistivity decreases with increase in mole % of Na_2O in the glass. Thus glass nos. 3 and 5 (with 3 mole % of Na_2O) show highest resistivity throughout the temperature range 100-400°C, whereas glass no. 1 (with 10 mole % of Na_2O) shows lowest resistivity. The activation energies are of the same order as for other alkali glasses and decrease with the increase in Na_2O content of the glass (fig. 10). These facts indicate that conductivity in these glasses in the above temperature range is due to the motion of alkali ions. At higher temperatures there is slight deviation from linearity. Thismay be due to polarization at the electrodes.

We can make an approximate calculation to see the order of decrease in resistivity with increase of Na_2O content of the glass, by using Stevels[15] expression for the variation of resistivity with temperature,

$$\rho = \frac{6kT}{\nu b \eta^2 e^2 n} \exp(E/kT) \qquad (6.1)$$

where ν is the vibrational frequency, b is the number of adjacent wells an ion can jump into, η is the average jump distance, n is the number of mobile ions/c.c. and E is the energy barrier.

The activation energies for glass nos. 1, 2 and 3 by d.c. measurements are 0.85, 1.27 and 1.40 eV respectively (table 2).

If the resistivities for glass nos. 1 and 2 at a temperature T°K are ρ_1 and ρ_2 and if we assume for a moment that all the terms in the preexponential factor of equation (6.1) are the same for glass nos. 1 and 2 we get

$$\frac{\rho_1}{\rho_2} = \frac{n_2}{n_1} \exp^{(E_1/E_2)} \qquad (6.2)$$

Substituting for ρ_1 and ρ_2 (from fig. 9, taking ρ values for 1/T = 1.925) and above values for E_1 and E_2 we get,

$$\frac{n_2}{n_1} = 1.09 \times 10^{-3} \qquad (6.3)$$

Similarly for glass nos. 1 and 3 we get

$$\frac{n_3}{n_1} = 2.02 \times 10^{-5} \qquad (6.4)$$

By knowing the molecular weight of the glass we can calculate the number of sodium atoms present in the glass per c.c.

Ratio of number of Na atoms in glass no. 2 (5 mole % Na_2O) to the number of Na atoms in glass no. 1 (10 mole % Na_2O) is 0.495.

Ratio of number of Na atoms in glass no. 3 (3 mole % Na_2O) to the number of Na atoms in glass no. 1 is 0.296.

The ratios of Na atoms in equations (6.3) and (6.4) are orders of magnitude smaller than the ratios of Na atoms calculated by molecular weight. But our calculations here are very approximate. Actually ν, b and η in equation (6.1) change with the composition of the glass. As Na_2O content of the glass is increased, the vibrational frequency ν and the number of adjacent wells b decrease, but the average jump distance η increases. If we take into account these variations also, the ratios of Na atoms calculated by Stevels model may approach the ratios calculated by molecular weight.

6.2 Surface Resistivity

6.2.1 Virgin Glasses

The virgin surface conductivities of all the glasses are shown in fig. 33 for comparison. All the curves can be divided into 4 distinct regions as shown in

the figure. In region I (low-temperature region) the resistivities of the glasses increase as the temperature is lowered below room temperature. In region II the resistivities increase as the temperature is increased above room temperature, showing a negative activation energy. In region III the resistivities decrease as the temperature is increased further. In region IV, the resistivities of glass nos. 3, 4 and 5 show some peculiar behaviour. A second peak is observed in this region. The conduction mechanisms in different regions of these curves are discussed below.

As discussed in Chapter 2, the surface resistivity of clean glasses in dry air will be of the order of 10^{14} ohm/□. The low resistivity observed at and slightly above room temperature in region II must be due to some external factors.

Experiments done by various workers (fig. 4, also ref. 67) indicate that surface conductivity is increased drastically if the humidity content of the ambient is higher. Iizima et al.[80] measured the surface conductivity of As-Te-Ge system after subjecting the surface of the glass to heat treatment, by boiling in water. In the temperature range 20-90°C, they observed a negative activation energy for surface conduction. They attributed this to the

formation of a conductive surface layer induced by water contained in the ambient. Hence it is possible that in the case of As_2O_3 containing glasses also, water molecules adsorbed on the surface do play a role in determining the surface conductivity. During the period in which experiments were done, % relative humidity of the ambient was 50-65%.

It is also known that SiOH groups occur on the surface of glasses and also that Na ions present in glass react with water to form an electrolyte film on the surface. The underlying layers of glass also influence the surface electrical conduction to some extent. During polishing a gel layer will form on the surface of the glass.

If we assume the presence of water molecules on the surface of glasses, the increase of resistivity with temperature in region II can be explained as due to protons acting as charge carriers. Protons are thought to be present in hydroxyl groups bound to Si atoms, and when migrating to jump from a hydroxyl group to a nearby terminal oxygen atom[80]. Conductivity increases with the concentration of both the OH groups and the terminal oxygen atoms. Since the sum of these concentrations is constant, there is an optimum ratio of concentration at which the conductivity is greatest. In As_2O_3 glasses under study, the lowest resistivity is observed near room temperature. As the temperature of the

sample is increased above room temperature, some of the water molecules may be driven off and the contribution to the total conductivity due to protons goes on diminishing, until at about 120°C ($1/T \simeq 2.5$), beyond which the conductivity is mainly due to sodium ions.

In region III the conductivity can be due to the movement of Na ions. Activation energy values support this.

In region IV, glass nos. 3, 4 and 5 show a small but distinct peak, whereas glass nos. 1 and 2 which have higher mole % of Na_2O do not exhibit this behaviour. This may arise due to some sort of order disorder phenomena in the glasses containing lesser mole % of Na_2O. However this peak is not observed during cooling cycle.(figures 13, 14 and 15) and also for the sample 5 for which measurements were done after giving 12 hours of heat treatment at 120°C. This may be explained if we assume that the phase giving this type of behaviour is destroyed due to heat treatment. It is also significant that in region IV, the conductivity increases with the increase in Na_2O content of the glass indicating that at higher temperatures ionic conduction is the main conduction mechanism.

This rapid increase of resistivities of all the glasses in region I, resulting in high activation energies of the order of 2 to 7 eV can be explained if we assume the

conduction mechanism in this region also to be due to protons. As the temperature is lowered below room temperature, the water content on the surface of the glass may increase drastically upsetting the optimum ratio between the concentrations of hydroxyl groups and terminal oxygen atoms. The high activation energy observed may be due to the presence of large number of water molecules which decrease the mobility of protons. Since water molecules will be adsorbed only by a thin outer layer, it appears that electrical conduction takes place predominantly in this thin layer.

It will be interesting to study the variation of resistivity with temperature for fresh leached surfaces of these glasses and to see whether the variation of resistivity with temperature will show the same kind of behaviour. Also, detailed experiments to study the influence of water content present in the ambient on surface conductivity of these glasses should be carried, by keeping the sample under vacuum and then measuring the resistivities, to support the above arguments.

6.2.2 Reduced Glasses

The variation of surface resistivity with temperature for all the reduced glasses is shown in fig. 34. For reduced glasses also the curves can be divided into 4 regions;

By a comparison of figures 33 and 34 we find that

(1) Both for reduced and virgin glasses the minimum surface resistivities (observed near R.T.) are of the same order.

(2) Virgin surface resistivity curves show a maximum at about 120°C for all the glasses studied, except glass no. 1. For reduced glasses the maxima are observed at different temperatures for different glasses which in general occur at slightly lower temperatures (about 90°C) than for virgin glasses.

(3) In region III, for virgin surface resistivity measurements, the resistivity levels do not vary much with the composition of the glass. But in reduced glasses the resistivities vary markedly with the composition in this region.

These differences can be explained if we examine the reduction process in reduced samples taking place in the surface layers due to hydrogen.

When the glasses are reduced in hydrogen atmosphere, some hydrogen may remain in the surface layers after the reduction process. But due to the absorption of water by top surface layers, the room temperature resistivities of both virgin glass and reduced glass might be approximately the same. As the temperature of the specimen is raised

above room temperature the water molecules from the topmost layer will be driven off and the reduced glass may follow a different path, as shown in fig. 36, reaching the level of conduction due to alkali ions at a temperature T_2, which is less than the temperature T_1, where the ionic conduction for virgin glasses starts. Thus in region II, though the conduction mechanism is assumed to be due to protons, the difference between virgin surface conductivity and conductivity of reduced samples can be attributed to the reduction treatment given to the latter.

In region III, the reduced glasses show marked variation in resistivity levels. The exact knowledge of the state of As_2O_3 after reduction process and its role in conduction process may help us in understanding these differences in resistivity levels. That the variation in resistivity levels in region III is due to reduction process itself is evident from the fact that for virgin glasses the variation in resistivity levels with composition is not much. However ionic conduction may also play a role in conduction in this region. Resistivity level of reduced glass no. 3 is much lower than the resistivity levels for other glasses in region III. This may be due to some crystallization process taking place, during slow heating of the sample, while measuring resistivity at different temperatures.

In region IV, reduced glass nos. 1 and 3 show small peaks. This may again be due to some order-disorder phenomena. A PbO glass of composition 6 (table 1), containing 1 mole % of As_2O_3 was reduced and resistivity measurements were done for this sample in the temperature range 100-200°C. It gave a straight line (fig. 26) in this temperature range. This shows that the peculiarities observed for the variation of surface resistivity with temperature may be characteristic features of alkali borosilicate glasses containing As_2O_3.

6.2.3 Ion-Exchanged and Reduced Glasses

For ion-exchanged and reduced glasses, plots of log ρ vs. 1/T are given for all the glasses studied in fig. 35. These curves can be divided into 3 regions. These curves differ from similar plots for virgin surface resistivity and reduced surface resistivity in that no second peak at higher temperatures is observed for any of these glasses except for a small hump for IER glass no. 2.

For ion-exchanged and reduced glasses also, the conduction in region I can be assumed to be due to protons. In region II, conduction can be again explained as due to protons with humidity lowering the resistivity near room temperature. In the IER silicate glasses containing Bi_2O_3[73], bismuth particles have been identified and the

conduction is explained as due to the presence of these particles. The electronic conduction in these glasses was explained, as due to the hopping of electrons between the conducting islands of bismuth. Also, there will be Ag particles in IER glass surfaces due to ($Ag^+ \rightleftharpoons Na^+$) ion-exchange reaction which again lead to electronic conduction. Hence in region II and III for IER glasses, conduction will be the combined effect of water molecules, ionic conduction and electronic conduction due to metallic particles. This may explain the differencesin resistivity levels in region II and III between virgin glasses and IER glasses. However detailed microstructural studies of virgin glasses, reduced glasses and IER glasses may help us in understanding the different conduction mechanisms operative in these glasses.

These peculiarities in variation of surface resistivity with temperature (particularly a deep minimum in resistivity near room temperature) for reduced glasses and IER glasses have also been observed for Sb_2O_3 [77] containing glasses.

6.3 DTA Studies

DTA curves recorded for glass nos. 4 and 5 show a minimum at about 160°C suggesting an endothermic reaction at this temperature. This may be due to expelling of water

molecules bonded to silicon atoms in which case DTA curves support our arguments discussed in the previous section. Or it may be due to the nucleation of some new phase, in the glassy matrix.

6.4 Switching

Out of the few glasses studied for switching behaviour only IER glass no. 2 showed switching behaviour below room temperature, at about 28°C. This glass also did not show switching at higher temperatures even when high voltages (upto 1000 V) were applied. The switching observed was of threshold type. This switching of the glass from high resistance state (10^{11} ohm) to low resistance state (10^{5} ohm) can be attributed to the fact that because of the thermal effects or Joule heating produced in the glass, current channels are induced implying thereby that the switching mechanism is thermal in nature. We have seen that for all the IER glasses the resistivity shoots up as the temperature of the sample goes below room temperature. Hence, in this temperature region, even a slight variation in temperature of one or two degrees will result in a large change in the resistivity of the sample. In particular, if the temperature of the sample increases by one or two degrees because of Joule heating, the resistivity of the sample will decrease considerably. By an approximate

calculation we can show that the rise in temperature of the sample due to Joule heating will be of the order of one or two degrees.

If I is the current passing through the sample just prior to switching (7 volts for IER glass no. 2) and R is the OFF state resistance, the heat generated will be I^2R. We can equate this to mct, where m is the mass of the sample, c is the specific heat of glass and t is the rise in temperature in °C.

For IER glass no. 2, with an electrode gap of 0.7 mm and an electrode width of 11 mm, and assuming that only a thin surface layer at the top of about 100 Å thickness is effective in conduction we get the mass of the sample through which conduction occurs as 1.54×10^{-7} gm where a density of 2 gms/c.c. for the glass is assumed.

Taking the specific heat for this glass to be 0.1 cals/gm/°C we get from the relation

$$I^2R = mct , \qquad (6.5)$$

$$2.02 \times 10^{-8} = 1.54 \times 10^{-8} \times t.$$

Thus t is of the order of 1°. This is consistent with our arguement above. Hence the switching mechanism seems to be thermal in nature.

However switching could not be observed in bulk glass no. 1. Further studies have to be done to establish the switching mechanism in these glasses and to determine the compositions of glasses which give better and stable switching characteristics.

6.5 Optical Absorption

Absorption edge was observed for all the glasses studied at about 3000 Å. The absorption edges lie in the range of 2.8 to 3.1 eV. These are more than twice the activation energy determined by d.c. measurements for these glasses. It is known that the activation energies for conduction in oxide glasses are much less than E_{gap}, whereas for chalcogenide glasses like As_2S_3 and As_2Se_3 they are similar to E_{gap}. Hence the absorption edges determined for these As_2O_3 glasses are consistent with the results for other oxide glasses.

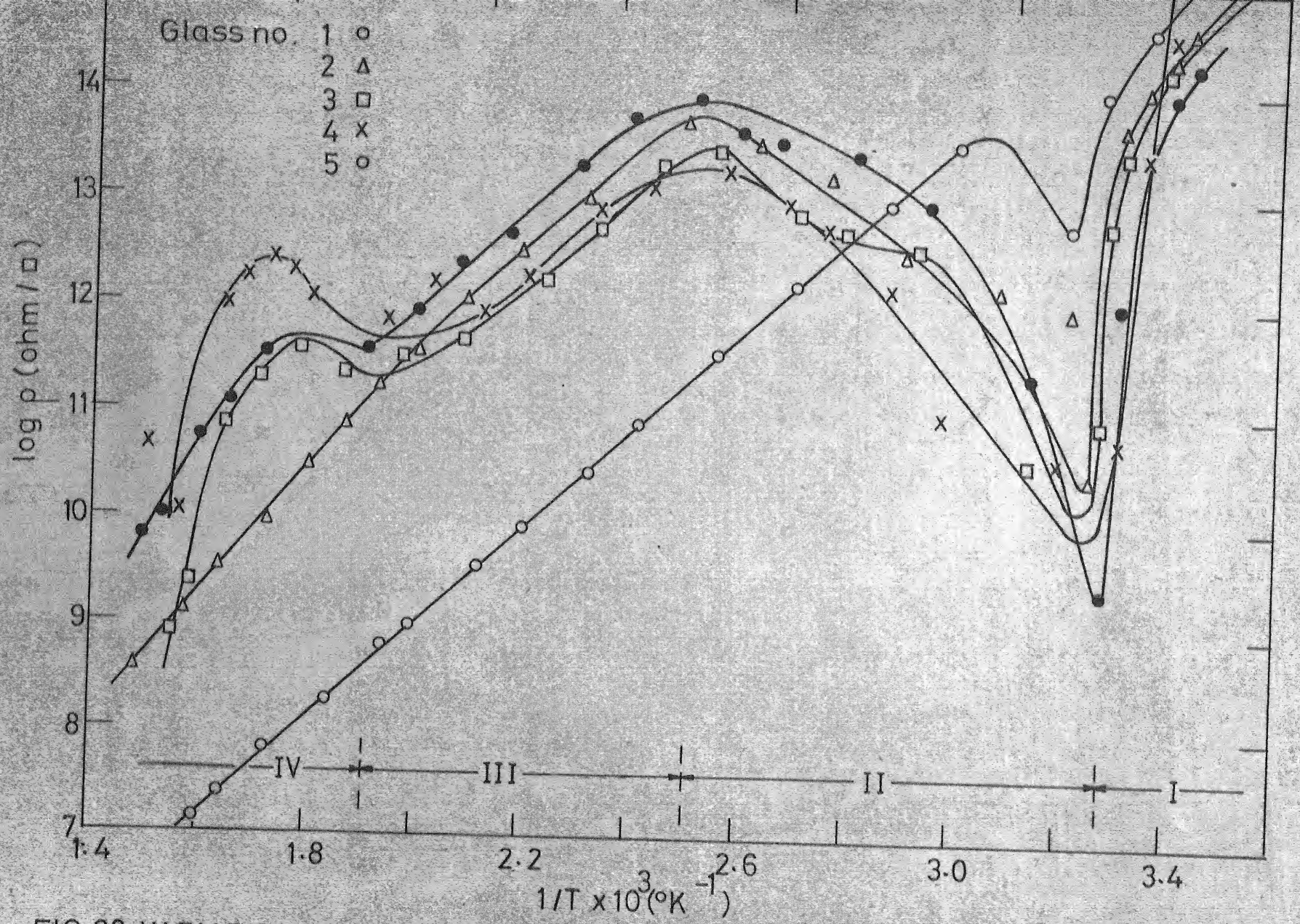

FIG.33 VARIATION OF SURFACE RESISTIVITY WITH INVERSE OF ABSOLUTE TEMPERATURE FOR VIRGIN SPECIMENS.

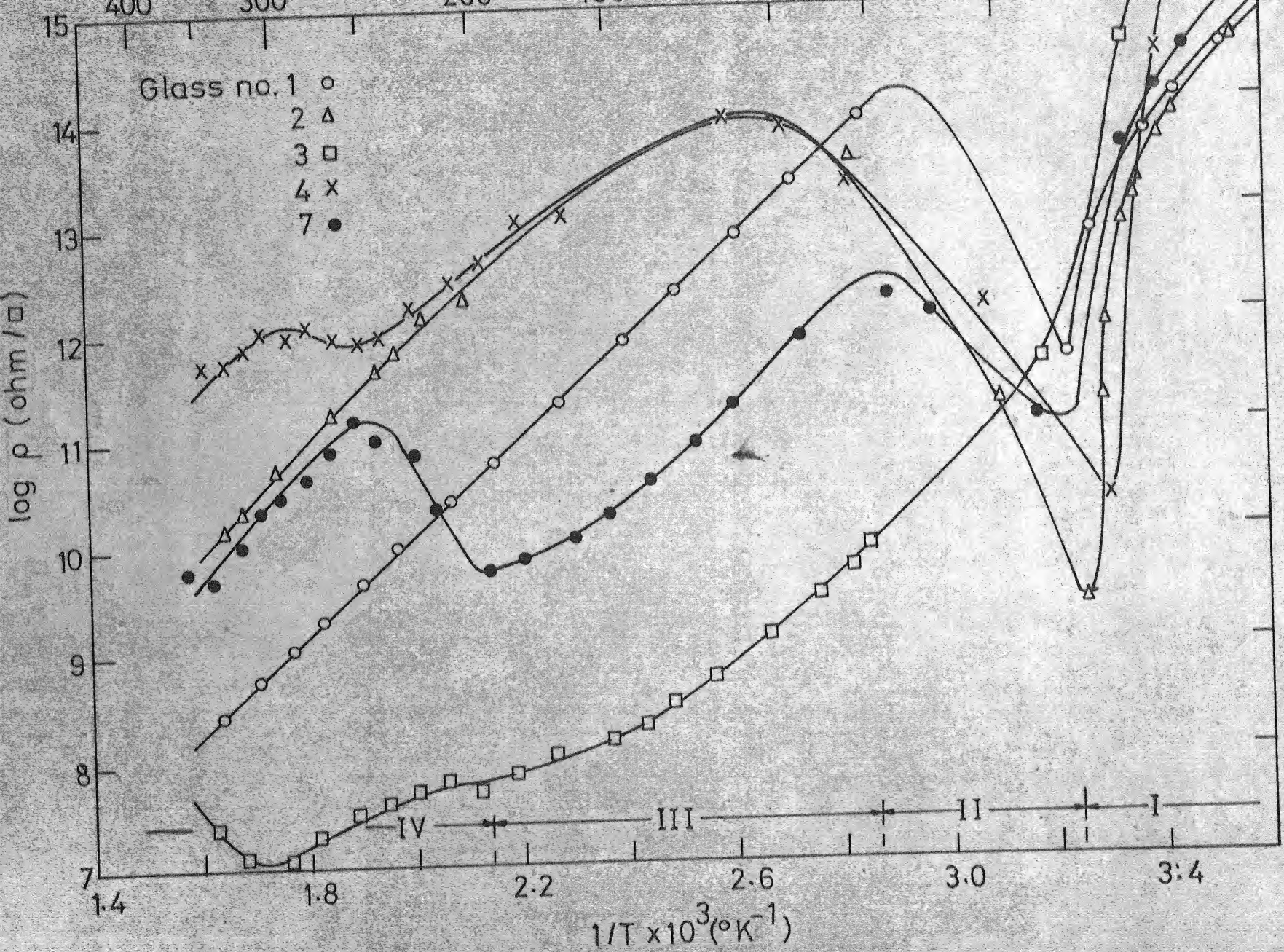

FIG 24 VARIATION OF SURFACE RESISTIVITY WITH INVERSE OF ABSOLUTE TEMPE-

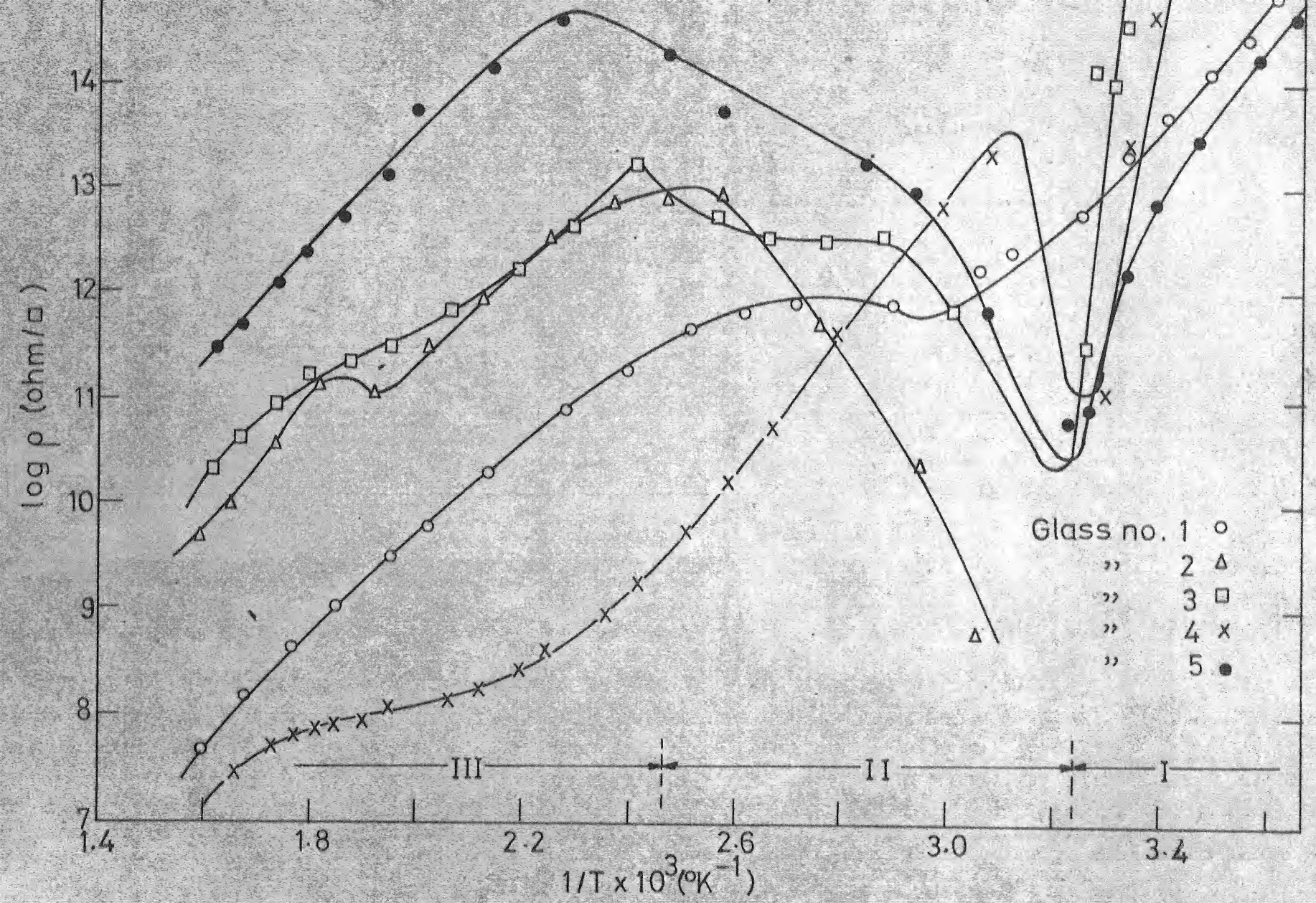

FIG.35 VARIATION OF SURFACE RESISTIVITY WITH INVERSE OF ABSOLUTE TEMPERATURE FOR ION EXCHANGED AND REDUCED GLASSES

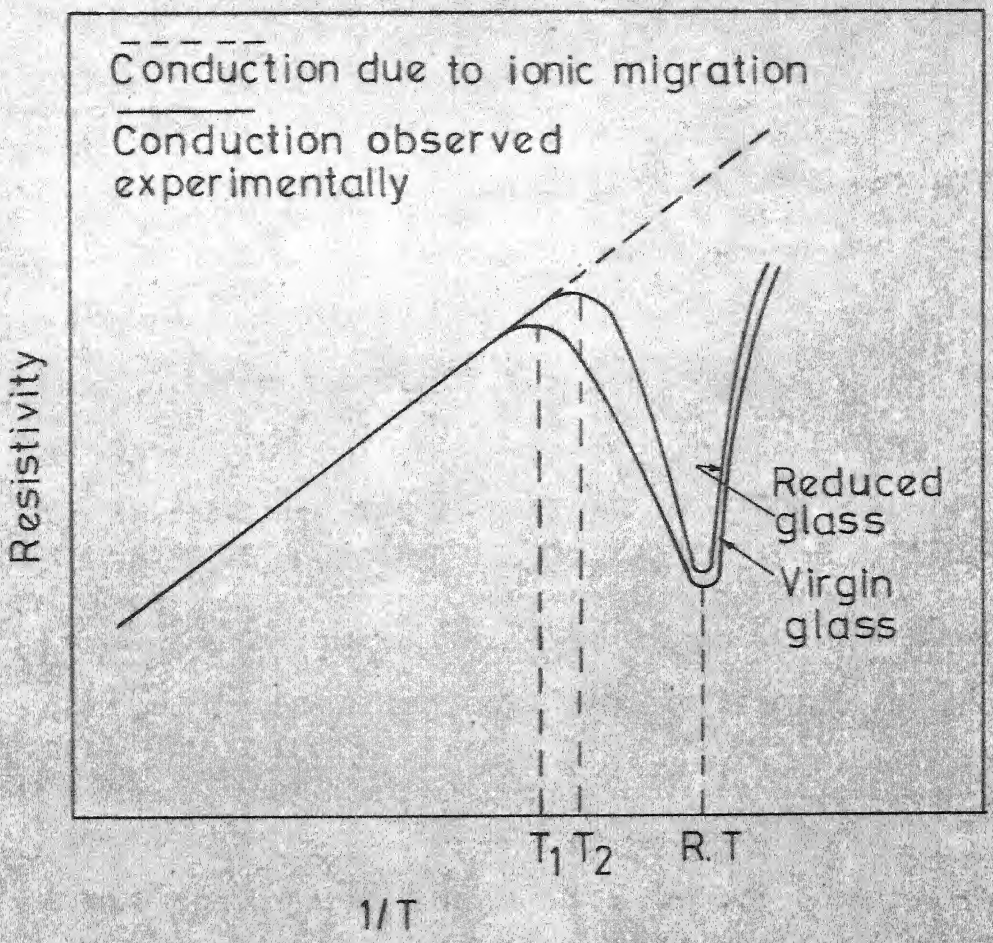

FIG.36 SCHEMATIC DIAGRAM SHOWING THE VARIATION OF SURFACE RESISTIVITY WITH TEMPERATURE FOR REDUCED AND VIRGIN GLASS.

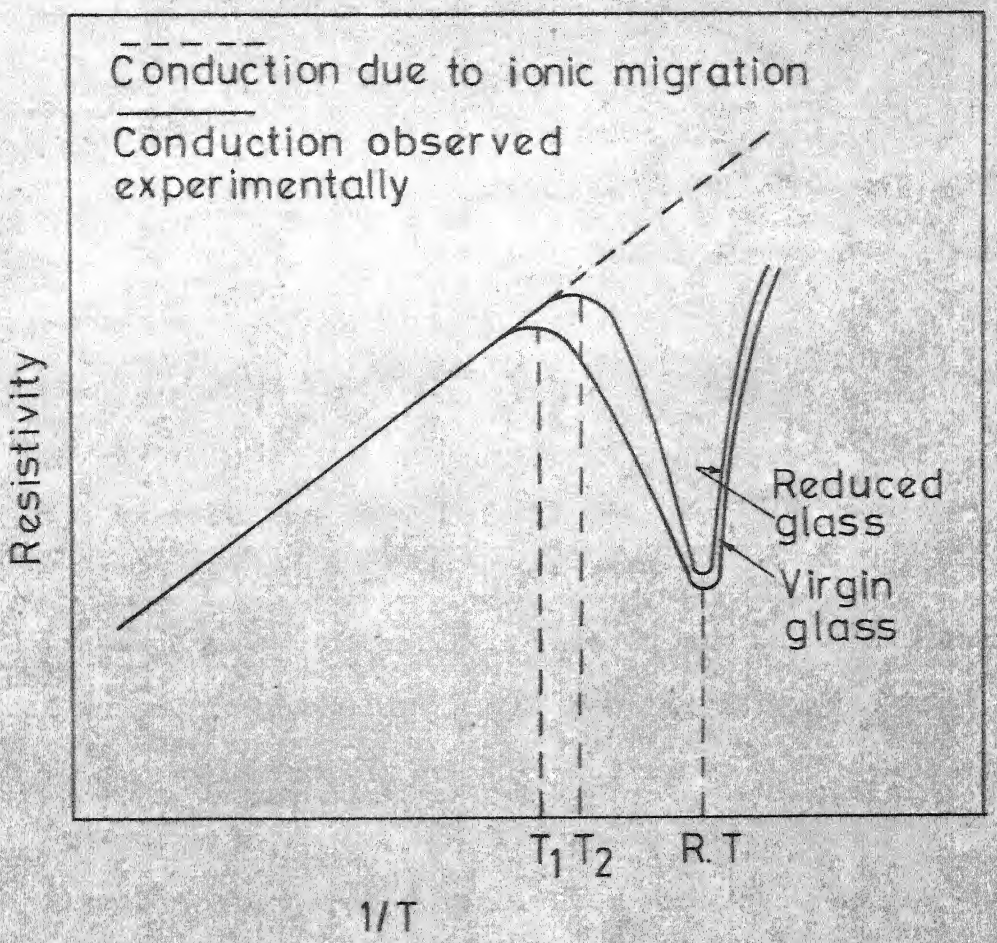

FIG.36 SCHEMATIC DIAGRAM SHOWING THE VARIATION OF SURFACE RESISTIVITY WITH TEMPERATURE FOR REDUCED AND VIRGIN GLASS.

CHAPTER 7

CONCLUSIONS AND SCOPE FOR FURTHER WORK

7.1 Conclusions

The following conclusions could be drawn from the studies made on the glasses belonging to the system SiO_2 - B_2O_3 - Na_2O - As_2O_3.

(1) The d.c. conductivity of these glasses is due to the motion of Na ions.

(2) The surface resistivities of all the virgin glasses studied and surface resistivities of all the reduced or ion-exchanged and reduced glasses exhibit a minimum near room temperature. The resistivities increase both below room temperature and just above room temperature. The increase in resistivity below room temperature is attributed to proton conduction and the increase just above room temperature is explained as due to water molecules and their interaction with silicate network of the glass. At higher temperatures these glasses show ionic conduction.

(3) Surface resistivities of glasses for which reduction treatment or ion-exchange and reduction treatment was given follow different kind of variation with temperature than for virgin glasses. This difference is

attributed to the surface treatment given to the glasses, resulting in different conduction mechanisms.

(4) A glass which had 5 mole % of Na_2O showed threshold type of switching after ion-exchange and reduction treatment of the surface. The switching mechanism is believed to be thermal in nature.

7.2 Scope for Further Work

(1) The glasses studied in the present investigation contained either 8 or 6 mole % of As_2O_3. It will be interesting to study the bulk and surface properties of glasses containing different mole % of As_2O_3.

(2) All the surface resistivity measurements were done for samples polished with 120 mesh size silicon carbide powder. It is necessary to investigate the dependance of surface resistivity on polishing medium and surface structure.

(3) In order to confirm the dependence of surface resistivity on water molecules adsorbed by the surface, it is necessary to carry out the following experiments.

   (a) Measurement of surface conductivity under vacuum and in dry nitrogen atmosphere

   (b) Measurement of surface conductivity at different

relative percentage of humidity by controlling the humidity of the ambient.

(c) Measurement of surface conductivity on fresh leached surfaces and also on samples exposed to boiling water for different periods of time.

(4) To study the surface conductivity of reduced and ion-exchanged and reduced samples as a function of temperature at which surface treatment was carried out. This study may help us in understanding the role of reduction or ion-exchange and reduction in surface conductivity mechanisms.

(5) To study in detail the microstructure of these glass surfaces and to identify the different species present on glass surfaces using different techniques such as IR spectroscopy, X-ray analysis, Electron diffraction and DTA.

(6) To investigate the switching properties of these glasses in more detail.

REFERENCES

(1) R.G. Neale, J. Non-Cryst. Solids, 2, 558 (1970).

(2) S.R. Ovshinsky and H. Fritzsche, IEEE Trans. Electron Devices, ED-20-2, 91 (1973).

(3) D.L. Nelson, J. Non-Cryst. Solids, 2, 528 (1970).

(4) M.H. Cohen, H. Fritzsche and S.R. Ovshinsky, Phys. Rev. Letters, 22, 1065 (1969).

(5) H. Fritzsche and S.R. Ovshinsky, J. Non-Cryst. Solid., 2, 393 (1970).

(6) A.W. Owen and J.M. Robertson, J. Non-Cryst. Solids, 2, 40 (1970).

(7) D. Chakravorty, Appl. Phys. Letters, 24-2, 62 (1974).

(8) G.W. Morey, 'The Properties of Glass', Rainhold, New York (1954).

(9) M. Schwartz and J.D. Mackenzie, J. Amer. Ceram. Soc., 49, 582 (1966).

(10) A.E. Owen, Phys. Chem. Glasses, 2, 87 (1961).

(11) K. Hughes, J.O. Isard and G.C. Milnes, Phys. Chem. Glasses, 9, 43 (1968).

(12) M. Schwartz, Thesis, Rensselaer Polytechnic Institute, Troy, New York, (1969).

(13) E. Gough, J.O. Isard and J.A. Topping, Phys. Chem. Glasses, 10, 89 (1969).

(14) E. Rasch and F. Hinrichsen, Z. Electrochem, 14, 41 (1908).

(15) J.M. Stevels, Encyclopedia of Physics, Vol. 20, 350, Springer Verlag, Berlin (1957).

(16) O.V. Mazurin, 'Electrical Properties and Structure of Glass', Consultants Bureau, New York (1965).

(17) A.E. Owen, Progress in Ceramic Science, Vol. 3, (J.E. Burke Ed.), Pergamon Press, New York (1963).

(18) B. Lengyel and Z. Boksay, Z. Phys. Chem., 203, 93 (1954); 204, 157 (1955).

(19) G.L. McVay and D.E. Day, J. Am. Ceram. Soc., 53, 508 (1970).

(20) C.C. Sartain, W.D. Ryden and A.W. Lawson, J. Non-Cryst. Solids, 5, 55 (1970).

(21) K.W. Hansen, J. Electrochem. Soc., 112, 994 (1965).

(22) E.P. Denton, H. Rawson and J.E. Stanworth, Nature, London, 173, 10 (1954).

(23) J.D. Mackenzie, in 'Modern Aspects of the Vitreous State', Ed. J.D. Mackenzie, Vol. 3, Butterworths, Washington (1964).

(24) J.D. Mackenzie, J. Am. Ceram. Soc., 47, 211 (1964).

(25) V.A. Joffe et.al., Sov. Phys. Solid State, 2, 609 (1960).

(26) D. Emin, C.H. Seager and R.K. Quinn, Phys. Rev. Lett., 28, 813 (1972).

(27) M. Nunoshita, H.Arai, T. Taneki and Y. Hamakawa, J. Non-Cryst. Solids, 12, 339 (1973).

(28) H.L. Uphoff and J.H. Healy, J. Appl. Phys., 32, 950 (1961).

(29) B.T. Kolomiets, Phys. Stat. Solids, 359, 713 (1964).

(30) Bandyopadhyay, M.Tech. Thesis, I.I.T. Kanpur (1974).

(31) V.K. Nagesh, M.Tech. Thesis, I.I.T. Kanpur (1974).

(32) J. Stuke, J. Non-Cryst. Solids, 4, 1 (1970).

(33) M.H. Cohen, J. Non-Cryst. Solids, 4, 391 (1970).

(34) N.F. Mott, in 'Electronic and Structural Properties of Amorphous Semiconductors', Ed. P.G. LeComber and J. Mort, London, Academic Press (1973).

(35) N.F. Mott, Advan. Phys., 16, 49 (1967).

(36) M. Cohen, H. Fritzsche and S.R. Ovshinsky, Phys. Rev. Letts., 22, 1065 (1969).

(37) E.A. Davis and N.F. Mott, Phil. Mag., 22 903 (1970).

(38) M.H. Cohen, J. Non-Cryst. Solids, 4, 391 (1970).

(39) E.A. Davis, in 'Electronic and Structural Properties of Amorphous Semiconductors', Ed. P.G. LeComber and J. Mort, London, Academic Press (1973).

(40) H. Fritzsche, J. Non-Cryst. Solids, 6, 49 (1971).

(41) N.K. Hindly, J. Non-Cryst. Solids, 5, 17 (1971).

(42) K. Hulls et.al., J. Phys. D (5) P.L. 865 (1972).

(43) B.T. Kolomiets and E.A. Lebedev, Radio Eng. Electron. USSR 8, 1941 (1963).

(44) A.D. Pearson, J.F. Dewald, W.R. Northover and W.F. Peck, in 'Advances in Glass Technology', Plenum Press, New York (1962); Vol. 1, 357; Vol. 2, 145.

(45) C. Feldman and K. Moorjami, J. Noncryst. Solids, 2, 82 (1970).

(46) A. Szymanski, D.C. Zarson and M.M. Laber, Appl. Phys. Letters, 14, 280 (1970).

(47) M.H. Omar et.al., Proceedings of IX Int. Congress on Glasses, Paris (1971).

(48) C.W. Gildart, J. Appl. Phys., 36, 335 (1965).

(49) C.F. Drake et.al., Phys. Status. Solidi, 32, 193 (1969).

(50) S.R. Ovshinsky, Phys. Rev. Letters, 21, 1450 (1968).

(51) H. Fritzsche and S.R. Ovshinsky, J. Non-Cryst. Solids, 4, 464 (1970).

(52) H.K. Henisch, J. Non-Cryst. Solids, 4, 538 (1970).

(53) A.D. Pearson, IBM J. Res. Develop., 13, 510 (1969).

(54) S.R. Ovshinsky, J. Non-Cryst. Solids, 2, 99 (1970).

(56) J.E. Stanworth, 'Physical Properties of Glass', Clarenden Press, Oxford (1950).

(57) J.H. Frazer, Phys. Rev., 33, 97 (1929).

(58) K.S. MacDonald, J. Phys. Chem. 62, 1168 (1958).

(59) R.H. Doremus, J. Phys. Chem., 75, 3147 (1971).

(60) L. Holland, 'The Properties of Glass Surfaces', Chapman and Hall, London (1964).

(61) M. Navez and C. Sella, C.R. 250, 4325 (1960); 257, 4183 (1963).

(62) J.J. Antal and A.H. Weber, Phys. Rev. 89, 900 (1953).

(63) F.M. Einsberger, in 'Annual Review of Materials Science', 2, 529 (1972).

(64) R.L. Green and K.B. Blodgett, J. Am. Ceram. Soc., 31, 89 (1948).

(65) E.M. Guyer, Proc. I.R.E., 32, 743 (1944).

(66) N.H. Kachalov, 'Foundations of the Grinding and Polishing Glass', Academy of Sciences, U.S.S.R., Press, Moscow-Leningrad (1946).

(67) Z. Boksay, M. Varga, A. Wikby, J. Non-Cryst. Solids, 17, 349 (1975).

(68) M. Tomozawa, C.H. Kim and R.H. Doremus, J. Non-Cryst. Solids, 19, 115 (1975).

(69) A. Wikby, J. Electroanal. Chem., 38, 429 (1972).

(70) K.B. Blodgett, J. Am. Cer. Soc., 34, 14 (1951).

(71) J.T. Randall and R.E. Leeds, J. Soc. Glass. Techn., 13, 16T (1929).

(72) A.K. Varshneya, J. Non-Cryst. Solids, 19, 355 (1975).

(73) D. Chakravorty, J. Non-Cryst. Solids, 15, 191 (1974).

(74) D. Chakravorty and C.S.N. Murthy, J. Phys. D.: Appl. Phys., 8, L162 (1975).

(75) C.S.N. Murthy, M. Tech. Thesis, I.I.T. Kanpur (1974).

(76) C.A. Neugebauer and M.B. Webb, J. Appl. Phys., 33, 74 (1962).

(77) Devendra Kumar, M.Tech. Thesis, I.I.T. Kanpur (1975).

(78) K. Hughes and J.O. Isard, Phys. and Chem. of Glasses, 9, 37 (1968).

(79) J. Tauc et.al., in 'Physics of Non-Crystalline Solids'', Ed. J.A. Prins, North-Holland, Amsterdam, page 606 (1965).

(80) S. Iizima, M. Sugi, M. Kikuchi and K. Tanaka, Solid State Communications, 9, 795 (1971).